Alma Mater Studiorum · Università di Bologna

SCUOLA DI SCIENZE
Corso di Laurea in Fisica del Sistema Terra

Simulation of plastic particles in the Western Mediterranean Sea

Relatrice:
Prof. Nadia Pinardi

Correlatore:
Dr. Baptiste Mourre

Presentata da:
Emma Ferri

Sessione IV
Anno Accademico 2021-2022

Ai miei genitori

Acknowledgements

I wish to show my appreciation to my supervisor at SOCIB, Baptiste Mourre, who has helped me and guided me during this work and gave me constant support. I also want to thank my Professor and supervisor Nadia Pinardi for giving me the opportunity to do this Thesis. I would also like to thank Alex Santana, Jaime Hernández Lasheras and Ismael Hernández for their patience and their help. Moreover, I wish to extend my special thanks to SOCIB and IMEDEA for hosting me and allowing me to carry out my thesis at their institutes.

I want to thank my family for being always by my side, to my mum for being the best emotional support one could ask for, and for always showing interest in what I was studying, always being there when I needed a shoulder to lean on and good advice. To my dad and Camilla, who have always supported me and celebrated my every minor success, and to my sister, my forever friend. Endless thanks go to my friends, for the constant help they gave me and for making every day better. I want to thank Cri, who walked with me to the finish line, and helped me with everything, both academically, and as a friend. I'm beyond grateful to Damiano, who was always there, with patience, kindness, and much appreciated scientific help. To Sofi, Rocìo, Vie, and all my Bologna friends, and my Reggio friends, who mean the world to me.

Abstract

In this Thesis we investigate the role of sea surface small-scale turbulence on the propagation of plastic particles from rivers Var (France, North West Mediterranean Sea) and Roya (Italy, Ligurian Sea), in the Western Mediterranean Sea (WMED). We simulate the dispersion of 60000 particles starting from the 3rd of October, 2020, immediately after a strong storm (Storm Alex) hit the area, causing the flooding of the two rivers and diffused damage across Europe. Storm Alex was a strong early-season extra-tropical cyclone that formed on the 30th of September 2020 and dissipated on the 3rd of October, 2020.
Storm Alex is just one of many extreme events that has struck Europe in the past decades; as global warming increases, extreme events are becoming much more frequent than in the past and the study and prediction of their effects have become a key topic in many scientific fields. We carry out our work by running numerical simulations of sea surface currents with the Western Mediterranean Operational Model (WMOP), developed by the Balearic Islands Coastal Ocean Observing and Forecasting System (SOCIB). We will also perform simulations using the Copernicus Marine Environment Monitoring Service-Monitoring Forecasting Centre (CMEMS-MED MFC), the outputs from the two models, which have a different spatial resolution ($\sim$2 km for the WMOP and $\sim$4.5 km for the CMEMS-MED MFC), will be then compared to look for similarities and differences in the results. We are interested in investigating how the particles disperse and where is their final position (on water, beached, or out of domain), and in which country. To filter out small-scale turbulence from the models outputs we perform four different types of simulations, with three-hourly outputs, in the WMED domain. The reference simulation is the output of the model, containing all the features representable by the model. We then make a temporal average of the currents to filter out short-lived turbulence and highlight the mean circulation of the WMED. The third simulation is obtained by making a 50 km running average of the models currents, in order to remove small-scale eddies and meanders of the Northern Current (the permanent rim current that flows Westward in the Northern part of the WMED). The fourth simulation is obtained by computing the geostrophic currents from values of sea surface height, from both models. The propagation of plastic is then simulated with these four currents, in order to find how different filters of turbulence impact the propagation of material. We learn that the role of the turbulence is that of keeping the material from reaching the North Balearic Front (NBC), the materials is slowed down and diffused in the total currents simulation, whereas in the three filtered simulations we observe: extensive beaching in the geostrophic simulation and on-water propagation in the temporal and spatial averages, in which the particles are carried through a substantial part of the domain's permanent circulation.

Sommario

In questa Tesi indaghiamo il ruolo della turbolenza superficiale di piccola scala sulla propagazione di particelle di plastica, provenienti dai fiumi Var (Francia, Mar Mediterraneo nord-occidentale) e Roya (Italia, Mar Ligure), nel Mar Mediterraneo Occidentale.
Simuliamo la dispersione di 60000 particelle a partire dal 3 Ottobre 2020, subito dopo che un forte temporale (tempesta Alex) colpì la zona, provocando l'esondazione dei due fiumi e danni diffusi in tutta Europa. La tempesta Alex è stato un forte ciclone extra-tropicale, di inizio stagione, che si è formato il 30 Settembre 2020 e dissipato il 3 Ottobre 2020. La tempesta Alex è solo uno dei tanti eventi estremi che hanno colpito l'Europa negli ultimi decenni; con l'aumentare del riscaldamento globale, gli eventi estremi stanno diventando molto più frequenti rispetto al passato e lo studio e previsione dei loro effetti sono diventati un argomento chiave in molti campi scientifici.
Svolgiamo il nostro studio eseguendo simulazioni numeriche delle correnti superficiali marine utilizzando il Western Mediterranean Operational Model (WMOP), sviluppato dal Balearic Islands Coastal Ocean Observing and Forecasting System (SOCIB) e il Copernicus Marine Environment Monitoring Service-Monitoring Forecasting Centre (CMEMS-MED MFC). Gli output dei due modelli, che hanno una diversa risoluzione spaziale ($\sim$2 km per il WMOP e $\sim$4.5 km per il CMEMS-MED MFC), saranno poi confrontati per cercare somiglianze e differenze nei risultati. Ci interessa indagare come le particelle si disperdono e qual è la loro posizione finale (in acqua, spiaggiata o fuori dominio), e in quale nazione. Per filtrare la turbolenza su piccola scala dagli output dei modelli, eseguiamo quattro diversi tipi di simulazioni, con output ogni tre ore, nel dominio WMED. La simulazione di riferimento è l'output del modello, contenente tutte le caratteristiche da esso rappresentabili. Dopodichè, facciamo una media temporale delle correnti per filtrare le turbolenze di breve durata ed evidenziare la circolazione media del WMED. La terza simulazione è ottenuta facendo una media mobile spaziale di 50 km delle correnti dei modelli, al fine di rimuovere vortici di piccola scala e meandri della Corrente Settentrionale (la corrente di bordo, permanente, che scorre verso ovest nella parte settentrionale del WMED). La quarta simulazione si ottiene calcolando le correnti geostrofiche con i valori altimetrici, da entrambi i modelli. La propagazione della plastica è poi simulata con queste quattro configurazioni di correnti, per trovare come diversi filtri di turbolenza influenzino la propagazione del materiale. Troviamo che il ruolo della turbolenza è quello di impedire al materiale di raggiungere il North Balearic Front (NBC), le particelle sono rallentate e diffuse nella simulazione delle correnti totali, mentre nelle tre simulazioni filtrate si osserva: spiaggiamento estensivo nella simulazione geostrofica e propagazione in acqua nelle simulazioni media temporale e media spaziale, in cui le particelle sono trasportate attraverso una parte sostanziale della circolazione permanente del dominio.

Contents

Chapter 1

Introduction

Between the end of September 2020 and the first few days of October 2020 Storm Alex, a strong extra-tropical cyclone, hit Europe and caused flooding damages and heavy rain. This extreme event caused rivers to overflow and increased watercourses discharges across the South-East coasts of France and the North-West coasts of Italy, as well as impacting Spain and other areas of Europe.
In this Thesis we focus on the discharge of two rivers, that flow into the Mediterranean Sea: river Var, which outflows between Nice and Saint-Laurent-du-Var, and river Roya, whose delta is located in the town of Ventimiglia; the rivers mouths are $\sim$37 km apart. Var is a 114 km long river whose course is entirely inside of France. On the other hand, river Roya , which is 59 km long, is shared between Italy (18.9 km) and France (40.1 km).
The objective is to study how virtual particles, representing floating plastic or marine litter, dispersed from these rivers into the Western Mediterranean Sea, following the exceptional stream output due to Storm Alex. In particular, we want to focus on the role of the small scale features of the Western Mediterranean circulation, and their importance in moving pollution across areas of water and land. We will examine how the meanders of the Northern Current influenced the movement of particles and the extent of their contribution compared to large scale features.
The simulations for the plastic particles and the surface currents are performed starting from the 3rd of October 2020 to the 30th of November 2020. Thus, allowing us to see the path of the particles in the immediate aftermath of the storm, and in the following weeks.
We conduct our investigation with the tools provided by the Western Mediterranean Operational System (WMOP), developed at the Balearic Islands Coastal Ocean Observing and Forecasting System (SOCIB), and Copernicus Marine Environment Monitoring Service- The Mediterranean Monitoring Forecasting Centre (CMEMS-MED MFC), in order to delineate the coastal and off-shore extent of pollution spillage.

1.1 The Western Mediterranean sea surface circulation

The Mediterranean Sea is a semi-enclosed basin located between 30°N and 46°N in the meridional direction and between 6°W and 37°E in the zonal direction. To the West, the Mediterranean communicates with the Atlantic ocean through the Strait of Gibraltar, which is a narrow strait separating the Iberian Peninsula from Morocco. To the East, the Turkish Straits, which consist of the Bosphorus and the Dardanelles, connect the Mediterranean to the Sea of Marmara and the independent Black Sea (Figure 1.1). Inside the Mediterranean sea we can find almost every

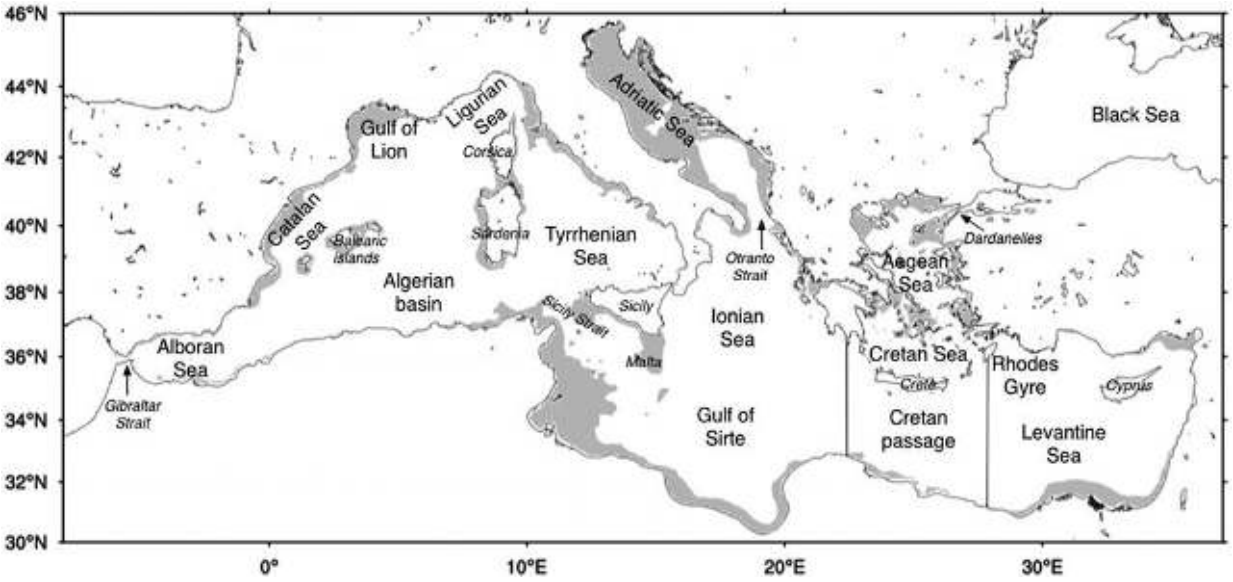

Figure 1.1: The main seas of the Mediterranean. Grey areas represent regions of depth less than 200 m. (borrowed from Pinardi et al. (2019))

oceanographic process observable in the world's oceans. Because of this, this basin is often referred to by oceanographers as a "miniature oceanographic laboratory" (Bethoux et al. (1999)). It can be divided into two different sub-basins, the Western Mediterranean (WMED) and the Eastern Mediterranean, which are connected by the Strait of Sicily. The depth of the Mediterranean waters is highly variable, we have both continental shelves, as in the Adriatic Sea and the Tunisian shelf, which have a depth of under 100 m, as well as deeper regions such as the Tyrrhenian, Ionic and Levantine Seas, where depths reach 5000 m.

In the Mediterranean Sea evaporation exceeds freshwater inputs from rivers and precipitation, therefore making it a concentration basin. Different factors, such as differences in water density due to variations in temperature and salinity, as well as wind and tide patterns give rise to an anti-estuarine circulation. The anti-estuarine circulation is opposite to the typical circulation we see in estuaries, where freshwater flows out to the sea. In the Mediterranean, seawater flows out into the Atlantic ocean through the Strait of Gibraltar.

When the less dense water of the Atlantic enters the Mediterranean, large-scale mo-

tions are generated. At the Strait of Gibraltar, Atlantic Water (AW) enters the basin on the surface (50 - 100 m); below, the saltier and warmer waters of the Mediterranean flow out of the basin, into the Atlantic. The Atlantic water entering the Mediterranean is termed Modified Atlantic Water (MAW) because of the mixing of Atlantic and Mediterranean waters, occurring in the Alboran Sea.
The circulation that is triggered from this exchange, characterises the surface motion of the WMED, which is the main focus of this work.
In Figure 1.2 are shown sea surface circulation patterns of the WMED. The AW entering the Mediterranean forms a quasi permanent anticyclonic gyre in the Alborian Sea. The current then flows eastward along the Algerian and Tunisian coasts, with various anticyclonic mesoscale eddies along the path, which are due to the unstable character of the flow (Robinson et al. (2001)). The current then moves Northward along the eastern coast of Italy, and subsequently flows South-Westward alongside the coasts of Northern Italy, France and Spain. The MAW flowing along the South-West European coasts forms the Liguro-Provenco-Catalan Current, or 'Northern Current' (NC). The southern branch of the cyclonic gyre in the north-western Mediterranean Sea is given by the North Balearic Front (NBC), which extends from the Balearic Current (BC) to the Ligurian Sea (Font et al. (1988)). In the winter, the NC intensifies and becomes narrower than in the summer months and the NBC is located at around 40°N.
The Northern Current represents one of the main focuses of our investigation, as it is its meanders and small-scale features that we analyse in the 2 months following Storm Alex. Overall, the WMED circulation is cyclonic, and numerous wind-induced eddies characterise the path in the interior of the sub-basin.

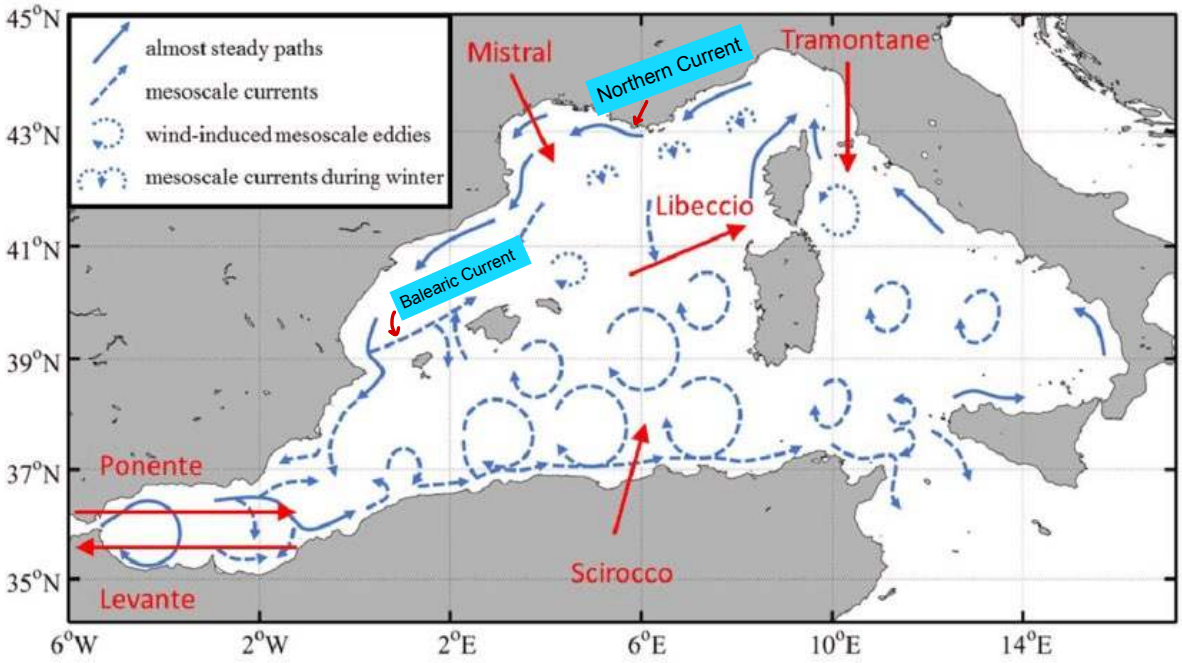

Figure 1.2: In blue: sea surface circulation of the WMED. In red: the main forcing winds. (Borrowed from Gade et al. (2018), the image has been modified to highlight the NC and the BC)

The Balearic Islands Coastal Observing and Forecasting system (SOCIB)

The work presented in this Thesis was carried out at SOCIB, the Balearic Islands Coastal Observing and Forecasting system (Tintoré et al. (2013)). SOCIB is a public research infrastructure, funded by the Spanish Science Ministry, the Balearic Islands Government and the Spanish Research Council. It has been operative since 2012, carrying out ocean observations and forecasts in the Western Mediterranean Sea, as well as gathering and analysing oceanographic data. Its results and investigations are presented into a European and international framework, with the aim of supporting operational oceanography and progress towards a sustainable development of marine and coastal research. It is part of the Joint European Research Infrastructure network for Coastal Observatory (JERICO), and it also collaborates with other research institutions in various international programs, such as CMEMS and EuroSea.
New observation technologies allow the real-time monitoring of the WMED, therefore dispensing to both the scientific and social communities products and services related to oceanographic prediction. In the European JERICO-S3 project (JERICO-RI), SOCIB participates in the North-Western Mediterranean pilot super-site, with specific interest in understanding the transnational transport throughout the region. This Thesis, also contributes to this activity.
SOCIB activities are branched into three major subsystems: oceanographic observations, the modelling and forecasting facility (MFF) and a data management sub-system. The observing system measures through different means, such as high-frequency radars (HFR), gliders, Lagrangian platforms, moorings, weather stations, tide gauges and a research vessel. The Data Centre Facility takes care of data curation and dissemination. The modeling and forecasting facility carries out three objectives:

1. forecasts of oceanic currents, temperature, salinity and sea level in the Western Mediterranean Sea;

2. forecasts and analysis of meteotsunamis in Ciutadella harbour (Menorca Island);

3. wave forecasting, implemented in the Balearic Islands area.

1.2 Context

In the last decades we have observed an increase of extreme weather events, including droughts, floods and episodes of extreme precipitation. The Mediterranean region suffers the pressure of around 100 million inhabitants living on its coastal regions (UN (2017)). As a consequence, pollution is specifically high in the shore regions and the urbanised environment is less equipped to contrast severe storms and precipitations. As we try to contrast the effects of climate change while new strategies are being implemented by policymakers, operational oceanography becomes increasingly important to study the consequences of these extreme weather

events in our seas. In this Thesis we want to study how plastic pollution, introduced by Storm Alex through the discharges of rivers Var and Roya, dispersed in the western Mediterranean.
Storm Alex hit southern France and northern Italy on the 2nd to the 3rd of October, causing extreme rainfall and flash flooding. According to Italian authorities, the Piedmont region saw its highest rainfall since 1958; in particular, in the 24 hours of the 3rd of October 2020, the Province of Verbano-Cusio-Ossola recorded 630 mm of rain. In the same period, Meteo France reported 500.2 mm of rain at Saint-Martin-Vésubie, which is more than three months worth of rain (according to FloodList and News (October 2020)). As we can see in Figures 1.3 and 1.4, in the aftermath of the storm the discharges of rivers Roya and Var were significantly increased and the two rivers flooded causing destruction of buildings and bridges. The rivers collected an abundance of natural and artificial debris and brought it into the Mediterranean sea.

Figure 1.3: Roya river before and after Storm Alex. The first image is from March 2016 (borrowed from account (a)), the second image is from October 2020 (borrowed from account (b)).

Figure 1.4: Var river before and after Storm Alex. The first image is from the 26th of September 2020 (borrowed from Sentinel Hub (2020b)), the second image is from the 3rd of October 2020 (borrowed from Sentinel Hub (2020c)).

1.3 Objectives of the work

According to Jambeck et al. (2015) the amount of plastic waste generated in 192 coastal countries in 2010 amounts to 275 million metric tons, with 4.8 to 12.7 million metric tons entering the ocean. This quantity is predicted to increase by an order of magnitude by 2025, unless proper waste management is refined and improved. Ocean plastic waste is a global catastrophe, having a huge impact on ecosystems

and the biodiversity of the seas. In this work we focus on the dispersion of plastic from one specific storm, but the conclusions are in fact relevant to a much more general framework. The study is carried out through numerical simulations, the final intent being to investigate the effect of small scale turbulence on the dispersion of materials.
We want to analyse the trajectories of plastic material input from the rivers, following Storm Alex. In particular, we want to assess how the small scale features of the WMED currents impacted the dispersion of virtual particles, representing floating plastic or marine litter, from rivers Var and Roya, following Storm Alex. To do this, we use three hourly sea surface current outputs from the WMOP and CMEMS models, which will be explained in the next Chapter. The current outputs from the two models are used to simulate the movement of plastic particles. Then, we produce different filtered versions of the original currents, in order to evaluate the effect of eddies and small scale features. Thus, we simulate again the dispersion of plastic particles using the different current simulations, in order to find differences due to small scale turbulence.
For both models, the currents studied, and the names with which they will be referred to, are:

- Total currents: these are the 3-hourly sea surface currents from the WMOP model and from the CMEMS-MED MFC model; they contain all the features of the sea surface currents, to the extent to which the models are able to reproduce them.

- Mean current: it is the time average of the total currents. We computed it over the entire period of study and it is therefore one single output over which the particles move.

- Spatially filtered currents: these currents are the result of a low-pass spatial filter, a 50 kilometers rolling space average, applied to the total currents.

- Geostrophic currents: these currents were obtained from values of the sea surface height, from the WMOP model and from the CMEMS-MED MFC model, through the geostrophic balance equations.

The total currents, which are our 3-hourly WMOP and CMEMS-MED MFC outputs, will be the reference to which we compare every other simulation obtained with different filters. We therefore accept that these are the currents that best resemble the real circulation of the WMED.
The mean current was studied in order to see how the particles would have moved in the absence of any small timescale features. By making a 60 days average (starting from the 3rd of October 2020), we were able to observe the movement of the material without any eddy or short lived turbulence.
The spatially filtered currents were obtained by computing a 50 km rolling average, for both models. The choice of which scale should be filtered out, in this case 50 km, was made by examining maps of sea surface height (SSH), in order to see the spatial scale of the meanders of the NC. These maps and the corresponding analysis, will be shown in the relative Sections.
Furthermore, we studied the geostrophic currents of the WMED. We computed them

from SSH data from the WMOP and CMEMS-MED MFC. Studying geostrophy allows us to better observe the mesoscale circulation, and since in this work we are interested in the small scale, it is a great tool to see what the circulation would look like without small scale features.
The means through which we obtained each type of current for our particles simulations will be further explained in the relative Sections. Overall, the goal is always to filter out small eddies, and in particular the meanders of the NC, to evaluate the role of these small scale features on the trajectories of plastic particles.

Chapter 2

Materials and Methods

2.1 Theoretical framework

Nowadays, ocean models, such as the ones we used in this Thesis, often describe the ocean dynamics by solving the primitive equations (Sommer et al. (2018)): a set of non-linear differential equations used to analyse both the atmospheric and oceanic flow. The primitive equations are an approximation of the Navier-Stokes equations, a simplified version used in most atmospheric and oceanographic models. They contain balance relations between velocity, salinity, and temperature, and their evolution over space and time.
Each model may use different approximations of these equations, but generally they consist of:

- The momentum equations, which describe the conservation of momentum for a hydrodynamical fluid moving on a rotating sphere. They assume hydrostatic equlibrium, and that the depth of the fluid is much smaller than the earth's radius;
- The continuity equation, representing the conservation of mass;
- The thermal energy equation and a salt equation, which relate these variables to their sources and sinks.
- The equation of seawater.

The momentum equations describe how momentum changes in a three-dimensional fluid flow; it is a set of three equations, one for each physical dimension. Assuming hydrostatic equilibrium, the equations are:

$$\frac{\partial u}{\partial t} + \vec{u} \cdot \nabla u - fv + f^* w = -\frac{1}{\rho_0}\frac{\partial p}{\partial x} + D_x + F_x \tag{2.1}$$

$$\frac{\partial v}{\partial t} + \vec{u} \cdot \nabla v + fu = -\frac{1}{\rho_0}\frac{\partial p}{\partial y} + D_y + F_y \tag{2.2}$$

$$\frac{1}{\rho}\frac{\partial p}{\partial z} = -g \tag{2.3}$$

where D_x,F_x,D_y,F_y are dissipation and forcing in the zonal and meridional directions, respectively, and $\vec{u} = (u, v, w)$.
Equations 2.1 and 2.2 describe the fluid flow in the zonal and meridional directions respectively. They include an acceleration term, an advection term and forcing terms on the right hand side of the equations. These are prognostic equations, meaning that they can be used to evaluate the velocity at later times, since they contain a time derivative. On the other hand, equation 2.3 is a diagnostic equation, because it is time-independent; the momentum equation in the vertical direction is the hydrostatic approximation, which states that at any point in the ocean, pressure is due to the weight of the water above it. The approximation arises from the assumption that the horizontal scale is large compared to the vertical scale.
The continuity equation is considered as for an incompressible fluid:

$$\vec{\nabla} \cdot \vec{u} = 0 \tag{2.4}$$

The thermodynamic equations are:

$$\frac{\partial T}{\partial t} = -\nabla \cdot (T\vec{u}) + D_T + F_T \tag{2.5}$$

$$\frac{\partial S}{\partial t} = -\nabla \cdot (S\vec{u}) + D_S + F_S \tag{2.6}$$

where D_S and D_T are diffusion of salinity and temperature, respectively, due to small-scale processes that are not resolved by the model. Equations 2.5 and 2.6 describe the evolution of the thermodynamic fields of temperature T and salinity S. Finally, the equation of seawater is

$$\rho = \rho(T, S, p) \tag{2.7}$$

and it relates density to temperature, salinity, and pressure.

2.2 Ocean circulation models

Understanding and reproducing the ocean's dynamics is a difficult and lengthy challenge. To tackle this challenge, ocean general circulation models (OGCMs) have become an essential tool. In the past decades, operational oceanography has advanced to the point where it is possible to make oceanic forecasts analogous to atmospheric predictions. In fact, we now have numerous OGCMs, which are used to make predictions and diagnostic assessments of the state of the ocean. In particular, the Mediterranean has become an international focus of study, given that it is an essential resource to multiple nations and it also serves as a natural ocean laboratory for operational oceanographers. Ocean modelling is a relatively recent field, the first underlying algorithm was proposed by (Bryan and Cox (1967)) and the field has been improved ever since, also due to the continuous progress of technology and increase in computational power. Oceanographic models allow us to exploit data in order to predict processes that are not directly measurable, such as forecast and hindcast predictions. These models are based on complex math which accounts for the interaction of energy and matter; these interactions are closely related to the

time intervals over which they evolve: a smaller time interval means a more precise prediction. All predictions and diagnostics performed by OGCMs are also bounded by space, in other words, grid size. A model with a smaller grid cell will have a better spatial resolution and will therefore be able to make more accurate predictions. An important aspect in modern numerical modelling is the advancement of data assimilation. Data assimilation (DA) is a method to combine observations with model products. It was initially developed in the field of meteorology, but it is now an established discipline in multiple fields. In numerical forecasting, DA is usually described as a process to define optimal initial conditions by using both the model and the observational data available. Furthermore, models and observations are used to correct the errors of one another; in the regions or times where the model lacks, data assimilation can help to fill in the blanks. Likewise, observations are also subject to errors which can be improved by merging with model outputs.

WMOP: The Western Mediterranean Operational System

In order to simulate the trajectories of tracers and pollutants descending from Var and Roya, a model for oceanic circulation and mesoscale variability is needed. In this thesis we initially use the Western Mediterranean Operational Model (WMOP, Juza et al. (2016); Mourre et al. (2018)), which provides daily predictions and hindcast simulations. The WMOP model generates forecasts as a regional configuration of the Regional Ocean Modelling System (ROMS); it was developed at SOCIB and it covers an area from the Strait of Gibraltar to the Sardinia/Corsica Islands (6°W-9°E, 35°N-44.5°N), with a Spatial resolution of ∼2 km. Regarding the vertical coordinate system, the grid is made up of 32 stretched sigma levels. In the sigma level coordinate system, the vertical coordinate is terrain-following, meaning that it is comprised of the same number of vertical grid points everywhere in the domain. As a consequence, each sigma layer does not have the same thickness, but it varies depending on the depth of the ocean in that point. Since the vertical layers follow the slope of the bathymetry, the sigma-layers are often more packed near the surface, thus allowing to better resolve the surface boundary layer. Therefore, WMOP has a vertical resolution varying from 1–2 m at the surface, 30–40 m at 200 m depth, around 250 m at 1000 m depth, and 500 m for depth levels deeper than 2500 m (Juza et al. (2016)). This is especially suitable for this Thesis, where we focus only on the sea surface circulation.
Moreover, the WMOP is nested in the Mediterranean model from the Copernicus Marine Service (CMEMS-MED), which has a spatial resolution of ∼4.5 km. The WMOP model is a primitive equations model with Boussinesq and hydrostatic approximations, which is forced by high-resolution atmospheric outputs and, at the boundaries, active and passive conditions (Marchesiello et al. (2001)) are imposed using daily forcing data from the CMEMS-MED simulations. The outputs from the model are three hourly. In the system is included the climatological runoff of the Var river, as a source of low salinity, obtained from a 5-years-long average (2008–2012) of daily runoff values provided by the French Hydro database. In this thesis we focus on the discharges of both the Var and Roya rivers, the latter is not included

in the model and we will therefore exploit the use of satellite data in order to locate its plume.

CMEMS: Copernicus Marine Environment Monitoring Service

In the second half of our work we will use the Copernicus Marine Environment Monitoring Service-Monitoring Forecasting Centre (CMEMS-MED MFC, Clementi et al. (2017); Simoncelli et al. (2014)). The CMEMS system includes seven monitoring and forecasting centers (MFCs) that provide short-term forecasts, hindcasts and reanalysis, it is also a primitive equations model with Boussinesq and hydrostatic approximations. In particular, we will be using the Mediterranean Forecast System (MFC) which is led by Fondazione CMCC - Euro Mediterranean Center on Climate Change (CMCC, IT). The CMEMS-MED MFC has a a resolution of $\sim$4.5 km, with 72 unevenly spaced vertical z-levels and a 6-hourly surface forcing from the European Centre for Medium-Range Weather Forecasts (ECMWF). The outputs are hourly, but we will only retrieve values every 3 hours, so to have the same data as the WMOP.
In the z-level vertical coordinate system, the vertical coordinate is depth. It is the simplest system and it is particularly effective in areas of constant bathymetry. Indeed, the 72 levels can be distributed unevenly in order to give more resolution to the layer of interest. Issues arise in areas of sloping bathymetry, where the layers intersect the sea bottom and can yield unrealistic velocities (Evan et al. (2019)).
Moreover, in the CMEMS-MED MFC model, river runoff is provided from the Global Runoff Data Centre archive, which does not include the runoff of neither Var nor Roya. The system's domain covers the entire Mediterranean as well as part of the Atlantic Ocean, but for juxtaposition purposes we cut the domain in order to match that of the WMOP.
We will be running the particles simulations with both models, showing the results and ultimately comparing the models outputs.

2.3 Lagrangian trajectory models

To simulate the trajectories of plastic particles, we generate the particles using OceanParcels: a set of Python classes and methods developed to create customisable particle tracking simulations using outputs from Ocean Circulation models (developed by van Sebille et al. (2019)). The particles are seeded starting form the 3rd of October 2020 to the 7th of October 2020; we initialise multiple sets, containing 1000 particles each, that start in sequence with a 3-hour gap. Overall, 60000 particles are launched from the rivers plumes, 30000 from each one, and we follow their trajectories up until the 30th of November 2020. Since we are simulating floating micro-plastics, the trajectories are generated following surface currents simulations from the WMOP and CMEMS-MED MFC models and are therefore bound to the surface as well. Their path is driven by advection and diffusion, which are implemented in sequence, every 30 minutes.

In more detail, advection from Oceanic General Circulation Models (OGCM) is executed using fourth-order Runge-Kutta integration; the advection kernel provided by OceanParcels has been modified in order to account for beaching. Each time an advected particle ends up on land, or its velocity is $\leq 10^{-14}$, then it is considered beached and its position is saved. After advection, a simple 2-dimensional diffusion is applied to the particles, the diffusivity is assumed uniform and the value implemented is equal to 50 m^2/s. After the particles have been diffused, their position is again tested for beaching. At the end of each simulation we therefore find how many particles have left the domain of the model, have remained on water, or have ended up on land.
We want to note that the choice of 50 m^2/s for diffusivity was made by producing differently diffused simulations and by comparison with different outputs in literature, the former will not be shown here as they are beyond the scope of this Thesis. Common values of diffusivity are usually derived from the relationship experimentally determined by Okubo (1971):

$$K_{cgs} = 0.0103 l^{1.15} \tag{2.8}$$

Where K_{cgs} is our diffusivity input in cm^2/s and l is the horizontal scale in cm. In our case, given that the horizontal scale is ∼2000 meters for WMOP and ∼4500 meters for CMEMS-MED MFC, the diffusivity K would be ∼1.29 m^2/s and ∼3.27 m^2/s, respectively. Nonetheless, using these values yields unrealistic simulations; as noted by (Brouwer et al. (2018)), higher values of diffusivity are a better fit and more accurate when compared to observational data.

Chapter 3

Lagrangian simulations from WMOP surface currents

In this Section we will show the results obtained while conducting our particles simulations with data from the WMOP model. We will analyse the positions of plastic material in the four different simulations of study.
Given that we initialise our experiment on the 3rd of October 2020, which is the last day of Storm Alex in our area of study, we display here the four different current outputs on this day at T00:00, from the WMOP model. We want to remind the reader that in these figures, and throughout this Thesis, the bars of magnitude in the graphs are sometimes different for the sake of readability.
In Figure 3.1 we see the total currents from the WMOP model: the currents show a number of eddies of different scales, and we also see that the NC is highly disturbed as it is almost imperceptible at this time, due to the storm still raging. In fact, the whole WMED domain shown here, is characterised by turbulence and the presence of small scale variability. Keeping the total currents of Figure 3.1 as a reference, we can compare the other WMOP currents to see the main differences. In Figure 3.2 we see the mean of the WMOP total currents, obtained for the 60 days of study; here the NC is evident and it stays relatively strong as it crosses the Gulf of Lion and reaches the longitude 3°E, where it meets a gyre above the Mallorca island and then dissipates. The rest of the WMED circulation is coherent with the literature (explained in Section 1.1) and we can therefore see that, after the storm, the sea surface circulation somewhat stabilised in the two months of the experiment. The spatially filtered currents are shown in Figure 3.3; here we can already foresee the effect of the low-pass filter on the total currents. The currents are smoothed out and we loose the smallest scale features that we see in the total currents. The overall shape of the patterns follows that of the total currents, but with less turbulence. In the geostrophic case (Figure 3.4), we note that the currents are weaker but overall follow the same large structures of the total currents, but they do not contain the currents due to the wind associated with the storm, especially in the area near Var and Roya. Furthermore, we have an enduring area of low speed just Southern of the Northern current, which is not present in the total currents.

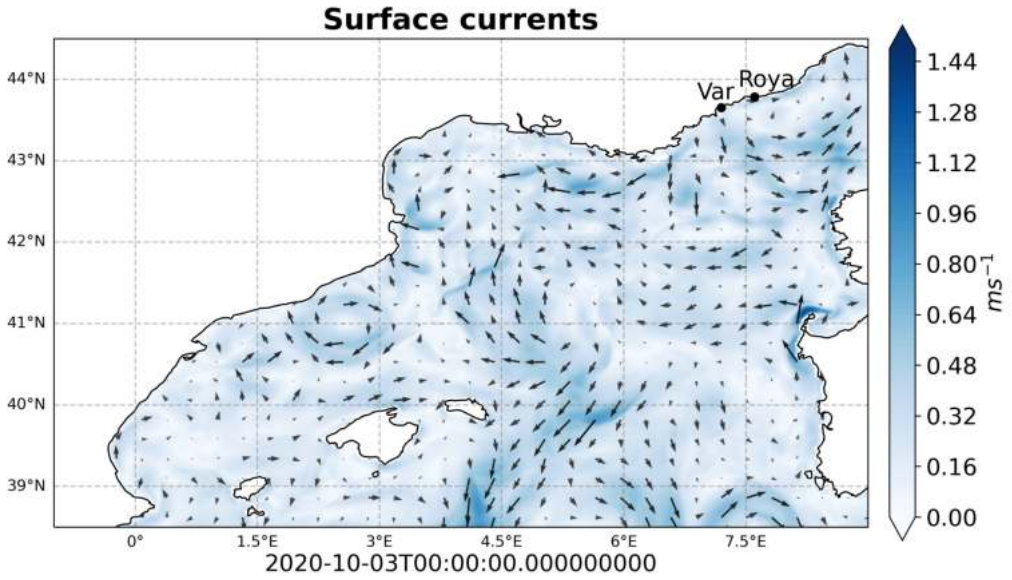

Figure 3.1: WMOP total currents simulation on the **3rd of October 2020, at T00:00**.

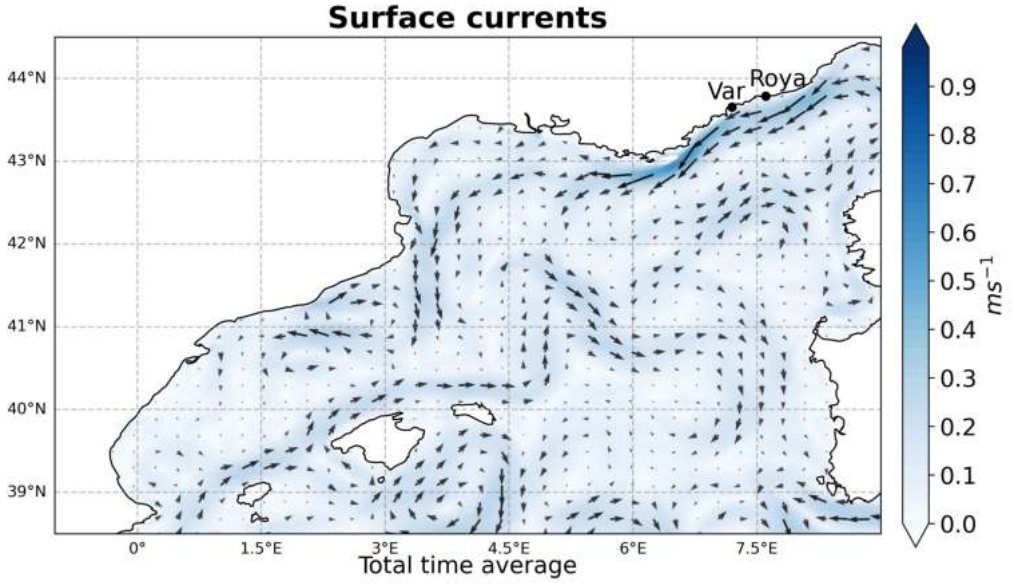

Figure 3.2: WMOP mean current simulation.

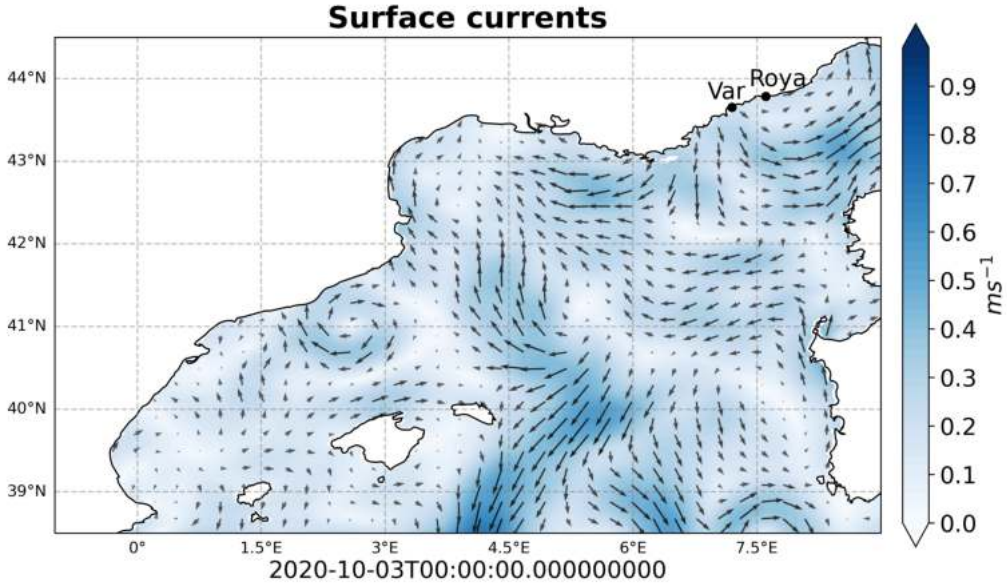

Figure 3.3: WMOP spatially filtered currents simulation on the **3rd of October 2020, at T00:00**.

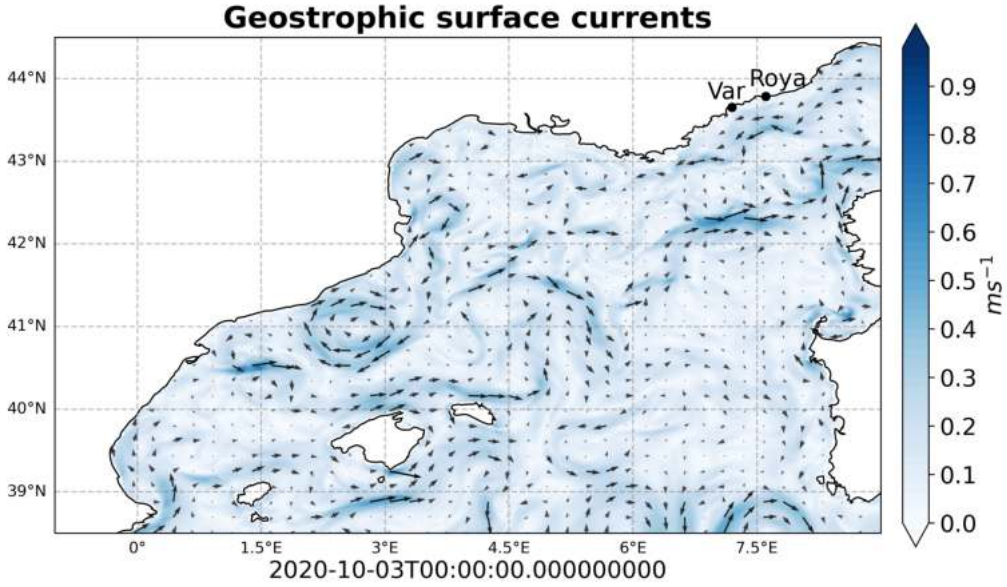

Figure 3.4: WMOP Geostrophic currents simulation on the **3rd of October 2020, at T00:00**.

In this work, we are evaluating the role of small scale turbulence in dispersing material in the WMED. To display a first and general view of the energy involved we show a kinetic energy map. We want to see the Eddy Kinetic Energy (EKE) of our period of study, as reproduced by the WMOP model. The method to compute the EKE was to first subtract the mean current output from the total currents outputs in order to obtain only the turbulence contribution. We computed the kinetic energy with the formula:

$$EKE = \frac{u^2 + v^2}{2} m^2/s^2$$

where u and v are the zonal and meridional velocities. Then, we averaged the EKE

over the whole period of study (60 days). The EKE map, for the WMOP model, is shown in Figure 3.5. We see that the NC shows various spots of higher energy, which are also present in the Gulf of Lion, beyond the 1000 m and 200 m bathymetry lines. We also see peaks of energy in the centre of the domain. Especially, a peak of EKE is noticeable at $\sim$ 3°E, 41.5°N, which corresponds to the position of a large eddy we observe throughout our experiment, and which was already visible in the currents maps shown above (Figures 3.1, 3.2, 3.3, 3.4).

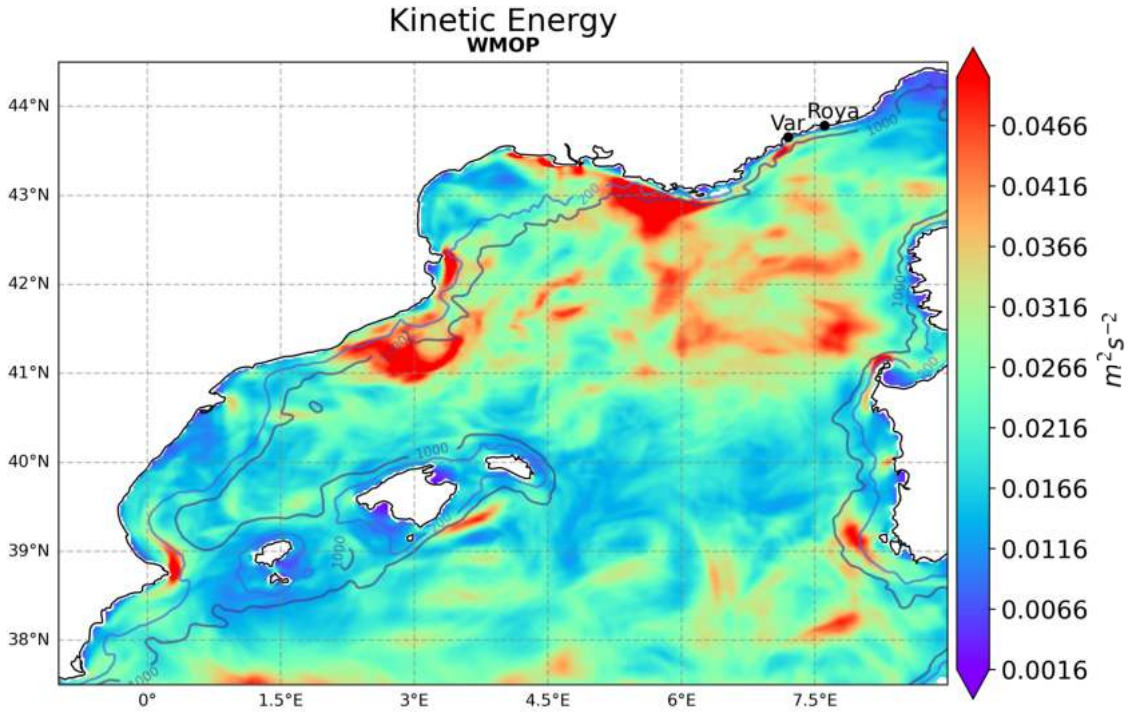

Figure 3.5: WMOP: Mean Eddy Kinetic Energy

3.1 Determining the initial positions

The positioning of the particles near the mouths of rivers Var and Roya has to be cautiously determined, in order to best represent positions in the river plumes on the 3rd of Ocotober and to be consistent with the model's land-sea mask. This is done by exploiting satellite images from the day in question, as well as model outputs. We want the particles to start their trajectories inside the plumes of the rivers, so to ensure that the simulation will be mirroring the spillage from the rivers discharge, and its consequent path. From the Sentinel Hub engine for processing satellite data (Sentinel Hub (2020a)), we obtained the image of Figure 3.6 where we can see the plumes of the rivers on the 3rd of October 2020. These plumes have an extension of a few kilometers: for Var, the plume extends $\sim$5 km from the mouth of the river and $\sim$4 km from the coast; Roya's plume is bigger, reaching up to $\sim$8 km from the mouth and $\sim$3 km from the coast. The rivers mouths are

located at, roughly, a latitude and longitude of (43.654°N, 7.199°E) for Var and (43.787°N, 7.606°E) for Roya. Using this image, we want to initialise our particles at a latitude and longitude of (43.609908°N, 7.205821°E) for Var and (43.749174°N, 7.693657°E) for Roya. To ensure that these positions are coherent with the model's land-sea mask, we examine a sea surface salinity map, shown in Figure 3.7. In the salinity map are shown the initial positions of the particles and the positions of the mouths of the rivers; by comparing this map with the satellite image we can deduce that the particles initial positions are reasonable. In fact, the Var particles are placed between the two smaller plumes branching out from near shore, which are observable in both the satellite image and the salinity map. On the other hand, the Roya particles are located to the right of the river's mouth, in order to follow the initial direction of the plume. To position the particles for the Roya river, we make extensive use of the satellite image, given that the WMOP model does not contain the river discharge coming from Roya.

Figure 3.6: False colour satellite image of the Var and Roya rivers plumes on the **3rd of October 2020**. The image is based on bands 8,4,3. (Borrowed from Sentinel Hub (2020a))

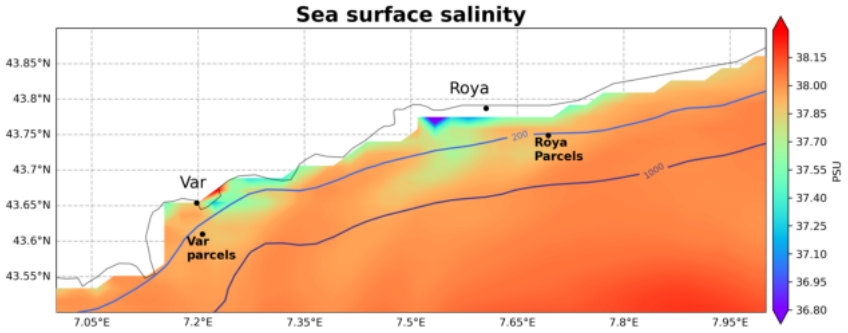

Figure 3.7: WMOP sea surface salinity on the **3rd of October 2020, at T00:00**.

Since the WMOP model has a spatial resolution of 2km, the simulation cannot start too close to the coast; moreover, to avoid that the particles will end up on land in the immediate start of the simulation, we look at a zoom of the total surface currents close to the coast and the winds blowing during the storm. In Figure 3.8 we can see the surface currents in the first time step of the 3rd of October output,

when we intend to start our particles simulation. We can see that the currents are directed Eastward and slightly Southward along the coast. Furthermore, we can see that the NC is undetectable at this time and the currents are significantly affected by the high winds, due to the storm still occurring.

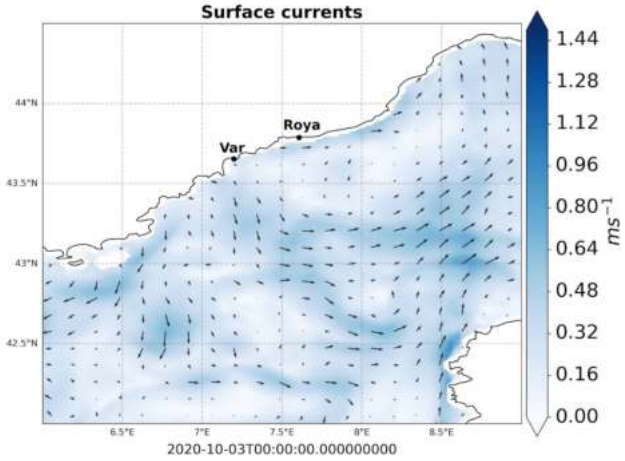

Figure 3.8: WMOP surface currents map on the **3rd of October 2020, at T00:00**.

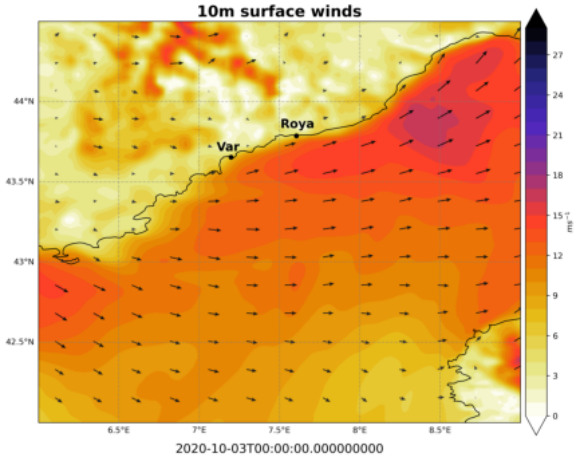

Figure 3.9: 10m wind currents simulation on the **3rd of October 2020, at T00:00**, produced from data from the Spanish Meteorological Agency model, which is used to force the WMOP model.

To better understand this unusual currents pattern, we show the 10 meter wind map on the 3rd of October 2020 at T00:00 in Figure 3.9. From this map we can see that the winds, blowing North-Eastwards, are overall consistent with the model sea surface currents. As we know, the Mediterranean Northern Current flows Westward along the coast of Liguria, Provence and Catalonia. Its interaction with winds directed the opposite way (Figure 3.9) causes a surface current directed, overall, South-Eastwards. We can therefore place the particles inside the plumes and near to the coast, as it was shown in Figure 3.7, with a dispersion of 500 meters from the specified latitudes and longitudes.

3.2 Particles dispersion

3.2.1 Using WMOP total currents

In this Section, we look at the particles simulation obtained with the WMOP total sea surface currents. In the following figures we can see various time steps of the particles simulation, produced with standard 3-hourly currents simulations from the WMOP. In the first half of October (in Figure 3.10 we can see the first day) some of the particles move towards the South-East, exiting the domain of the simulation and reaching Sardinia. In the second half of October (Figure 3.11), the Northern Current regains its strength and the particles are funneled towards the West, following along the coast of France. In November (Figures 3.12 and 3.13), a number of eddies perturb the main circulation, causing the particles to move off-shore, and disperse away from the Northern Current.

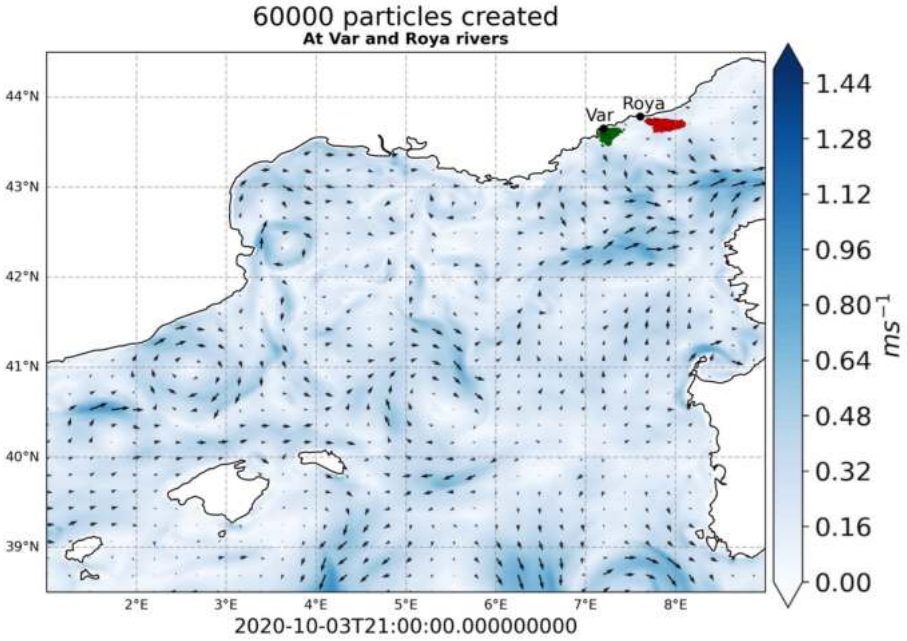

Figure 3.10: WMOP total currents particles simulation on the **3rd of October 2020 at T21:00**. Red: particles from river Roya. Green: particles from river Var.

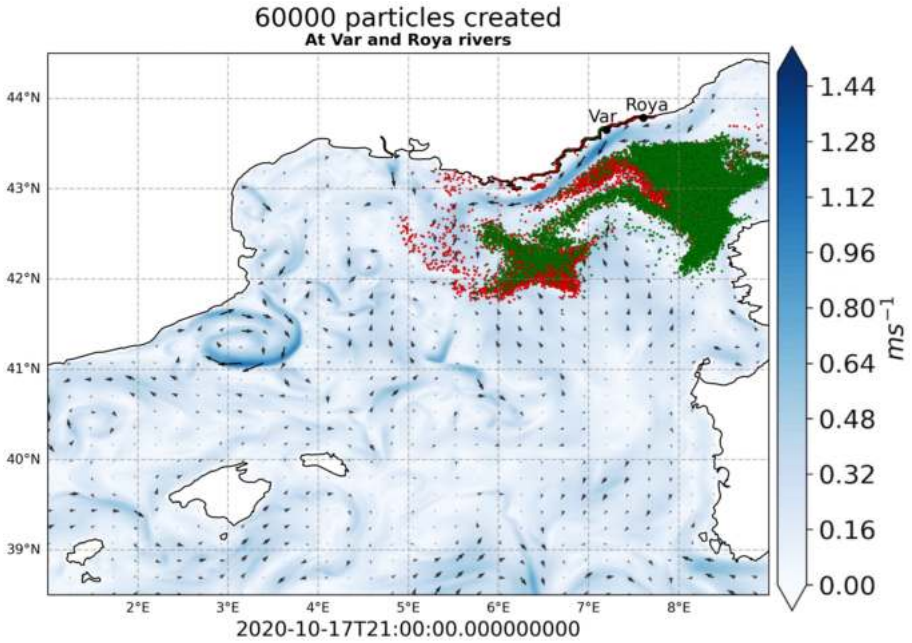

Figure 3.11: WMOP total currents particles simulation on the **17th of October 2020 at T21:00**. Red: particles from river Roya. Green: particles from river Var.

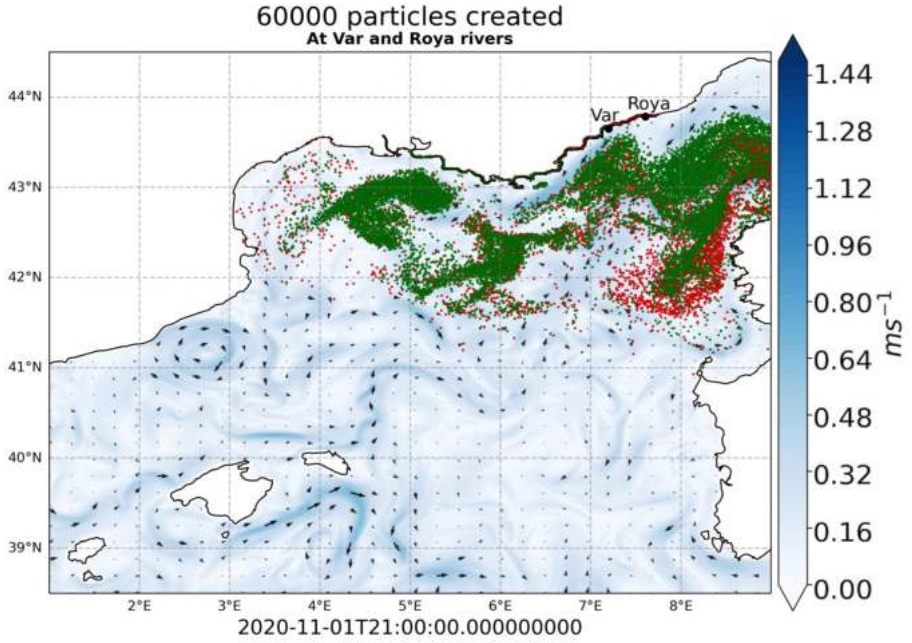

Figure 3.12: WMOP total currents particles simulation on the **1st of November 2020 at T21:00**. Red: particles from river Roya. Green: particles from river Var.

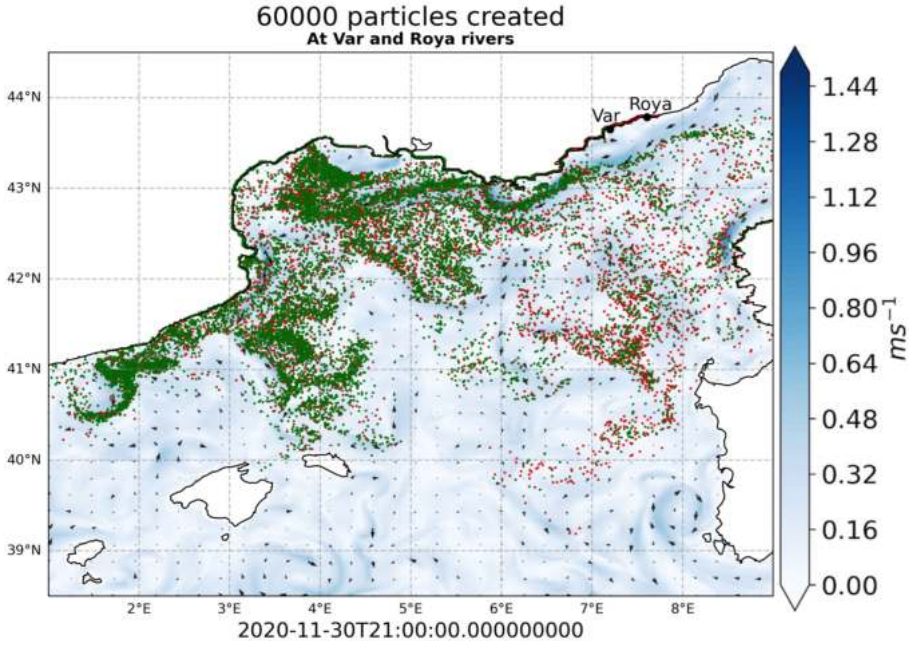

Figure 3.13: WMOP total currents particles simulation on the **30th of November 2020 at T21:00**, the last time step. Red: particles from river Roya. Green: particles from river Var.

In Figure 3.13 we can see the final image of the simulation: the particles dispersed into the domain and the presence of eddies and NC meanders is noticeable. For instance, the eddy present at $\sim$ 1.5°E, 41.5°N had a noteworthy impact in trapping the material flowing Southwards. The total currents include the main features of the WMED circulation, such as the NC, the wind driven wind due to the Mistral and Tramontane winds, which blow from the northwest and cause turbulence and interfere with the NC. Multiple eddies appear and dissipate during the simulation run, and this is shown in the propagation of plastic and its final position on the last day of the simulation.

3.2.2 Using WMOP mean current

The first step we take, in order to examine the importance of transient features, is to filter them out by averaging temporally. By producing a time average of our currents, we are fundamentally excluding any perturbation that lasts less than 60 days. What we obtain is one current output that resembles the mean circulation of the North Western Mediterranean. The particles are then initialised and moved following this single current field, as we previously did with the total currents. In the next figures we can see different time steps of the particles simulation, the same we have observed in the previous case. We note a substantial difference: first of all, as it can be seen in Figure 3.15, the particles move really fast towards the Gulf of Lion. They do so, while staying close to the coast with rather low dispersion. By the 1st of November (Figure 3.16) they are already much more South-East than what we saw in the total currents simulation.

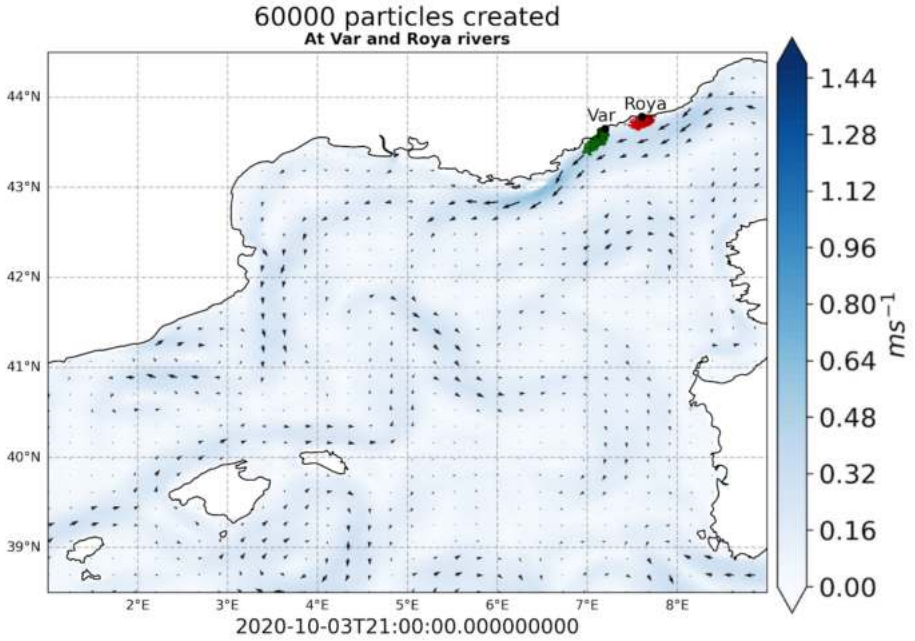

Figure 3.14: WMOP mean current particles simulation on the **3rd of October 2020 at T21:00**. Red: particles from river Roya. Green: particles from river Var.

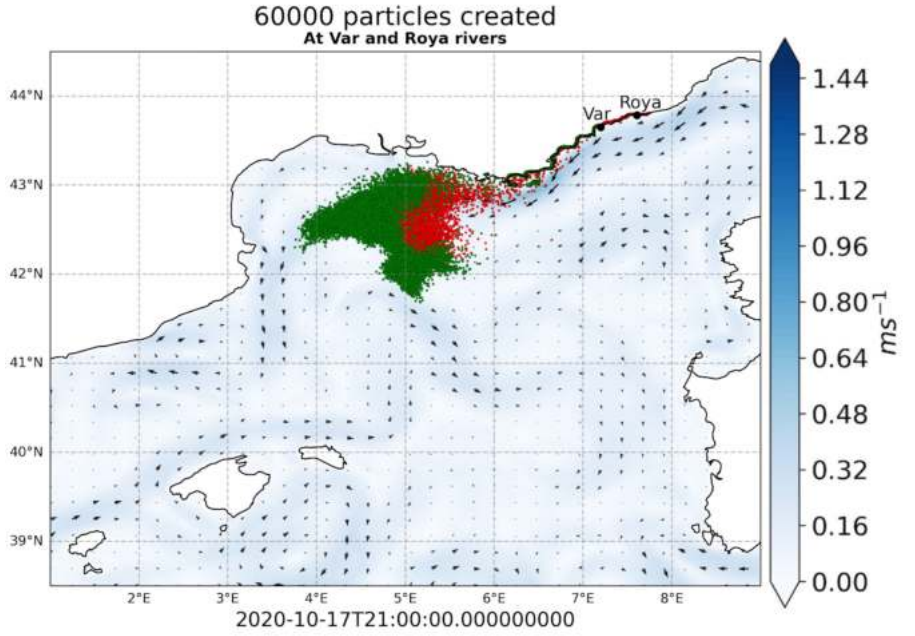

Figure 3.15: WMOP mean current particles simulation on the **17th of October 2020 at T21:00**. Red: particles from river Roya. Green: particles from river Var.

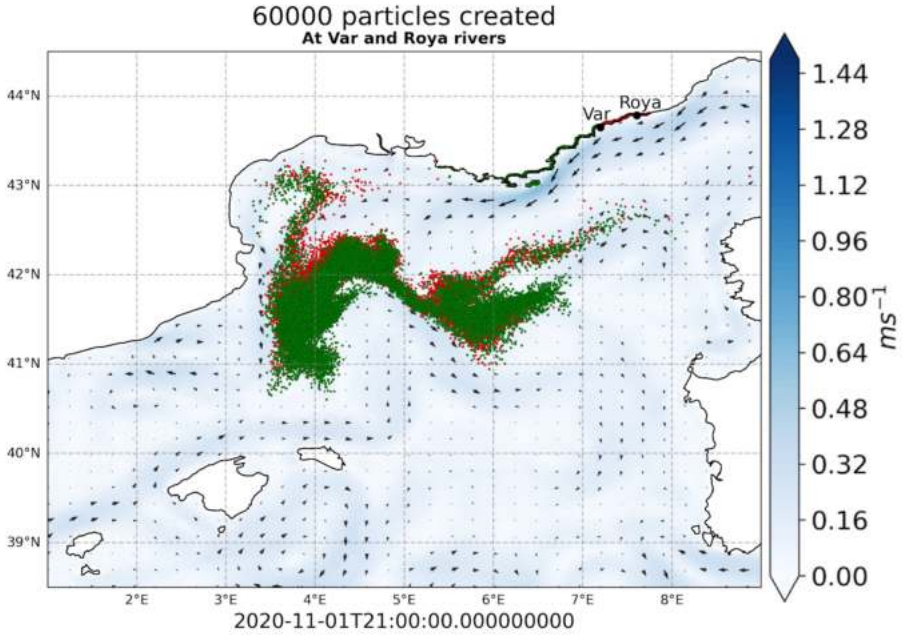

Figure 3.16: WMOP mean current particles simulation on the **1st of November 2020 at T21:00**. Red: particles from river Roya. Green: particles from river Var.

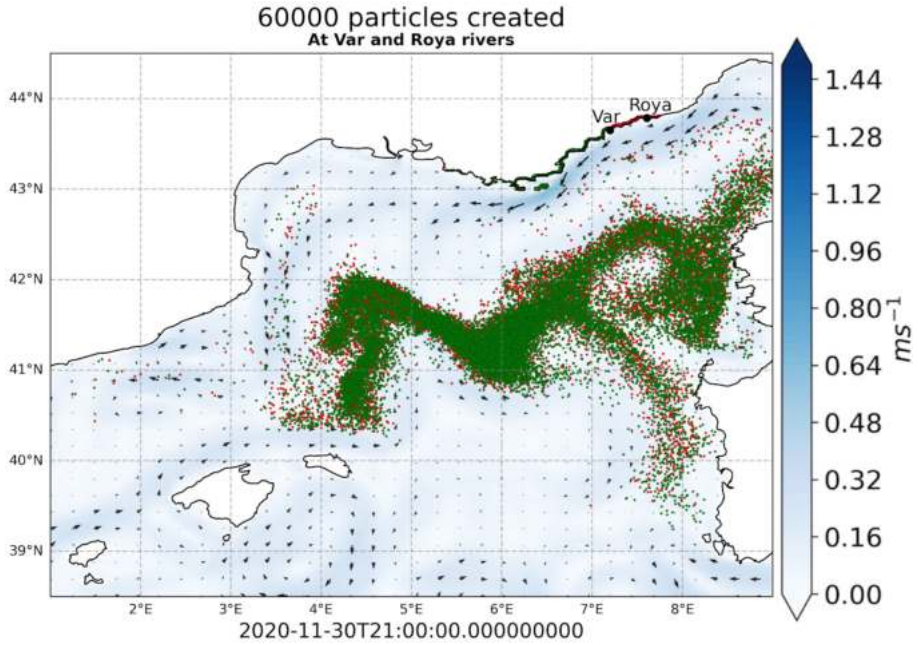

Figure 3.17: WMOP mean current particles simulation on the **30th of November 2020 at T21:00**, the last time step. Red: particles from river Roya. Green: particles from river Var.

In the last time step, shown in Figure 3.17, we can see that the particles moved compactly, with less dispersion and diffused movement than we previously observed. Particles return Eastwards towards Corsica and Sardinia Islands, following the Southern branch of the cyclonic circulation of the North-Western Mediterranean Sea. Without all the short lived eddies the particles are funneled along the main

streams.
Producing this simulation helps us obtaining a first insight into the impact of transient oceanic features on the plastic dispersion; the mean current field drives the particles paths as if no turbulence was present. We can see how much more close-packed they stay, meaning that, with a fore-look into practical applications as well, without turbulence it would be much easier to track them in real life and to possibly contain the polluting effect.

3.2.3 Using WMOP spatially filtered currents

To identify and subtract features with small spatial dimensions, while retaining the largest eddies, we make use of spatial filtering. To identify the filtering scales, we first need to identify the scale and extent of the meanders of the Northern Current near the rivers mouths. To do so, we examine a high resolution Sea Surface Height (SSH) map (3-hourly outputs) using Sea Level Anomaly data from the WMOP model. In Figures 3.18, 3.19 we show, as an example, two SSH contour plots from the 3rd of October 2020 T15:00 and the 6th of October 2020 T06:00. Here we can see that the SSH variations from the average sea level are of the order of tens of centimeters, reaching absolute values as big as 40 centimeters. This kind of meanders are the ones we are interested in removing.

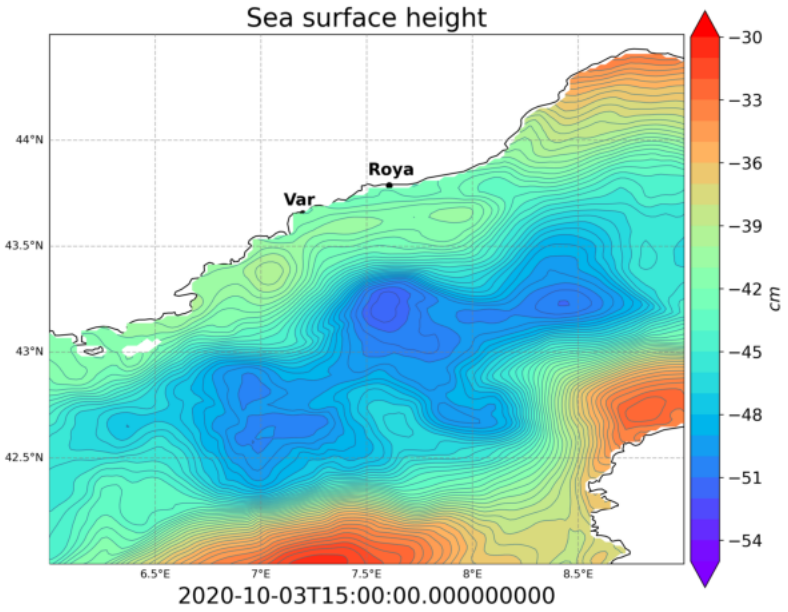

Figure 3.18: WMOP SSH map on the **3rd of October 2020 at T15:00**.

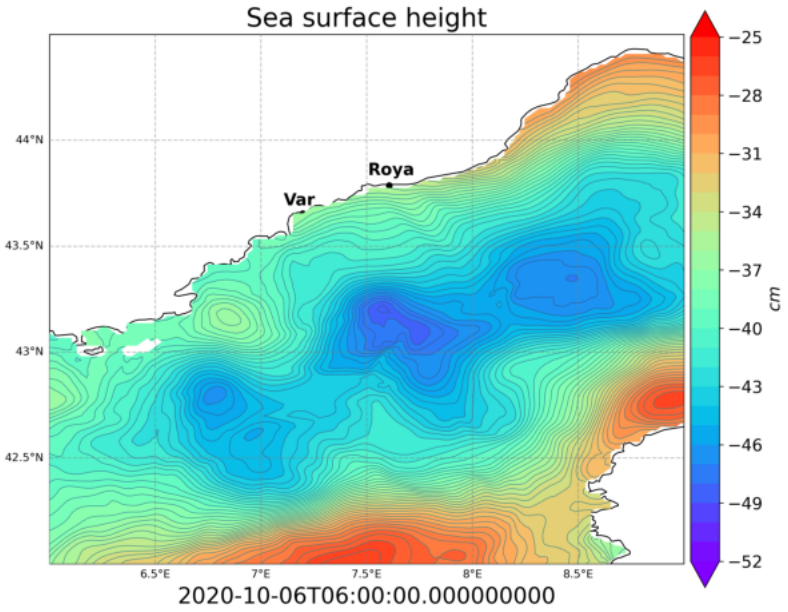

Figure 3.19: WMOP SSH map on the **6th of October 2020 at T06:00**.

Knowing that 1 degree of latitude covers about 111 kilometers, we find that the spatial extent of these coastal meanders is circa 50 km or less. With this information, and after having produced multiple simulations with different spatial filters, we decided to apply a 50 km moving average spatial filter. The computation consists of producing a 50 km centered rolling average that is applied to each point of the total currents, these outputs are then used to run the particles simulation. Again, we show the particles simulation for both rivers at different time steps. In this simulation the Northern Current magnitude is similar to that of the mean current case, the particles flow towards the South-East in a compact manner, but they are dispersed by large scale eddies, which were not present in the mean current simulation and that were dominated by small scale features in the total currents case. As more evident in Figure 3.23, compared to the total currents simulation, here the particles do not reach as far South-East, they divide in patches and move towards Catalonia, Corsica and Sardinia. We see that the central part of the domain is left quite untouched, especially in comparison with the mean current simulation. This reveals the role of small scale eddies, which seem to be driving the main dispersion of particles into the broad domain of study.
Furthermore, compared with the mean currents, the spatially filtered currents are much more dispersive; here, in the first week of the simulation the particles are pushed off-shore, whereas the mean currents where channelling them along the Northern Current. Large-scale perturbations in the WMED circulation, such as those due to strong and extended wind gusts, are still present after the spatial filter and cause dispersion away from the counterclockwise circulation of the WMED.

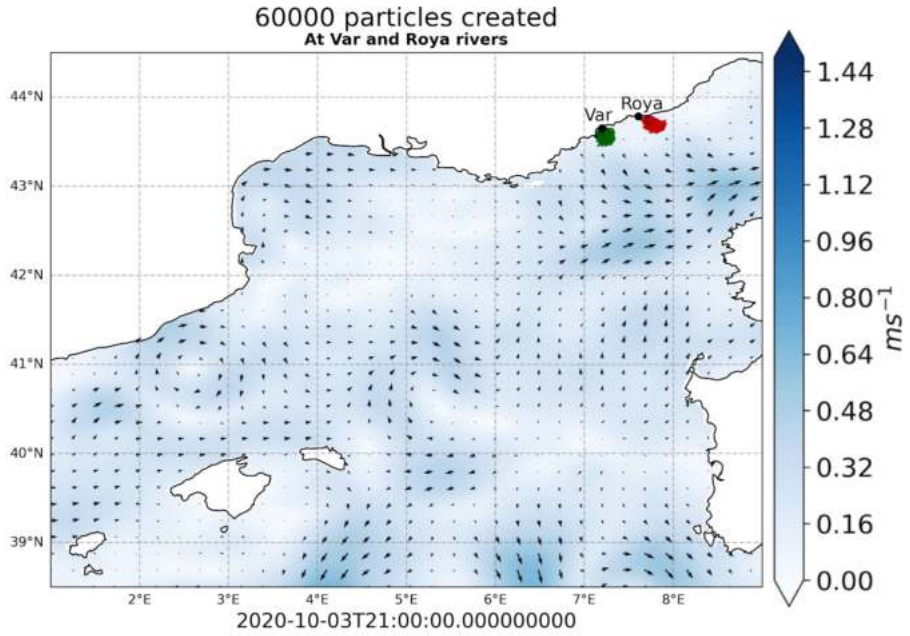

Figure 3.20: WMOP 50km spatially filtered particles simulation on the **3rd of October 2020 at T21:00**. Red: particles from river Roya. Green: particles from river Var.

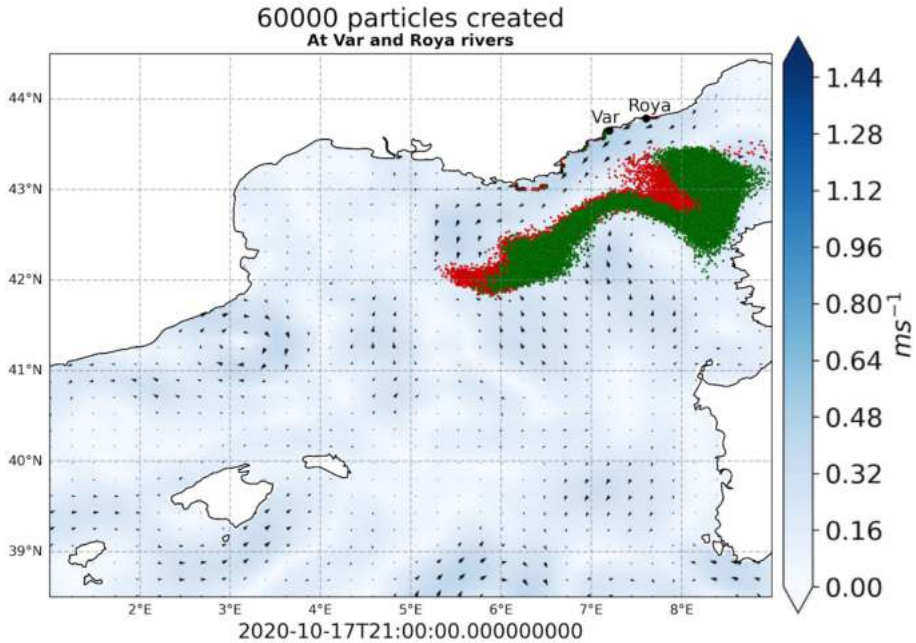

Figure 3.21: WMOP 50km spatially filtered particles simulation on the **17th of October 2020 at T21:00**. Red: particles from river Roya. Green: particles from river Var.

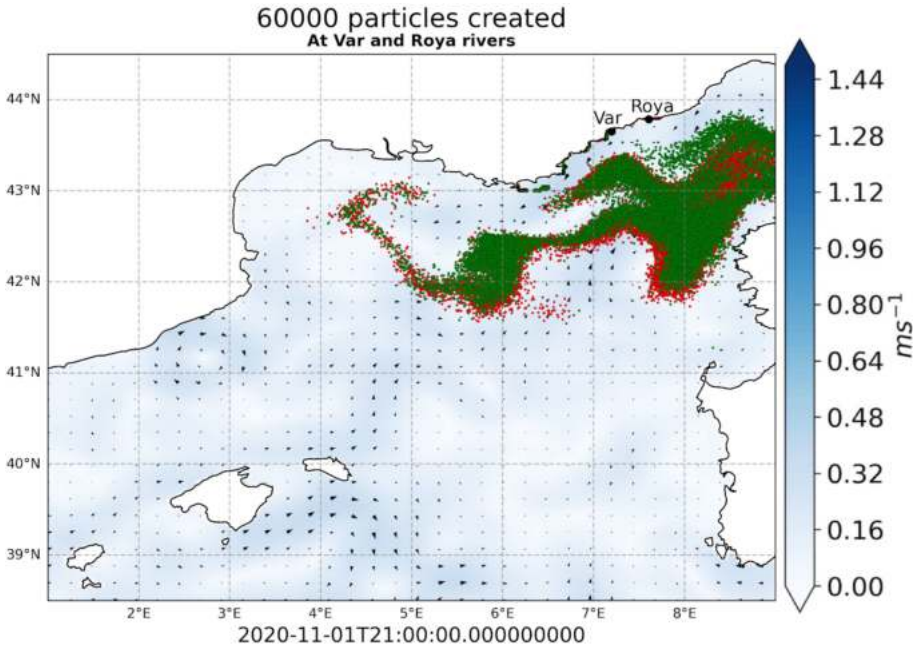

Figure 3.22: WMOP 50km spatially filtered particles simulation on the **1st of November 2020 at T21:00**. Red: particles from river Roya. Green: particles from river Var.

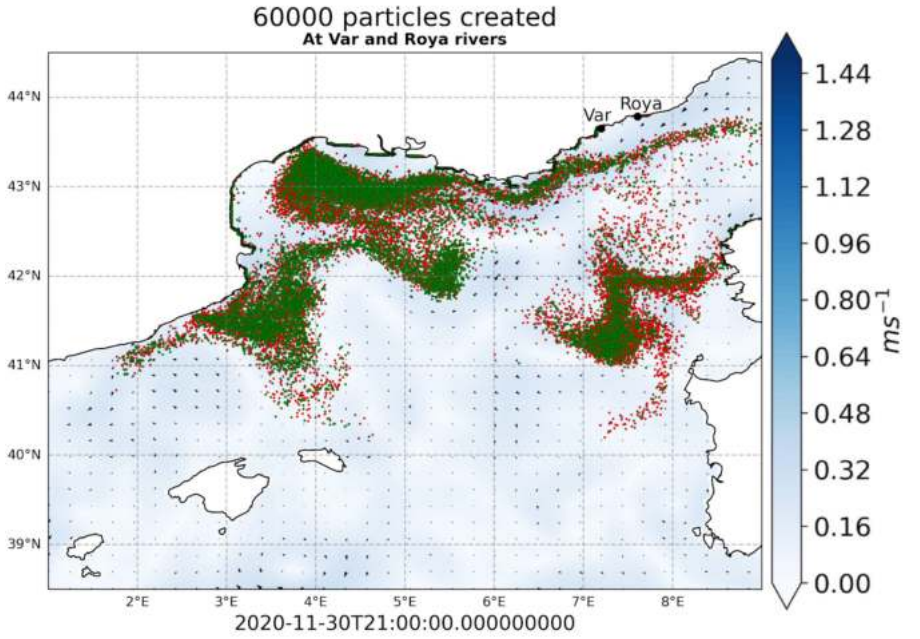

Figure 3.23: WMOP 50km spatially filtered particles simulation on the **30th of November 2020 at T21:00**, the last time step. Red: particles from river Roya. Green: particles from river Var.

3.2.4 Using WMOP Geostrophic currents

Studying the geostrophic field of the ocean permits us to observe the large scale patterns of oceanic circulation. Geostrophic currents are due to the balance of the

horizontal pressure gradient and the Coriolis force; as we know, water flows from regions of high pressure towards regions of lower pressure. At the same time, the Coriolis force deflects the motion towards the right (left) in the Northern Hemisphere (Southern). In the Northern Hemisphere, the result of this balance is a current that propagates perpendicularly with respect to the pressure gradient and Coriolis force, such that high pressure is to the right of the current's direction. In the Northern Hemisphere (Southern) anticyclonic eddies rotate around centres of high pressure (low), whereas cyclonic eddies rotate around centres of low pressure (high). Deviations from geostrophy, especially at the surface, are usually due to wind stress effects which interfere with the balance.
In particular, the NC is usually in geostrophical balance and directed South-Westwards, when no strong wind events are present. When such events occur, ageostrophy can become important and the response is directly linked to wind-induced stress. As described by Berta et al. (2018), strong westerly wind events, such as Storm Alex, can perturb the normal NC flow and weaken the zonal geostrophic transport by up to 40-50 %.
The Rossby Radius of Deformation indicates the length scale at which the water flow along the pressure gradient will be deformed by the Coriolis force, in other words the length at which geostrophy is predominant. It is defined as the horizontal length scale at which the Coriolis effect and the pressure gradient force balance each other. In the Mediterrenean, the Rossby radius is around 15 km, much smaller than the basin's scale and therefore we have that geostrophic currents are a good representation of the circulation of the Mediterranean. Furthermore, the direction of geostrophic currents teaches us about the direction of the prevailing winds, since they are the main forcing for surface pressure gradients.
At the sea surface, the geostrophic velocities are computed with the equations (Gill (1982)):

$$\begin{aligned} v &= \frac{g}{f}\frac{\partial \eta}{\partial x} \\ u &= -\frac{g}{f}\frac{\partial \eta}{\partial y} \end{aligned} \tag{3.1}$$

Where η is the sea surface height (SSH) obtained from the WMOP model; f is the Coriolis parameter, considered as constant, calculated for the average latitude of the domain; g is the gravitational acceleration = 9.81 m/s^2; x and y are the longitude and latitude; v and u are, respectively, the meridional and zonal velocities, i.e. the total currents from the WMOP model.

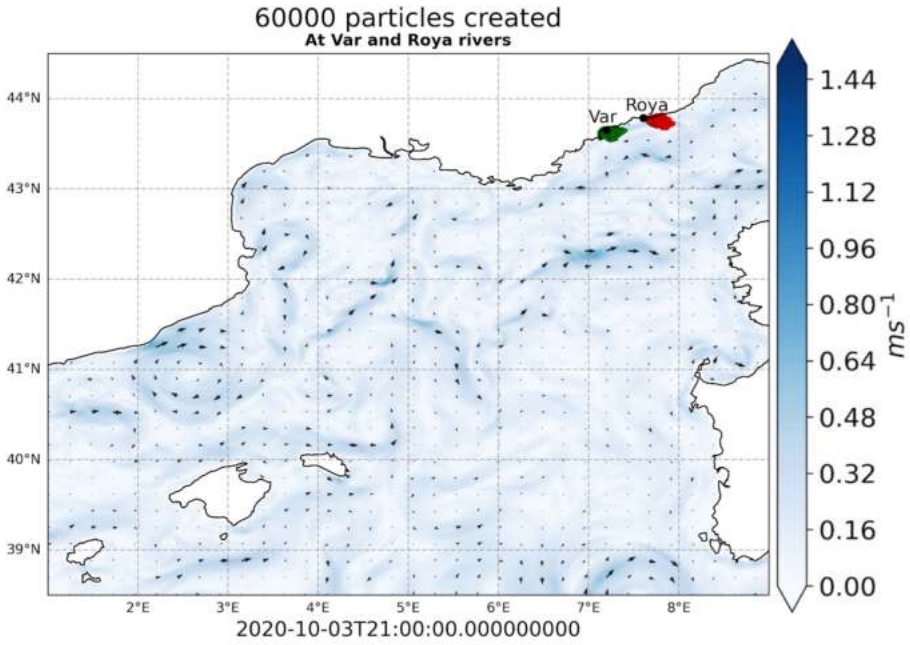

Figure 3.24: WMOP geostrophic currents particles simulation on the **3rd of October 2020 at T21:00**. Red: particles from river Roya. Green: particles from river Var.

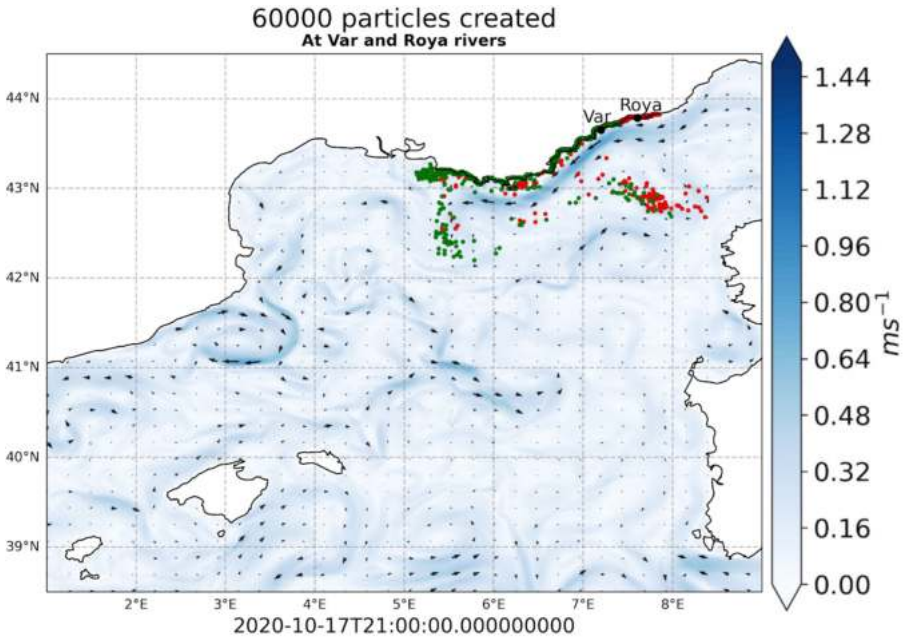

Figure 3.25: WMOP geostrophic currents particles simulation on the **17th of October 2020 at T21:00**. Red: particles from river Roya. Green: particles from river Var.

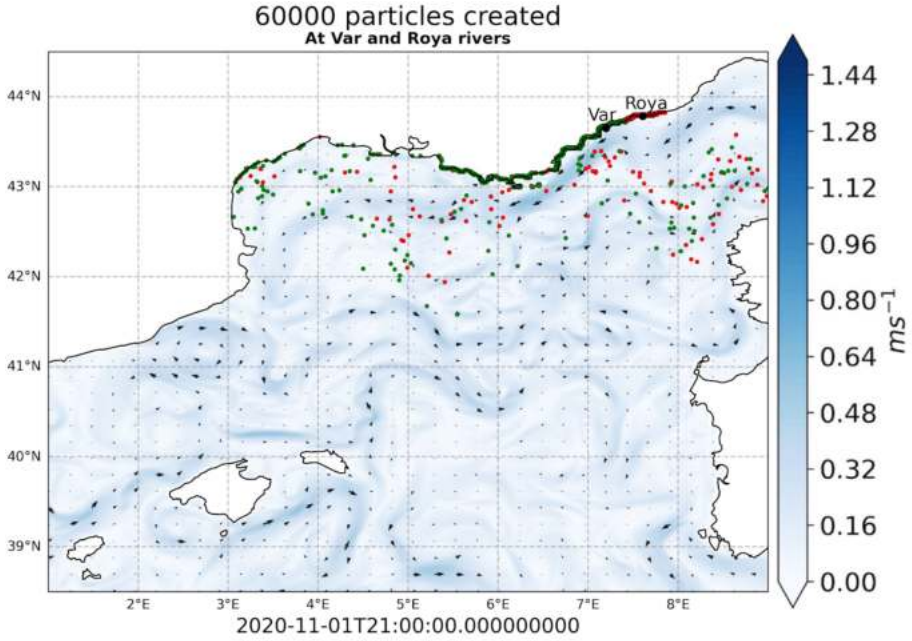

Figure 3.26: WMOP geostrophic currents particles simulation on the **1st of November 2020 at T21:00**. Red: particles from river Roya. Green: particles from river Var.

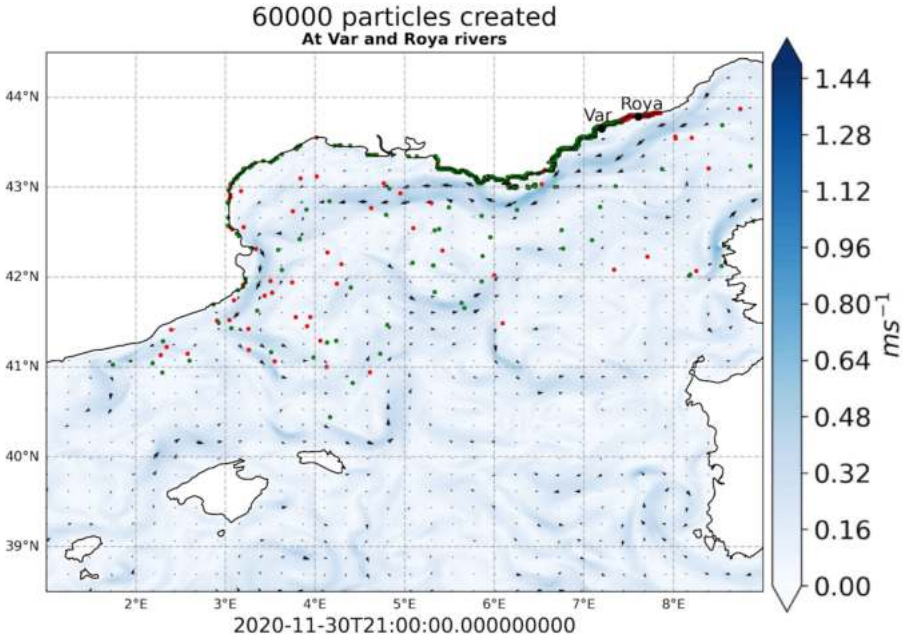

Figure 3.27: WMOP geostrophic currents particles simulation on the **30th of November 2020 at T21:00**, the last time step. Red: particles from river Roya. Green: particles from river Var.

In Figures 3.24, 3.25, 3.26, 3.27, we can see different steps of the simulation, here the particles sizes have been increased for clarity. We can see that an extremely small number of particles stray away from the coast. Small perduring eddies and meanders are weakened (but present), and the particles now closely follow the Northern

Current and a few larger eddies visible in the plots. We can see that at the end of the simulation only a few particles are left on water and most seem to have been beached. This behaviour was already found when using the mean currents, however to a smaller extent. This is due to the fact that particles get trapped between the coast and the main NC vein, with no average offshore current allowing them to enter the NC and disperse off-shore.
In the next Section we will see this in more detail, as we will study the final positions of the particles for all of our cases.

3.3 Analysis of final positions

In this work, we are especially interested in the polluting impact of the storm, and in particular in the extent of the transboundary transport and pollution[1]. We look here for how many particles have ended up on land and where they did so, as well as how many particles have ended up out of domain or stayed in the water, and how many have crossed the 200 m isobath.
In this Section we present the results of the final positions of the particles, obtained from the different simulations. A total of 60000 particles where initialised in each simulation, 30000 from each river. Underneath each map is plotted the average sea surface currents from the two months of simulation, that is the mean current. We also plot the Exclusive Economic Zones (EEZ) underneath each plot, since we are ultimately interested in the transnational impact of the plastic pollution as well. For the sake of clarity and as a reference, we first show the EEZ map in Figure 3.28.

[1]"Transboundary pollution is the pollution that originates in one country but is able to cause damage in another country's environment, by crossing borders through pathways like water or air" (Varkkey (2019))

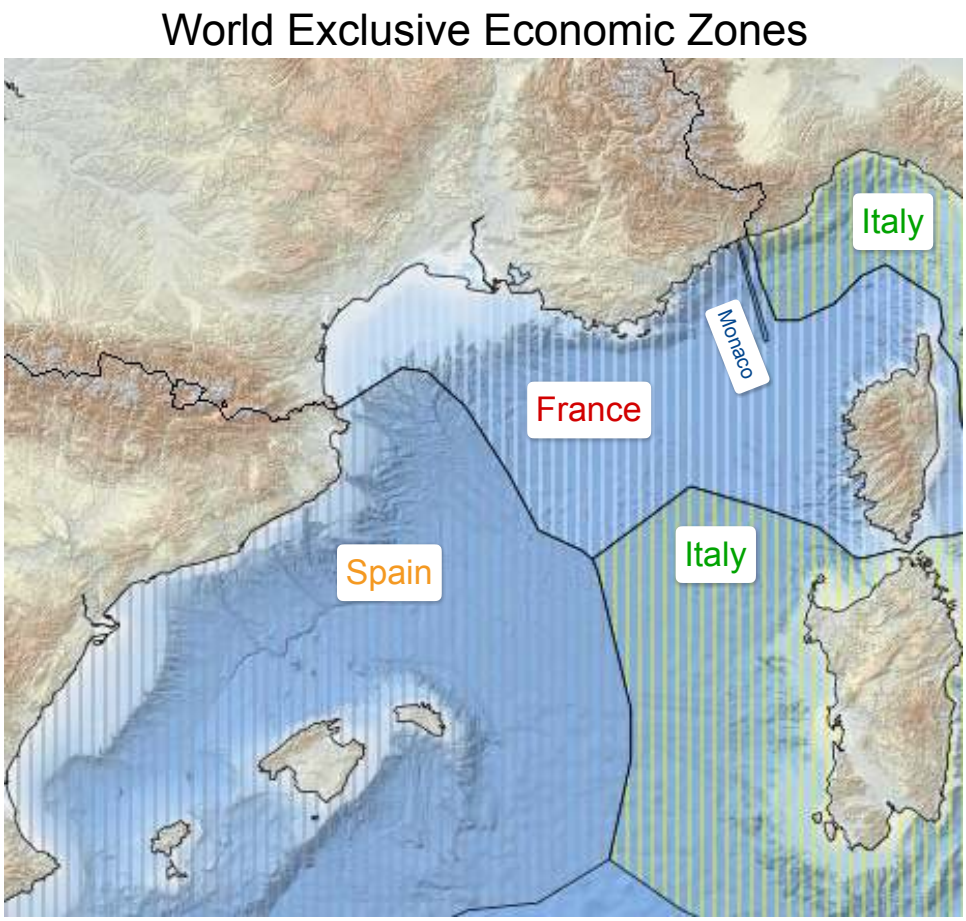

Figure 3.28: Exclusive Economic Zones (EEZ) map. Borrowed from maritime forum (2019).

3.3.1 Beaching

First of all, we are interested in seeing how many particles have been beached. In Figures 3.29, 3.30, 3.31 and 3.32 we can see the density plots of the particles on land, from both rivers; the total currents and the spatially filtered simulations yielded similar results, with a number of 17846 and 11068 beached particles, respectively. On the other hand, more than half of all the particles from the mean current simulation have ended up on land, while for the geostrophic case an astonishing number of 59857 particles have been beached.
Also, in the total currents case, the particles reached the Southernmost areas, all the way to Catalonia, Minorca, Corsica and Sardinia. In all four simulations, the majority of the particles were beached near the mouths of the rivers. In the geostrophic simulation, the particles did not strand far from the coast near the rivers, only 200 landed in Corsica and a few hundreds went beyond the Gulf of Lion.

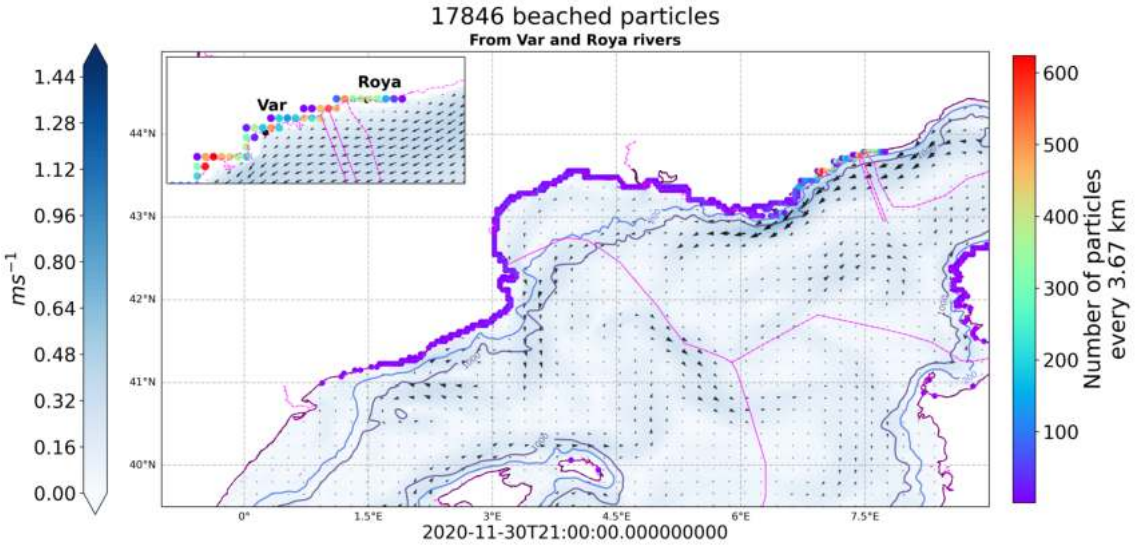

Figure 3.29: 17846 beached particles, from the WMOP total currents particles simulation.

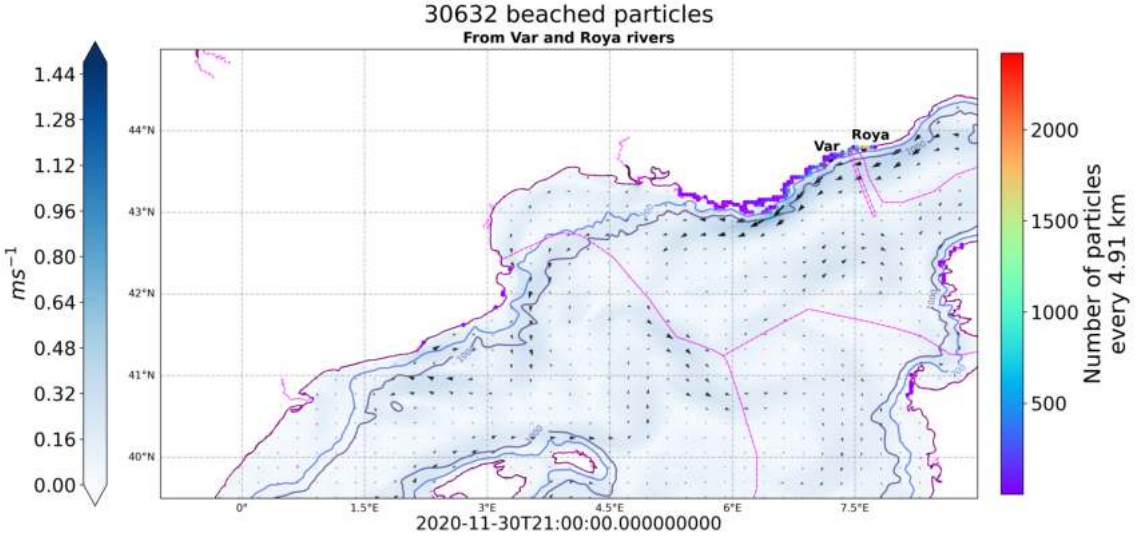

Figure 3.30: 30632 beached particles, from the WMOP mean current particles simulation.

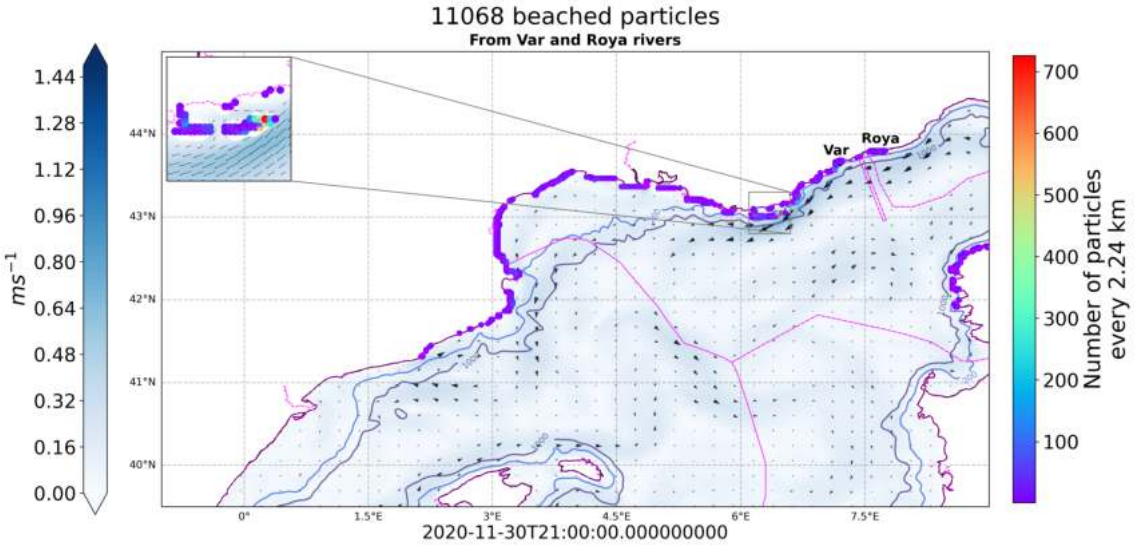

Figure 3.31: 11068 beached particles, from the WMOP spatially filtered currents particles simulation.

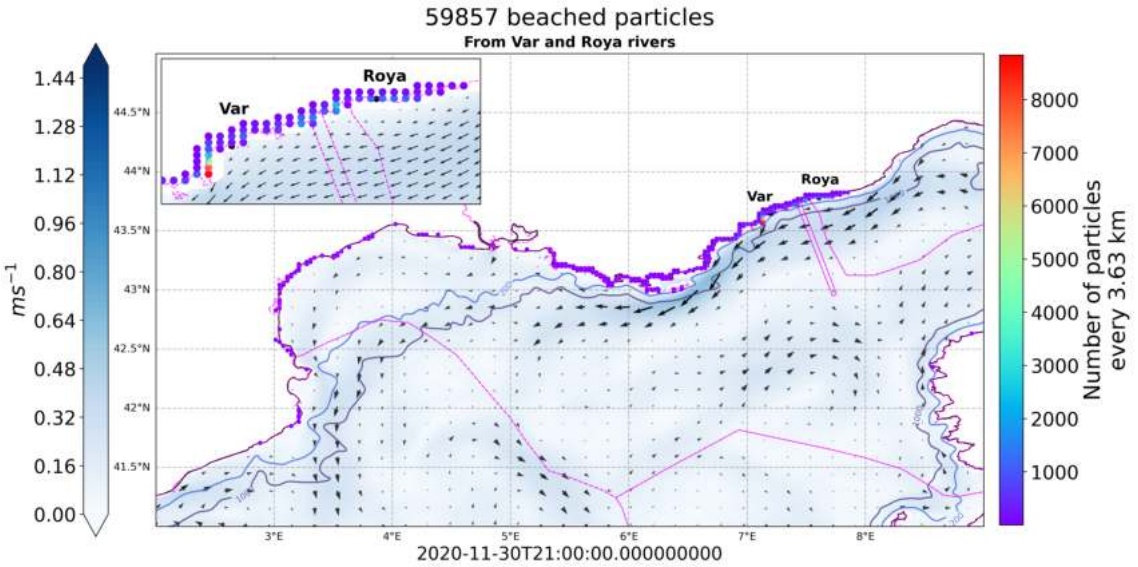

Figure 3.32: 59857 beached particles, from the WMOP geostrophic currents particles simulation.

In Figures 3.33, 3.34, 3.35 and 3.36 we can see that in all cases, particles left the domain of the simulation in the same area between France and Corsica; for the total currents case and the geostrophic case, where in the latter only 47 particles went out of domain, a few crossed between Corsica and Sardinia. We see that in the spatially filtered currents case 21540 particles left the domain and in the mean current case 598. The interesting factor here is that 27400 particles left the domain in the total currents simulation, indicating a counter-current, just Southern of the Northern Current, that pushed the particles North-East.

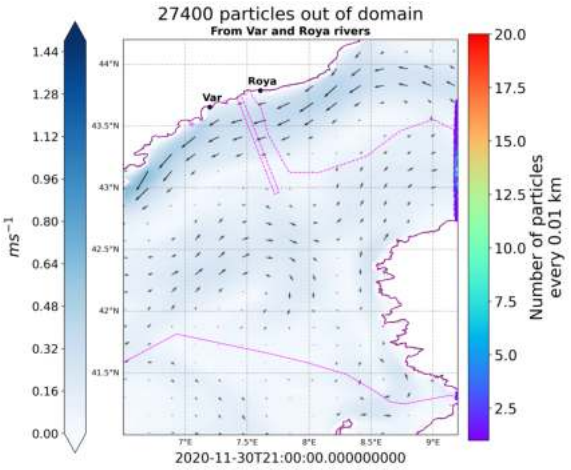

Figure 3.33: 27400 particles that left the domain of the simulations, from the WMOP total currents particles simulation.

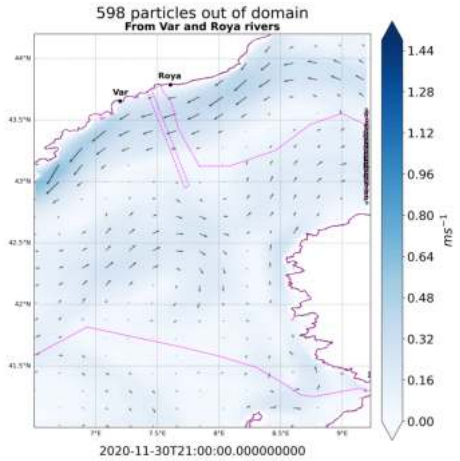

Figure 3.34: 598 particles that left the domain of the simulations, from the WMOP mean current particles simulation.

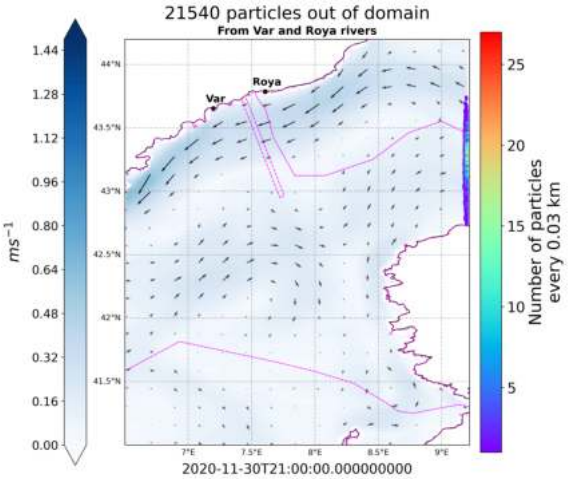

Figure 3.35: 21540 particles that left the domain of the simulations, from the WMOP spatially filtered currents particles simulation.

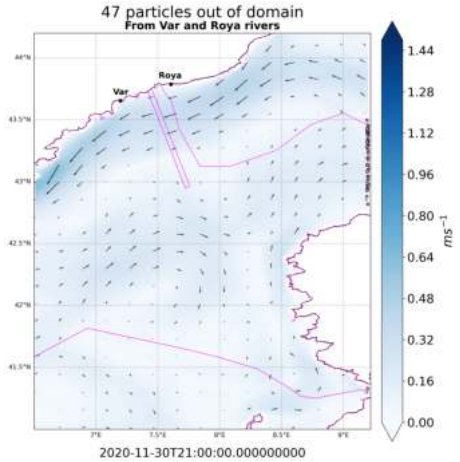

Figure 3.36: 47 particles that left the domain of the simulations, from the WMOP geostrophic currents particles simulation.

3.3.2 Floating particles

In Figures 3.37, 3.38, 3.39 and 3.40 we show how many particles remained on water during the simulations, and their last positions. While the mean current case and the spatially filtered simulation have a similar number of on-water particles (28770 and 27392, respectively), it is notable that their positions are quite different. In fact, the spatially filtered simulation mostly resembles that of the total currents, which presents 14754 on-water particles; we see that they both have a peak in the Gulf of Lion, even though the spatially filtered simulation is less dispersed and did not reach as far South and West as the total currents one. In the mean current simulation, the particles stayed closely packed and barely dispersed: we see a large number in

the centre of the Lion Gyre, in the middle of our domain. Furthermore, and given its high number of beached particles, the geostrophic currents simulation presents only 96 particles on water. We also note that the shape of the water particles positions of the mean current simulation (Figure 3.38) and that of the total currents (Figure 3.37) simulation show a remarkable complementarity. This is even more visible between the mean current simulation and the spatially filtered simulation: as we know, the low-pass filter removed eddies with a spatial extent less than 50 km, on the other hand, the mean simulation lacks any feature that lasted less than 60 days. Therefore, short-lived features could be responsible for preventing the particles from entering the central gyre. The mean current simulation is the one where the WMED general circulation is better represented, we can see both the Northern Current as well as the North Balearic Front, which moves North-Eastwards from ∼40°N to ∼43°N. Thus, in the mean simulation the particles follow the NC and are then channeled North-East. In the total and spatially filtered simulations we can observe that the particles are moved in the general direction given by the mean currents, but they are much more dispersed and slowed down by the presence of eddies which are absent in the mean current simulation.

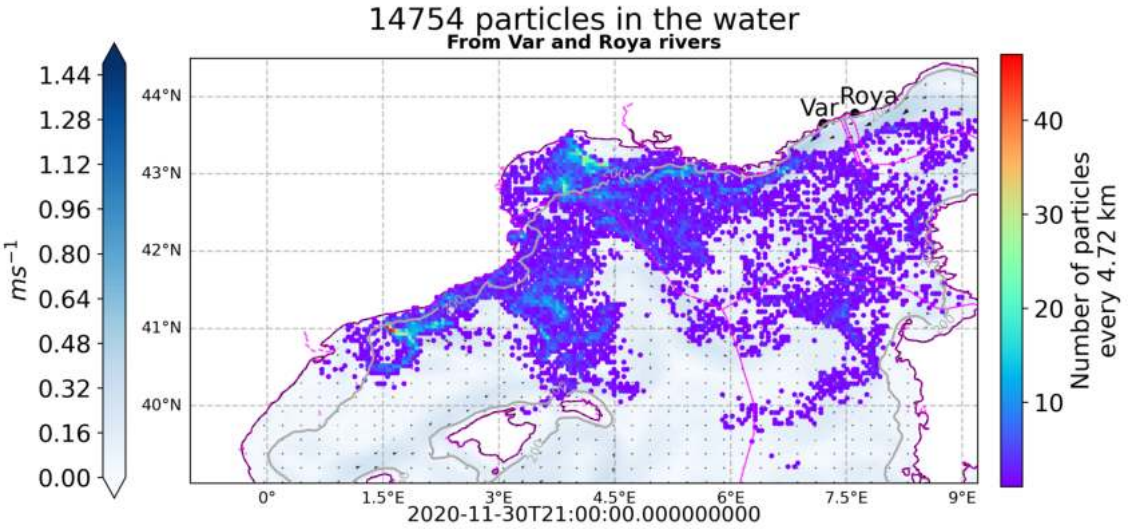

Figure 3.37: 14754 particles on water, density plot from the WMOP total currents particles simulation.

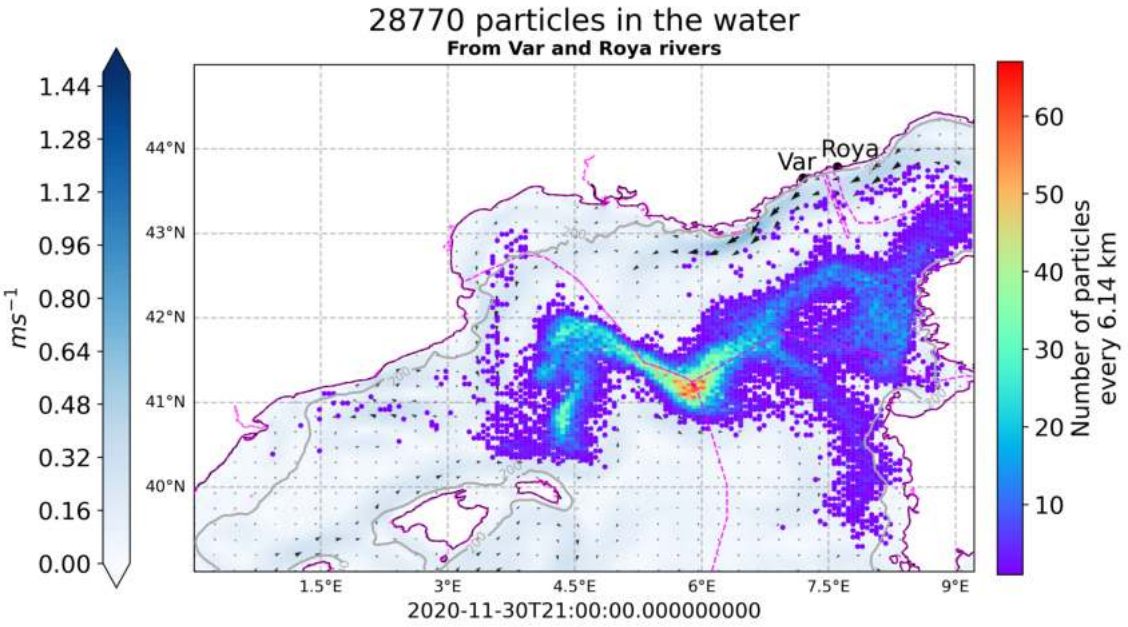

Figure 3.38: 28770 particles on water, density plot from the WMOP mean current particles simulation.

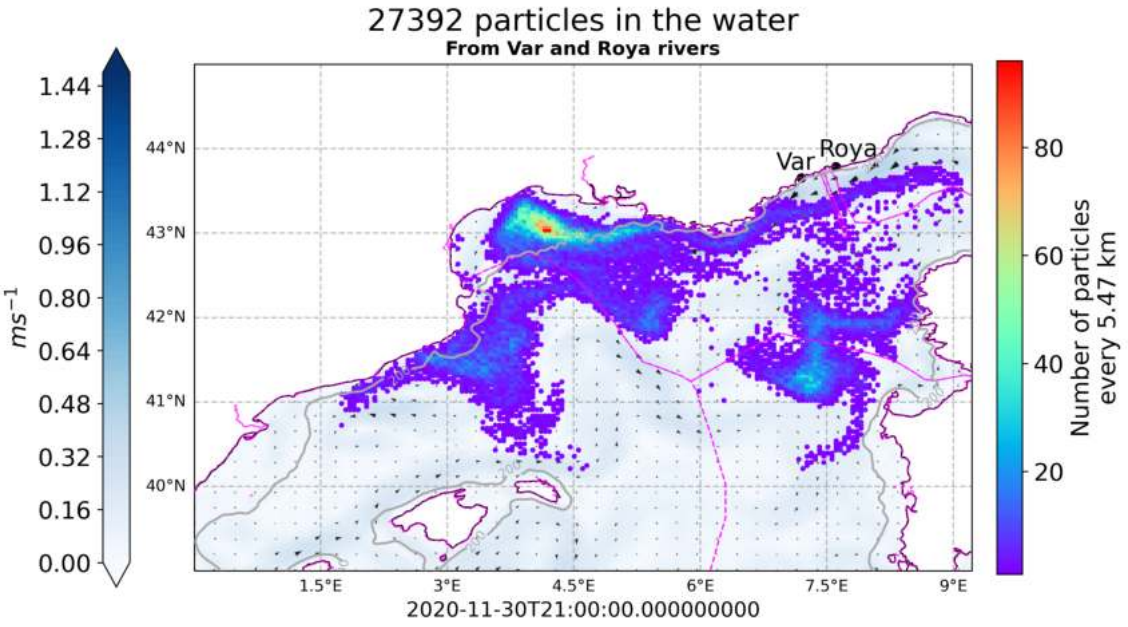

Figure 3.39: 27392 particles on water, density plot from the WMOP spatially filtered currents particles simulation.

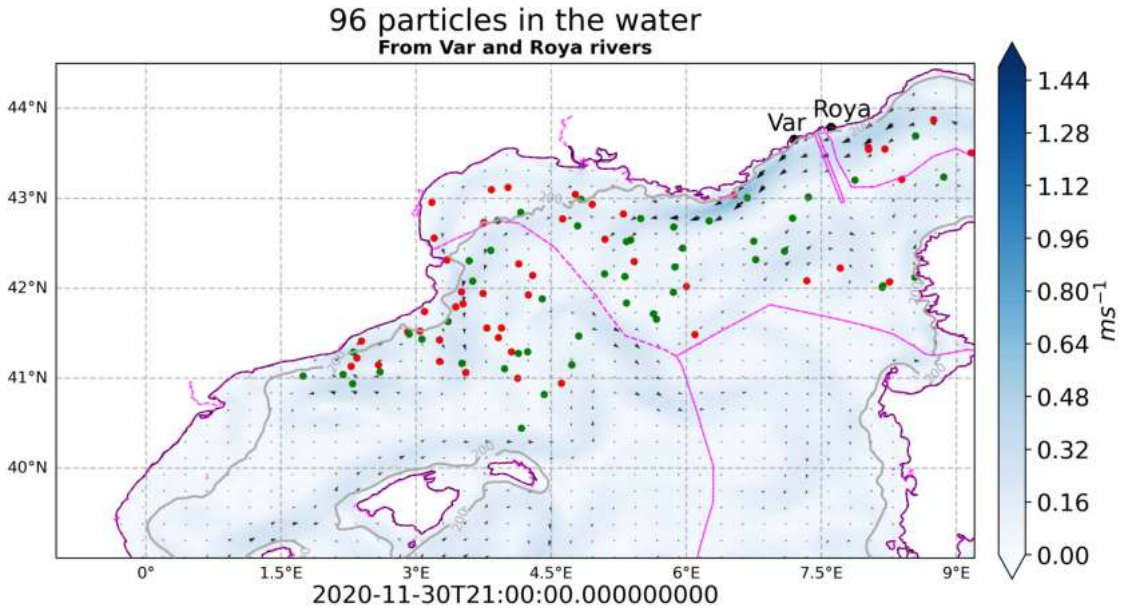

Figure 3.40: 96 particles on water, from the WMOP geostrophic currents particles simulation.

3.3.3 Shelf-slope exchanges

In order to see the extent of the shelf-slope exchange, we compute the percentages of all particles that crossed the 200 meter bathymetry line. The values, along with the percentages of particles that stayed on water, were beached and went out of domain, are shown in Table 3.1. Out of all the simulations, the one that saw the highest percentage of particles crossing the 200 m bathymetry line is the mean current simulation, with a value of ∼47.67 %. In the geostrophic simulation, almost all of the particles were beached, and we therefore see only ∼0.14 % crossing the 200 m isobath. Moreover, we see that ∼19.04 % and ∼30.72 % of the particles from the total and spatially filtered simulations, respectively, crossed the isobath.

Simulation	Total	Mean	Spatially filtered	Geostrophic
On water	24.6%	47.9%	45.7%	0.16%
Beached	29.7%	51.1%	18.4%	99.76%
Out of domain	45.7 %	1.0%	35.9%	0.08%
Percentage beyond the 200m bathymetry line	19.04 %	47.67%	30.72%	0.14%

Table 3.1: For each WMOP simulation, from both rivers: percentage of particles on water, beached and out of domain and the percentage that crossed the 200m bathymetry line.

3.3.4 Transnational transport

As we introduced previously, we want to know which countries felt the effect of the pollution the most. We know that the mouth of river Var is located between Nice and Saint-Laurent-du-Var, with its course being entirely in France. Roya discharges in the town of Ventimiglia, Italy, and its course is shared by both Italy and France, with France retaining most of it ($\sim$ 68% of the river's course). In this Section we will be making a distinction between the final positions of the particles from one river and the other. We do so, because the rivers discharge in different countries and we want to specifically see where the plastic from Italy and France ended up, in the different simulations.

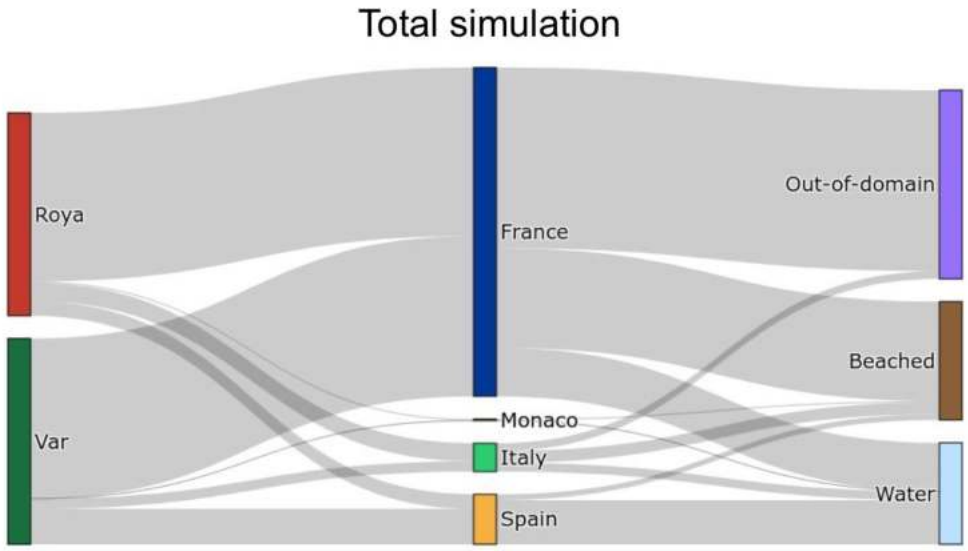

Figure 3.41: WMOP total currents: Sankey plot of transnational transport of particles from rivers Var and Roya.

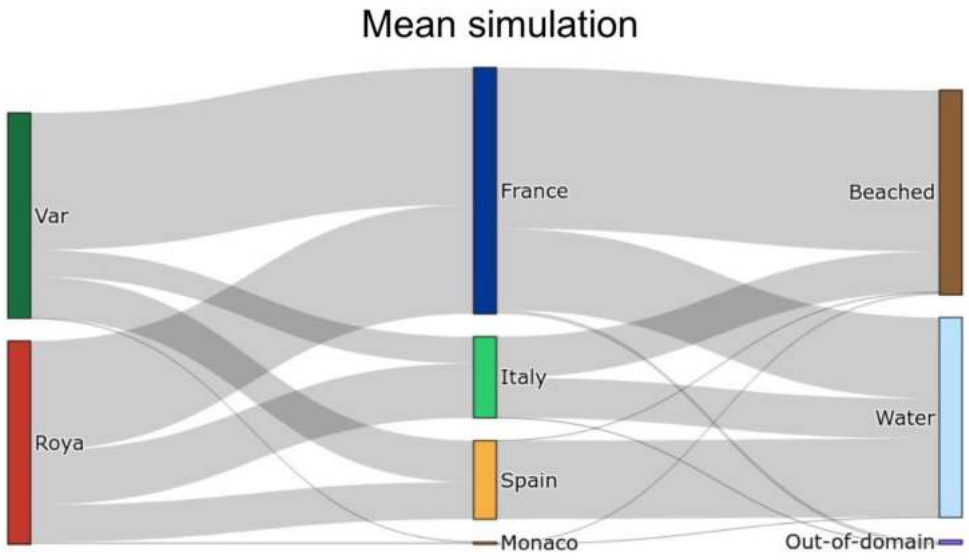

Figure 3.42: WMOP mean current: Sankey plot of transnational transport of particles from rivers Var and Roya.

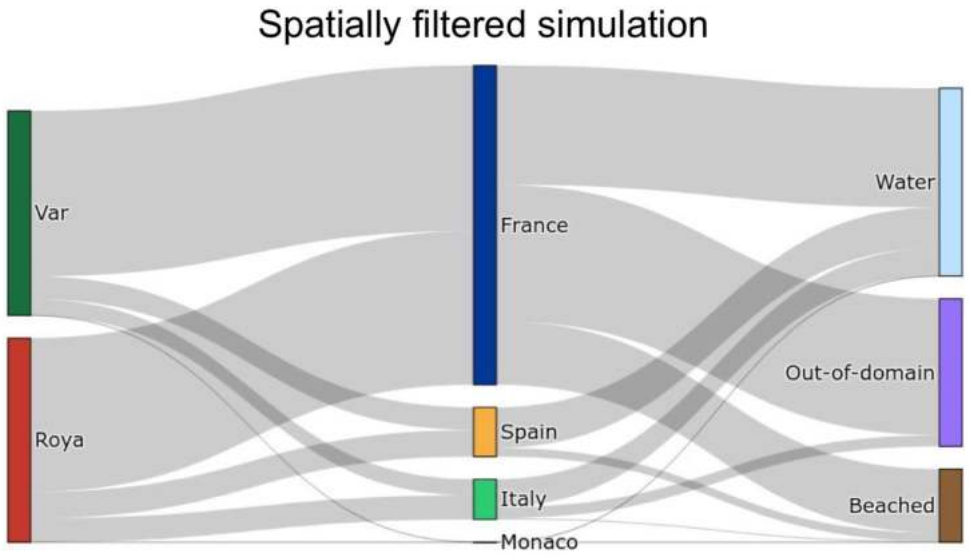

Figure 3.43: WMOP spatially filtered currents: Sankey plot of transnational transport of particles from rivers Var and Roya.

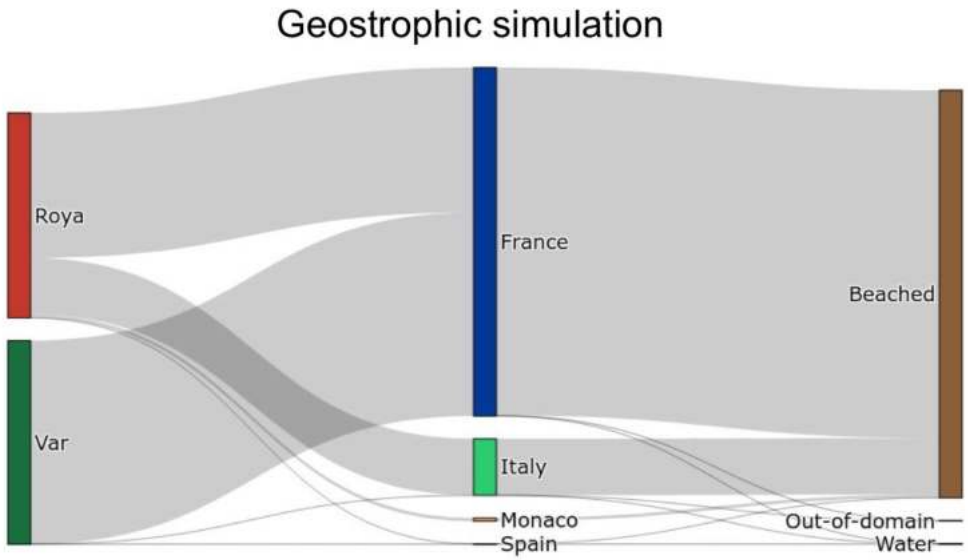

Figure 3.44: WMOP geostrophic currents: Sankey plot of transnational transport of particles from rivers Var and Roya.

In Figures 3.41, 3.42, 3.43 and 3.44 are shown the Sankey diagrams of the transnational transport for the four WMOP simulations. The diagrams show the flow of material from each river, in which country the material ended up and whether it was on water, beached, or out of domain.
In the total currents simulation (Figure 3.41), which contains all the scales of circulation representable by the model, we see that most particles from both rivers ended up in the French economic zone. In particular, most of these went out of domain, a smaller fraction was beached and a part stayed on French water. A small portion of particles from Var and Roya went to Spain and Italy, with Spain collecting most of the plastic into its waters, whereas in Italy the particles were fairly divided between land, water and out-of-domain. Obviously, only a really small percentage of the particles, in all four simulations, ended up in the small Monaco economic zone. If we now keep the total currents simulation as a reference, we can look at how the absence of small scale features impacted the transnational transport.
In the mean current simulation (Figure 3.42) France is still the country receiving the highest percentage of plastic particles, but here we see that Italy and Spain collected more pollution than in the reference, and that now most particles were either beached or remained on water. In the spatially filtered simulation (Figure 3.44), again France retained most of the pollution, followed by Spain, Italy and then Monaco. Here most of the plastic ended up on water, or out of domain, with a good portion ending up on land. In the geostrophic simulation (Figure 3.44), France collected the highest fraction of particles than in all the other simulations. Italy was second, followed by a paltry amount of material for Spain and Monaco. In the geostrophic simulation most of the material was beached, as we saw previously when analysing the final positions of the particles.
It seems that the effect of removing small scale features from our currents field

was that of reducing the amount of pollution arriving in the French economic zone. Moreover, when small eddies are present, the particles are mainly directed out of domain; whereas this configuration is secondary in the three "filtered" simulations. We show in Table 3.2 the exact percentages for the beached and water configurations in the total currents simulations; we do not show here the out-of-domain percentages because ultimately we do not know where the particles end up after exiting the domain.

WMOP	Roya	Var	Roya	Var
	On water		Beached	
Spain	6.32%	15.11%	0.75%	2.05%
France	9.10%	14.41%	38.30%	9.89%
Italy	2.34%	1.87%	5.67%	3.33%
Monaco	0.00%	0.00%	0.71%	0.00%

Table 3.2: WMOP total currents simulation: transnational transport.

Chapter 4

Lagrangian simulations from CMEMS-MED MFC surface currents

Here, we repeat all the previous analysis but with the CMEMS-MED MFC model. Again, before initialising the particles, we examine the sea surface currents from the four simulations, obtained from the CMEMS-MED MFC model. In Figure 4.1 we see the total currents from the CMEMS-MED MFC model: here we see a similar field to that observed for the WMOP (Figure 3.1), with the NC being undetectable and a number of eddies characterising the circulation. Nevertheless, there are noticeable differences between the two models total currents: near the Gulf of Lion, the CMEMS-MED MFC Northern Current is stronger, whereas in the centre of the domain the WMOP currents were slightly more pronounced. In the CMEMS-MED MFC mean field (Figure 4.2), we observe analogous patterns to that of the WMOP (Figure 3.2). The NC reaches the Channel of Ibiza, and gets progressively weaker on the way. From this channel, we see a counter current branching out and crossing the domain towards the East: the Balearic Current and North Balearic Front. Here, the gyre we observe above Mallorca island is essentially undetectable, meaning that in the CMEMS-MED MFC model it lasted less than 60 days. Again, the spatially filtered currents (Figure 4.3) follow the large scale pattern of the total currents, with significant wind effects and a weak signature of the NC. The geostrophic currents (Figure 4.4) follow the same large structures of the total currents, but small eddies and features are mostly missing. Compared to the WMOP geostrophic currents (Figure 3.4), here the NC near the rivers, and the return current just below it, are stronger in magnitude.

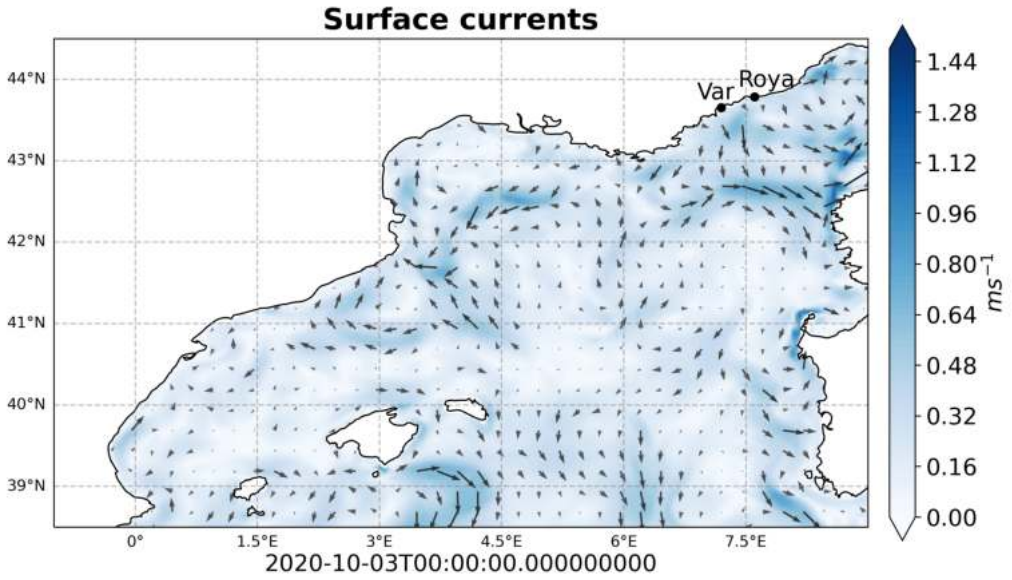

Figure 4.1: CMEMS-MED MFC total currents simulation on the 3rd of October 2020, at T00:00.

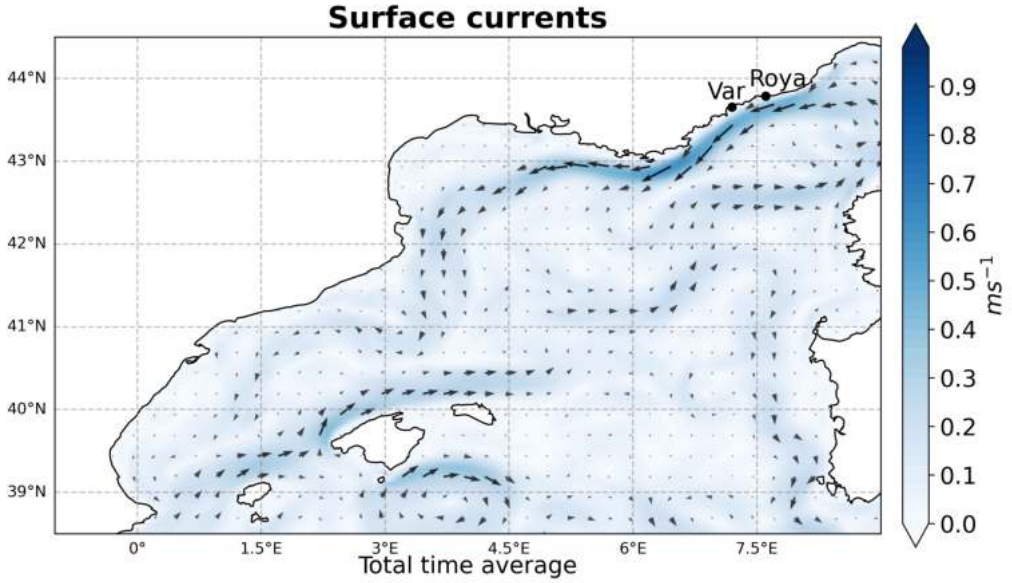

Figure 4.2: CMEMS-MED MFC mean current simulation.

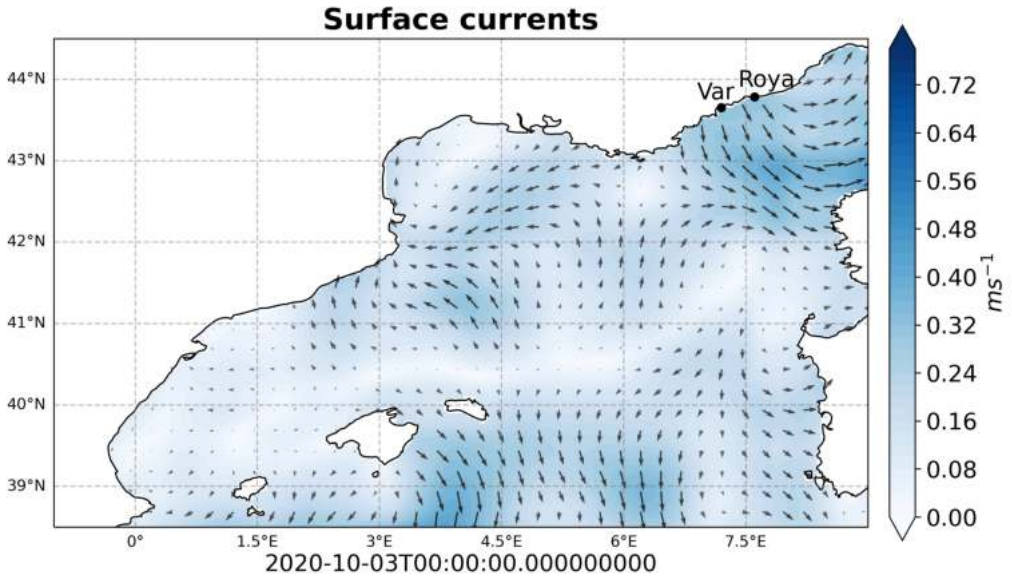

Figure 4.3: CMEMS-MED MFC spatially filtered currents simulation on the 3rd of October 2020, at T00:00.

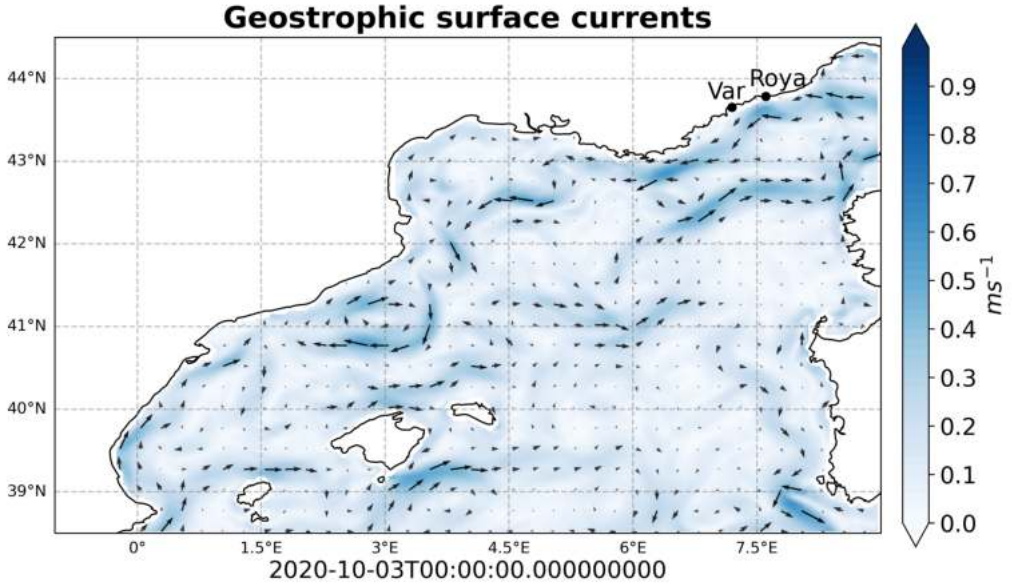

Figure 4.4: CMEMS-MED MFC geostrophic currents simulation on the 3rd of October 2020, at T00:00.

As we previously did for the WMOP model, we compute an EKE map of the sea surface currents from the CMEMS-MED MFC model, which is shown in Figure 4.5. The first thing we notice from the CMEMS-MED MFC EKE map is that this model detects less peaks of energy compared to what we observed in the WMOP EKE map (Figure 3.5), and these peaks are also less energetic overall, this is due to the higher resolution of the WMOP model. In particular, this is observable in the NC and in the centre of the domain as well as in the eddy above Mallorca island, which here is weaker and also a bit more Eastern than what we saw in the WMOP map.
Nonetheless, the EKE map from the CMEMS-MED MFC model is coherent with

the sea surface currents. The areas of highest energy are observed in the zones where currents form eddies and gyres.

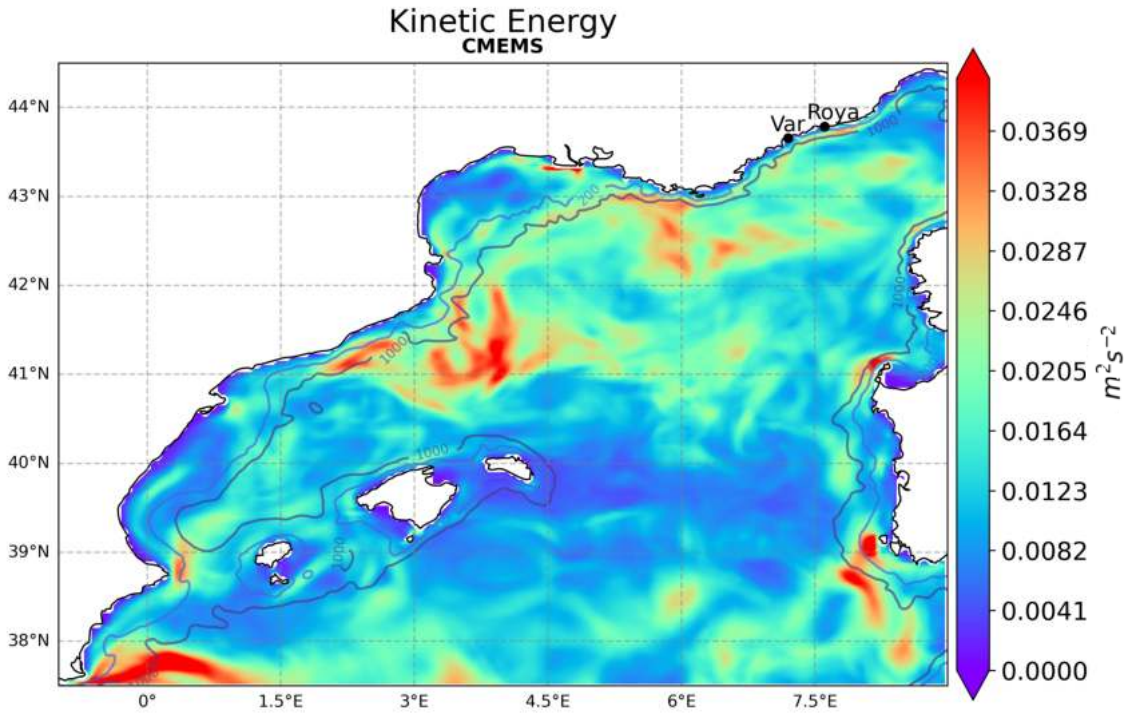

Figure 4.5: CMEMS-MED MFC: Mean Eddy Kinetic Energy

4.1 Determining the initial positions

To determine the initial position of particles for the CMEMS-MED MFC simulations we use the same logic as we did previously with the WMOP model. In this case, the crucial difference is that the CMEMS system does not contain the runoff values for Var and Roya. We therefore use the satellite image of Figure 3.6 to position the particles inside the plumes. Moreover, since the CMEMS-MED MFC domain and resolution are different from those of the WMOP (CMEMS-MED MFC has a spatial resolution of ~ 4.5 km, whereas the WMOP has a spatial resolution of ~ 2 km) we examine a salinity map to ensure that the particles are inside the model's domain.

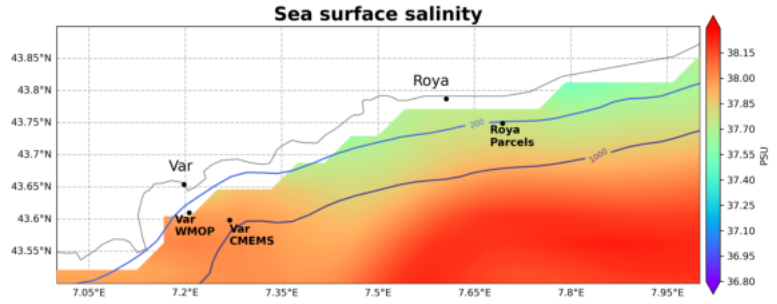

Figure 4.6: CMEMS-MED MFC model: sea surface salinity on the **3rd of October 2020, at T00:00**.

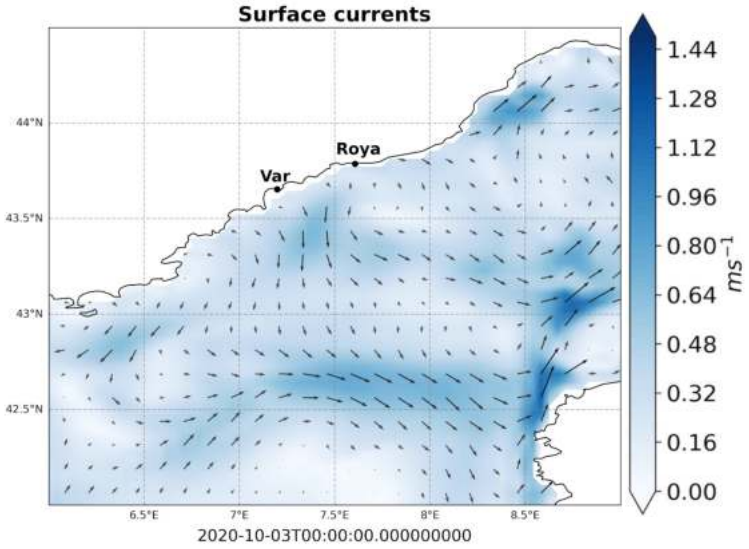

Figure 4.7: CMEMS-MED MFC model: surface currents simulation on the **3rd of October 2020, at T00:00**.

As we can see in Figure 4.6, the position of the Var particles used in the WMOP simulations is outside the CMEMS-MED MFC domain; this is due to the fact that the WMOP model and the CMEMS-MED MFC model have different land-sea masks. Thus, we move the Var particles initial position to a new spot of latitude and longitude of (43.5983°N, 7.268°E). The new position is still inside the plume of Var, according to the satellite image (Figure 3.6). For the Roya river particles, we are able to use the same location as for the WMOP, since they are inside the water domain of the CMEMS-MED MFC model. Moreover, we want to be sure that the particles will not end up on land immediately after starting the simulation; considering that we are initialising them rather close to the model's land mask we further corroborate this choice by looking at a zoom of the total sea surface currents patterns, shown in Figure 4.7: the currents are directed off-shore, as we previously observed in the WMOP simulations. This ensures that the immediate beaching of particles due to wrong positioning should be minimal.

4.2 Results

4.2.1 Using CMEMS-MED MFC total currents

In this Section, we look at the particles simulation obtained with CMEMS-MED MFC total sea surface currents. In Figures 4.8, 4.9, 4.10 and 4.11 we can see various time steps of the particles simulation, produced with total currents simulations from the CMEMS-MED MFC.
We can see that the particles move quite compactly towards the West; the combination of a large cyclonic gyre above Corsica and the Northern Current splits the movement: a large fraction of the particles remains trapped between the rivers mouths and Corsica, while the rest are brought South-West. This is evident in Figures 4.9 and 4.10 where we can see the two separate groups just described; by the end of the first week of November 2020, the particles above Corsica are starting to move either West, with the now intensified Northern Current, or East, with the Southern branch of the gyre. As they flow South-Westwards the particles fill the shelf of the Gulf of Lion, and do not spread much into the centre of the domain.
At the end of the simulation (Figure 4.11) a few particles have reached as South as ∼39°N and touched the coastal waters of the Valencian Community (∼0° longitude). The trajectories followed by the particles appear very concentrated, the total currents produced by the CMEMS-MED MFC model lack the same amount of small scale features that drove the particles paths in the WMOP total currents simulation.

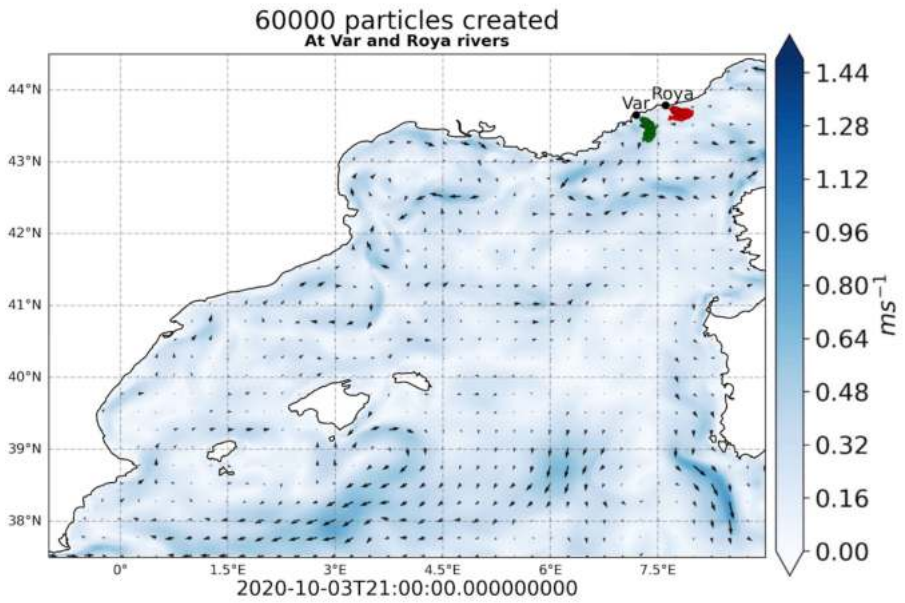

Figure 4.8: CMEMS-MED MFC total currents particles simulation on the **3rd of October 2020 at T21:00**. Red: particles from river Roya. Green: particles from river Var.

0.8

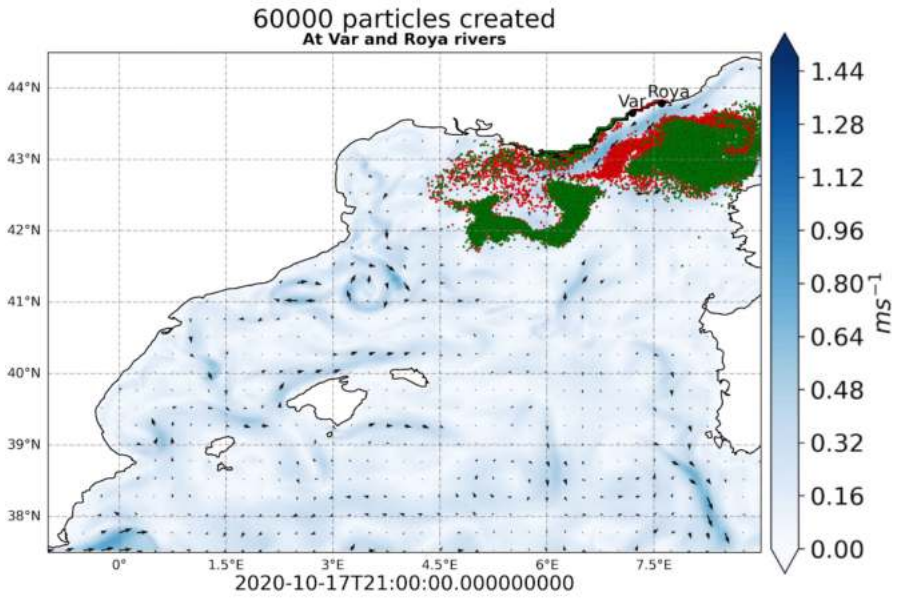

Figure 4.9: CMEMS-MED MFC total currents particles simulation on the **17th of October 2020 at T21:00**. Red: particles from river Roya. Green: particles from river Var.

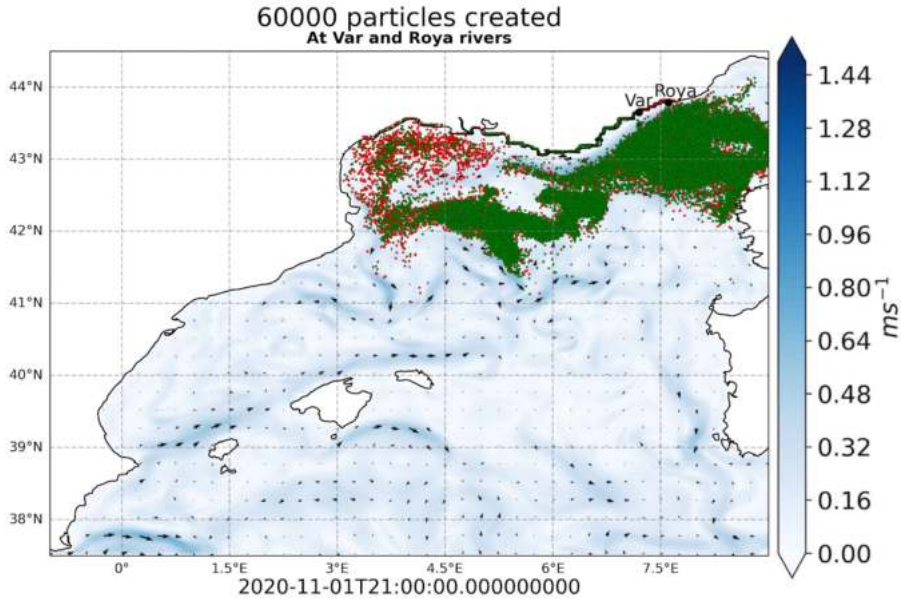

Figure 4.10: CMEMS-MED MFC total currents particles simulation on the **1st of November 2020 at T21:00**. Red: particles from river Roya. Green: particles from river Var.

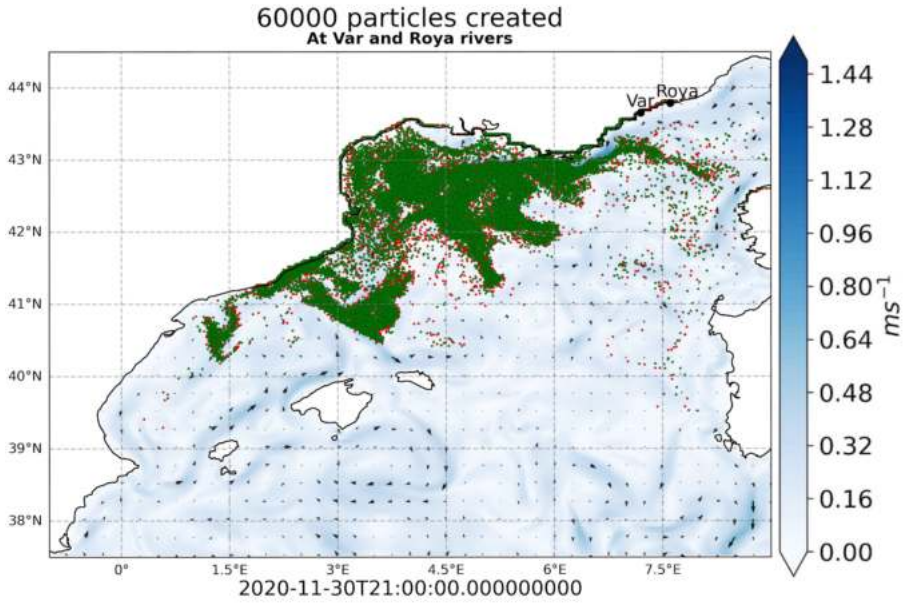

Figure 4.11: CMEMS-MED MFC total currents particles simulation on the **30th of November 2020 at T21:00**, the last time step. Red: particles from river Roya. Green: particles from river Var.

4.2.2 Using CMEMS-MED MFC mean current

As we previously did with the WMOP model, we now compute the 60 days average of the total currents produced with the CMEMS-MED MFC model. By removing any small scale feature that is short lived, we aim to examine the extent of the effect of these features on the currents and on the consequent particles trajectories. The current output we obtain should resemble the mean circulation of the Mediterranean as modelled by the CMEMS-MED MFC. As we noted in the WMOP simulation, the biggest difference between the CMEMS-MED MFC mean current simulation and the CMEMS-MED MFC total currents simulation is that the particles stay very close to each other. As observable in Figures 4.12, 4.13, 4.14 and 4.15 we see that the material moves South-West along the Northern Current, which is largely unperturbed. Then, the particles cross the Gulf of Lion and turn East along the North Balearic Front, which is located roughly in the same position we observed in the WMOP mean currents simulation, but is much weaker here. At the end of the simulation (Figure 4.15), we see that, compared to the total currents simulation, a lot more particles have reached the Valencian coast. Furthermore, only a smaller amount of material crossed the 200 m isobath and stayed in the Gulf of Lion. We observe very low dispersion, the domain is largely "untouched" by the particles, and the NC seems to be the main flow driving the material's movement.

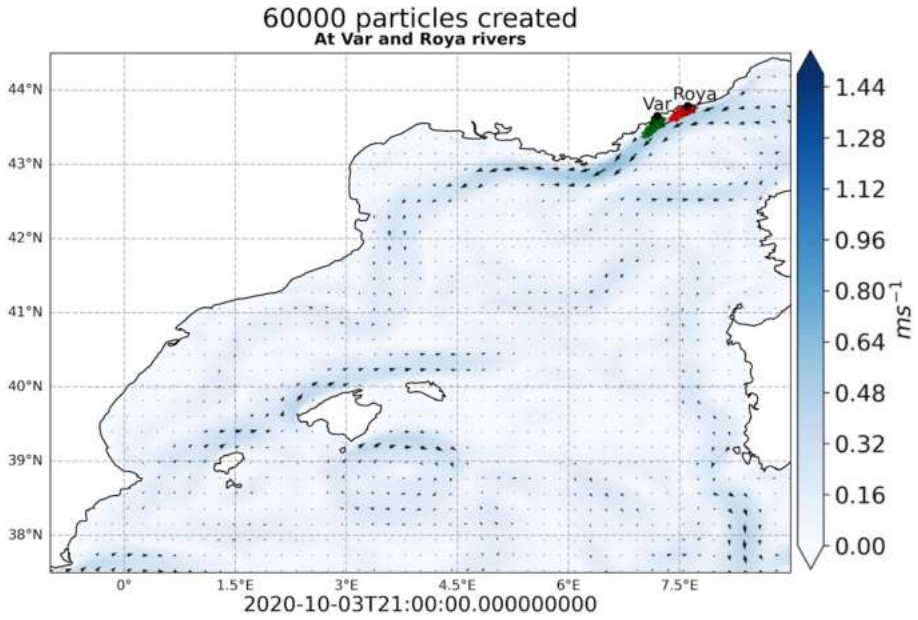

Figure 4.12: CMEMS-MED MFC mean current particles simulation on the **3rd of October 2020 at T21:00**. Red: particles from river Roya. Green: particles from river Var.

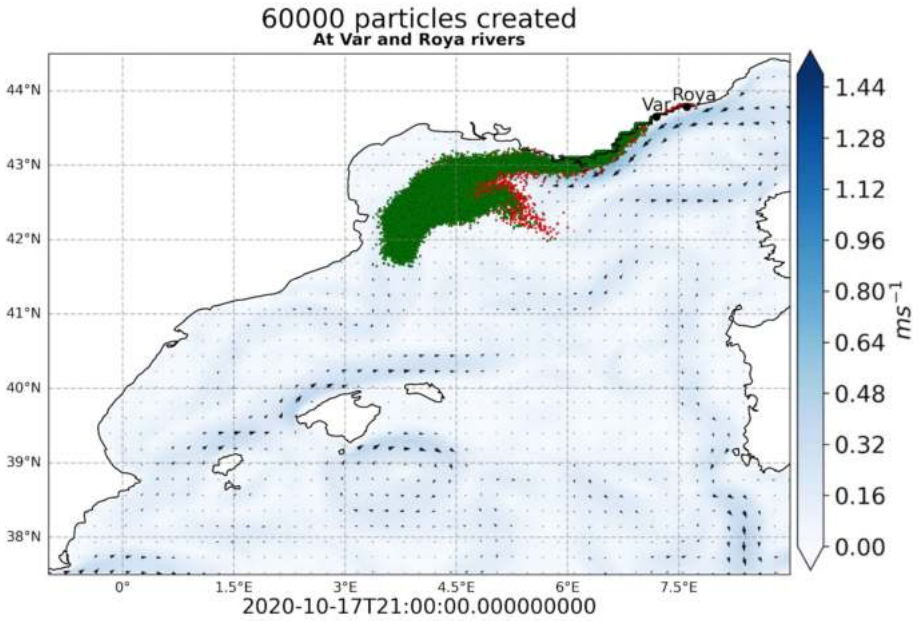

Figure 4.13: CMEMS-MED MFC mean current particles simulation on the **17th of October 2020 at T21:00**. Red: particles from river Roya. Green: particles from river Var.

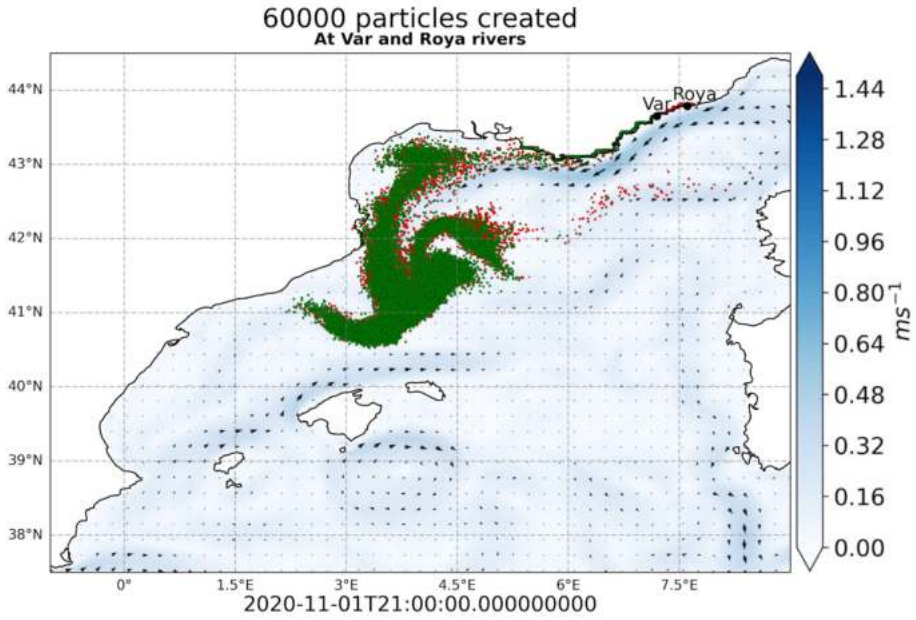

Figure 4.14: CMEMS-MED MFC mean current particles simulation on the **1st of November 2020 at T21:00**. Red: particles from river Roya. Green: particles from river Var.

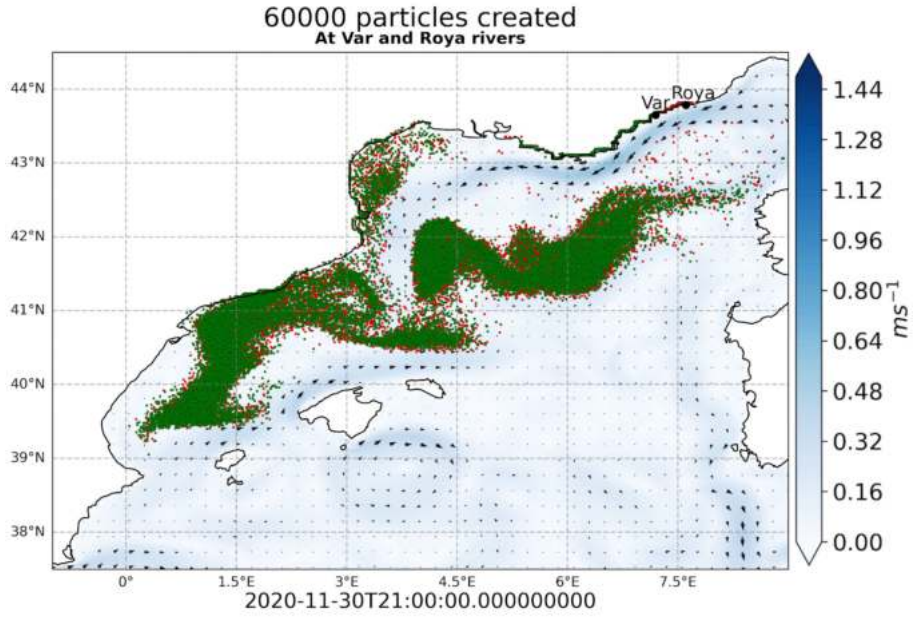

Figure 4.15: CMEMS-MED MFC mean current particles simulation on the **30th of November 2020 at T21:00**, the last time step. Red: particles from river Roya. Green: particles from river Var.

4.2.3 Using CMEMS-MED MFC spatially filtered currents

With the purpose of removing small scale features from the sea surface currents, and in particular from the NC, we produce a moving spatial average of the currents. To decide the size of the space filter, we examine SSH maps using Sea Level Anomaly data from the CMEMS-MED MFC model. In Figures 4.16, 4.17 we show two SSH contour plots from the 3rd of October 2020 at T15:00 and the 6th of October 2020 at T06:00. We show these two plots because they are indicative of what we were able to observe over the whole period of study. The size of the meanders of the Northern Current is roughly 50 km in the latitude and longitude directions; therefore, we can apply the same space filter we chose for the WMOP currents, which will also facilitate the comparison between the two models results. We also note that the SSH maps from the two models are quite different, which gives us an early clue of how diverse are the outputs from the WMOP and the CMEMS-MED MFC.

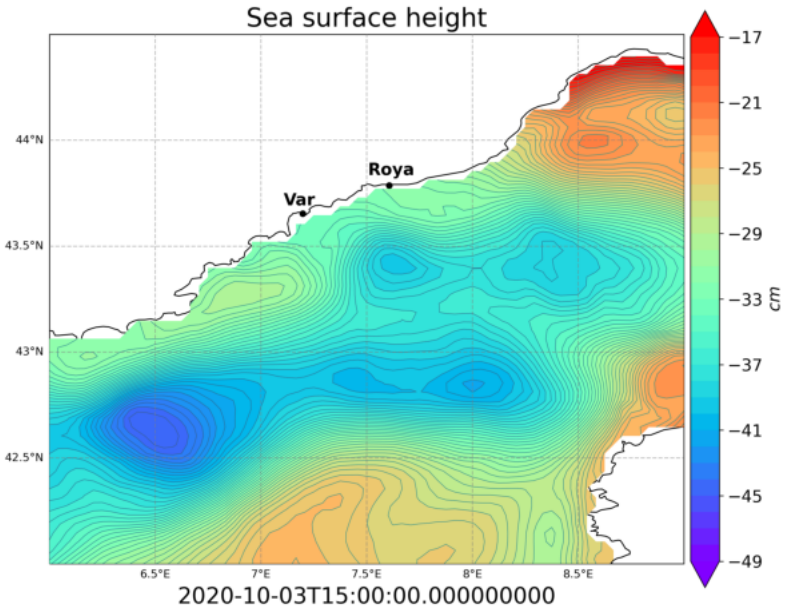

Figure 4.16: CMEMS-MED MFC SSH map on the **3rd of October 2020 at T15:00**.

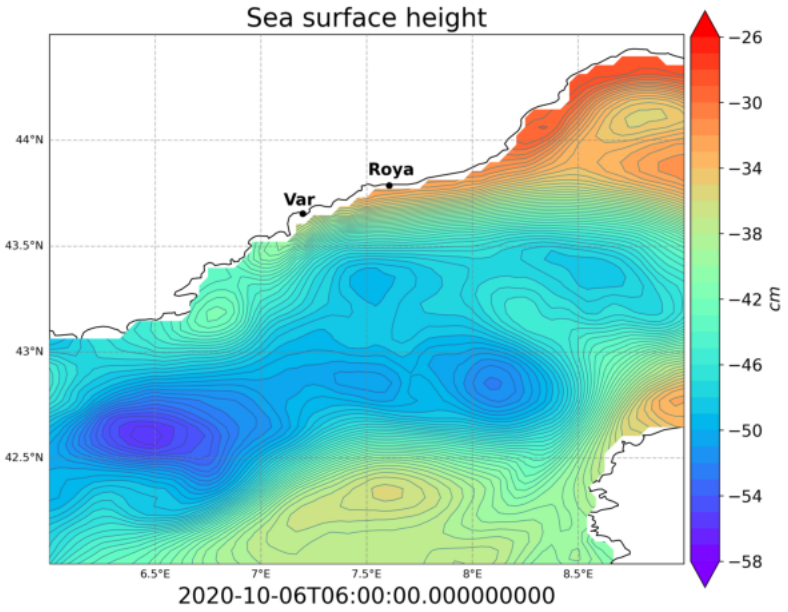

Figure 4.17: CMEMS-MED MFC SSH map on the **6th of October 2020 at T06:00**.

We show the particles simulation for both rivers at different time steps in Figures 4.18, 4.19, 4.20 and 4.21. The spatially filtered currents are really weak, barely detectable. Here, much more than in the mean current field, the particles move slowly and they stay cramped together. We observe very little dispersion, the weakest so far in our CMEMS-MED MFC simulations. The material does not reach as South-West as in the previous simulations, and it does not disperse into the shelf of the Gulf of Lion either. The space filter was effective in removing small scale meanders of the Northern Currents, but perhaps it also weakened important features of the main circulation as well, such as the Northern Current itself. Perhaps this is the reason why we do not see as many particles in the South-Western area of our domain.
Overall, the most evident aspect of this simulation is how much less dispersed the material is. We can therefore deduce, once again, that the role of small scale features seem to play a fundamental role in the dispersion of material in the area of study.

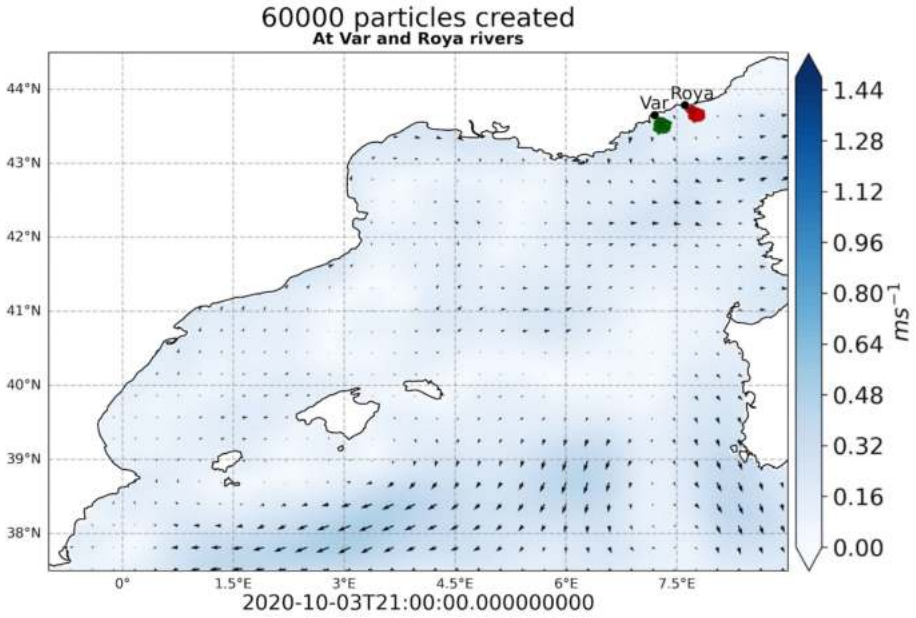

Figure 4.18: CMEMS-MED MFC 50km spatially filtered particles simulation on the **3rd of October 2020 at T21:00**. Red: particles from river Roya. Green: particles from river Var.

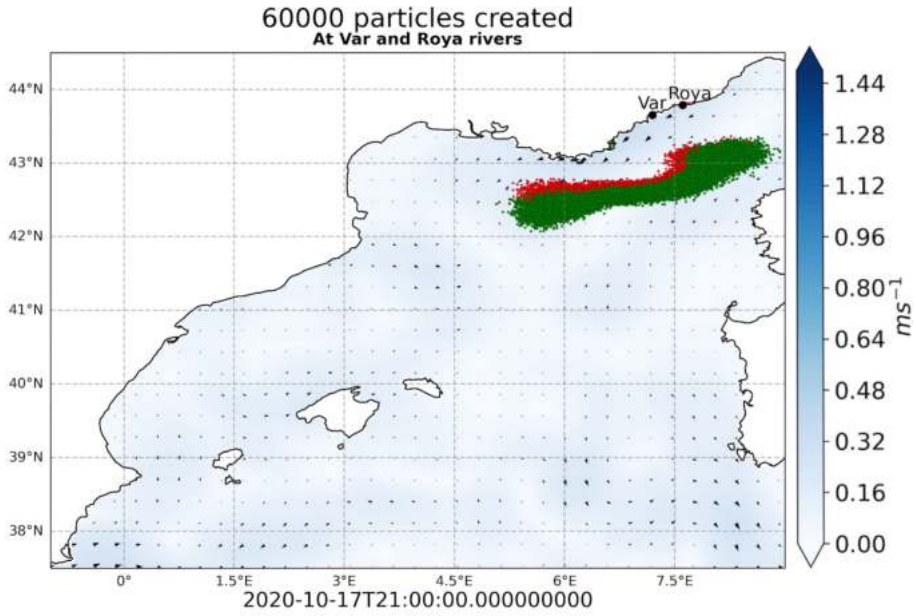

Figure 4.19: CMEMS-MED MFC 50km spatially filtered particles simulation on the **17th of October 2020 at T21:00**. Red: particles from river Roya. Green: particles from river Var.

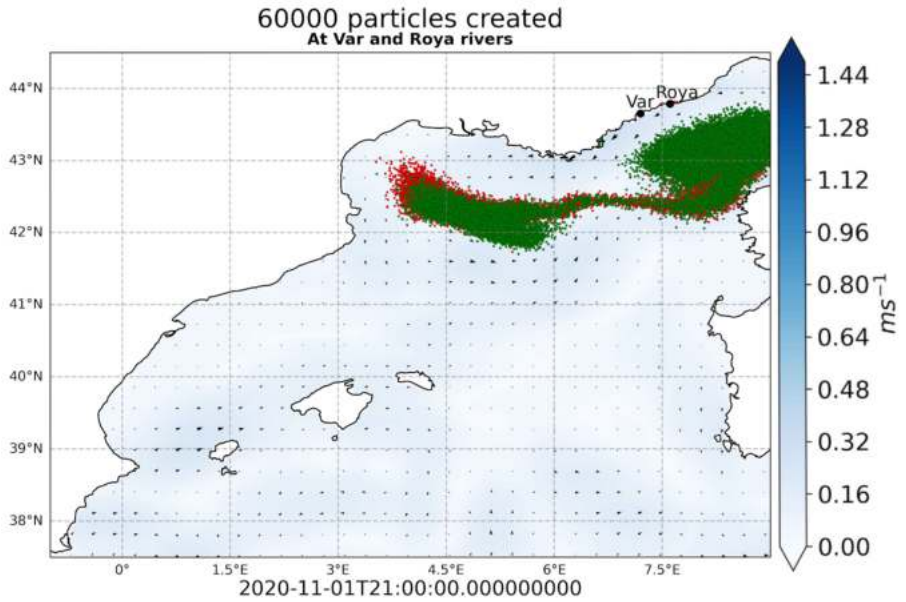

Figure 4.20: CMEMS-MED MFC 50km spatially filtered particles simulation on the **1st of November 2020 at T21:00**. Red: particles from river Roya. Green: particles from river Var.

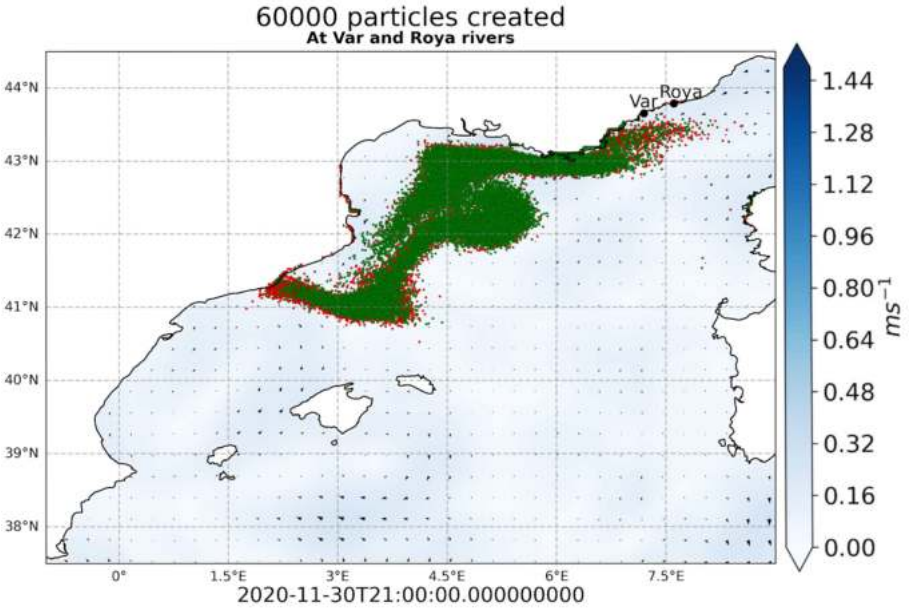

Figure 4.21: CMEMS-MED MFC 50km spatially filtered particles simulation on the **30th of November 2020 at T21:00**, the last time step. Red: particles from river Roya. Green: particles from river Var.

4.2.4 Using CMEMS-MED MFC geostrophic currents

As we did previously for the WMOP, we are now interested in producing geostrophic surface currents with CMEMS data of Sea Level Anomaly.
In Figures 4.22, 4.23, 4.24 and 4.25 we can observe the different time steps of the particles simulation. Compared to the CMEMS-MED MFC total currents simulation, here a remarkably low number of particles manage to move away from the coast near the rivers. We see in Figure 4.24 that on the 1st of November 2020 at T21:00, only a small amount of material is spreading in the Gulf of Lion's waters, and by the end of the simulation only a handful of particles are left on water domain in general. We can infer that this is due to the fact that the geostrophic currents present a strong Northern Current, weakly perturbed by small scale features, that traps the cross-shelf movement of the material. There is little to no shelf-slope exchange, compared to the other simulations, and the particles are not dispersed in the domain.

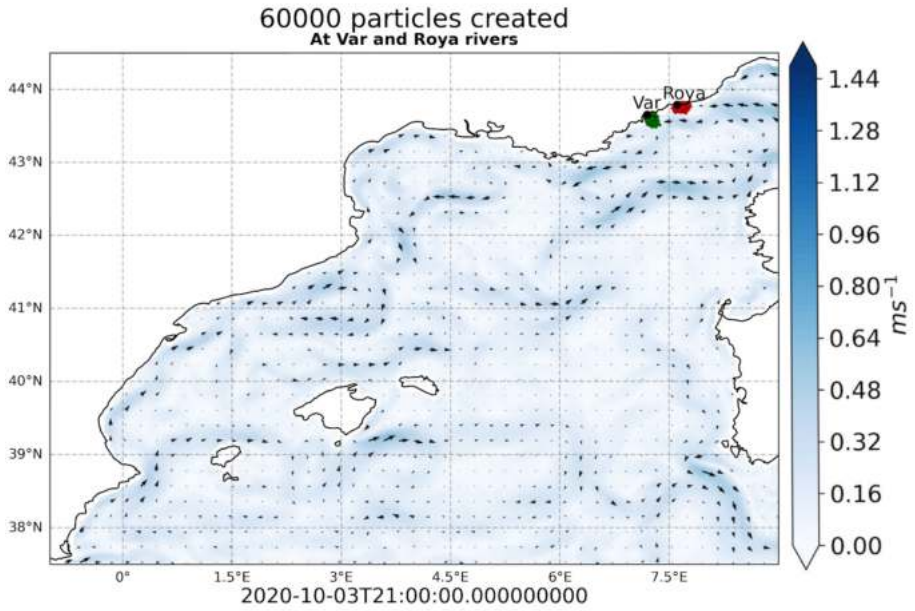

Figure 4.22: CMEMS-MED MFC geostrophic currents particles simulation on the **3rd of October 2020 at T21:00**. Red: particles from river Roya. Green: particles from river Var.

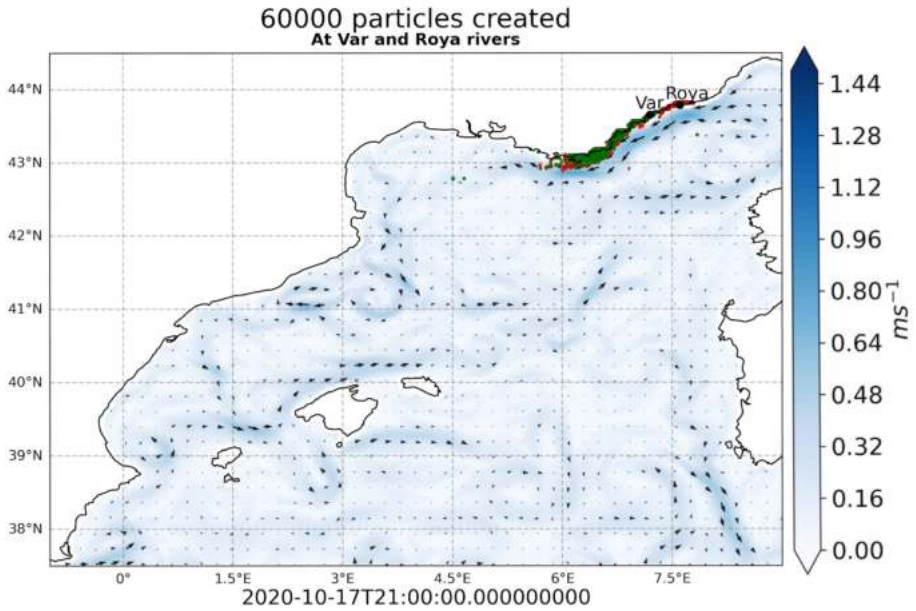

Figure 4.23: CMEMS-MED MFC geostrophic currents particles simulation on the **17th of October 2020 at T21:00**. Red: particles from river Roya. Green: particles from river Var.

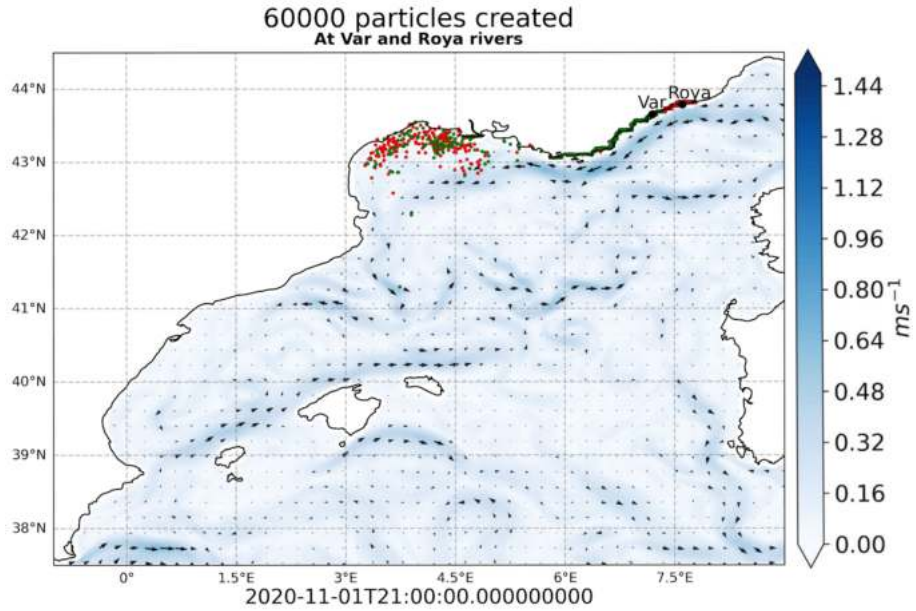

Figure 4.24: CMEMS-MED MFC geostrophic currents particles simulation on the **1st of November 2020 at T21:00**. Red: particles from river Roya. Green: particles from river Var.

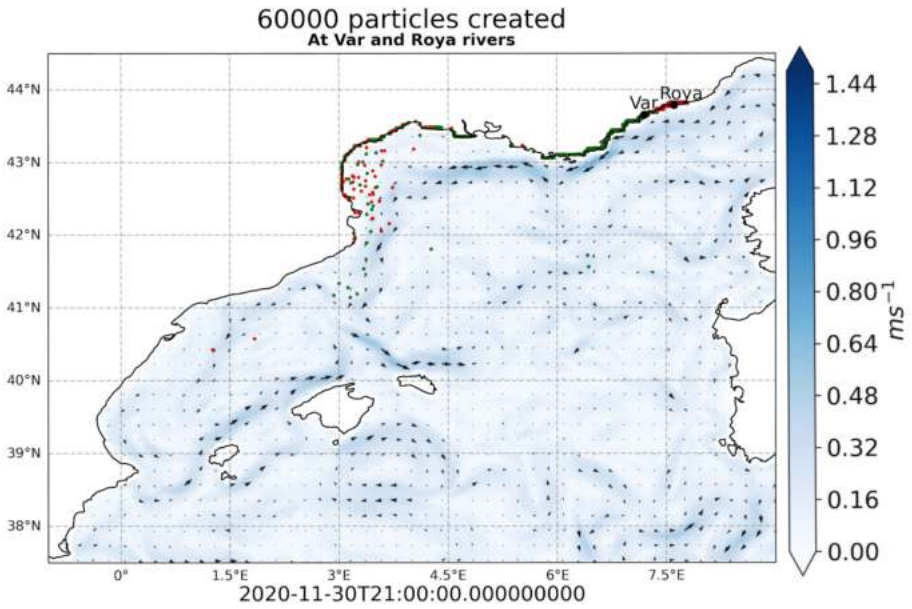

Figure 4.25: CMEMS-MED MFC geostrophic currents particles simulation on the **30th of November 2020 at T21:00**, the last time step. Red: particles from river Roya. Green: particles from river Var.

4.3 Analysis of final positions

Now, we want to examine the final positions of the particles in the CMEMS-MED MFC simulations.

4.3.1 Beaching

As we did with the WMOP results, we want to see what role the small scale features of the WMED played in the beaching of particles or in keeping the material on water or pushing it out of domain. A total of 60000 particles where initialised in each simulation, 30000 from each river. Furthermore, underneath each map is plotted the 60-days average of the currents in question and the borders of the exclusive economic zones.

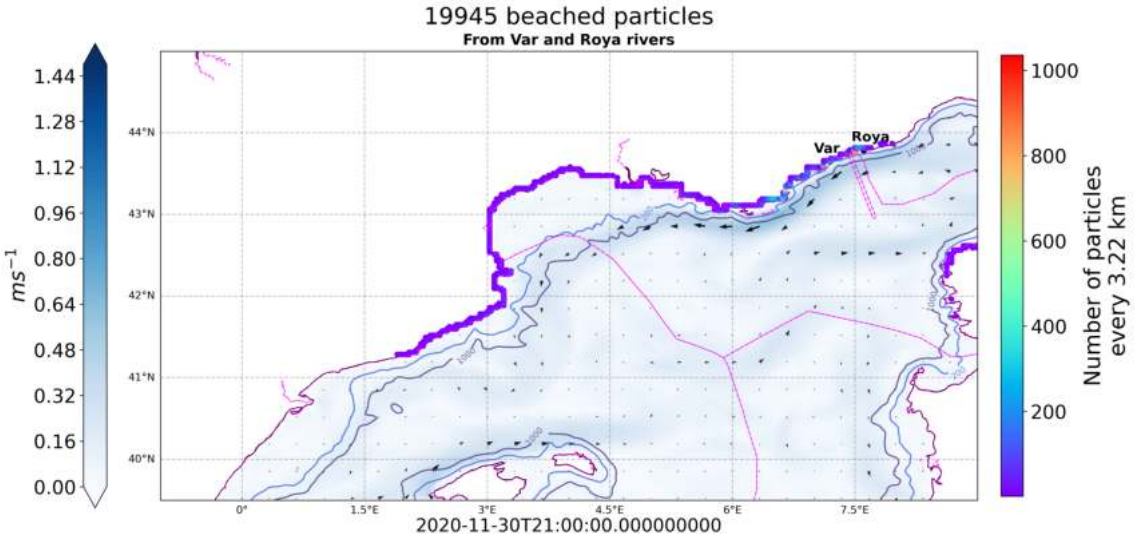

Figure 4.26: 19945 beached particles, from the CMEMS-MED MFC total currents particles simulation.

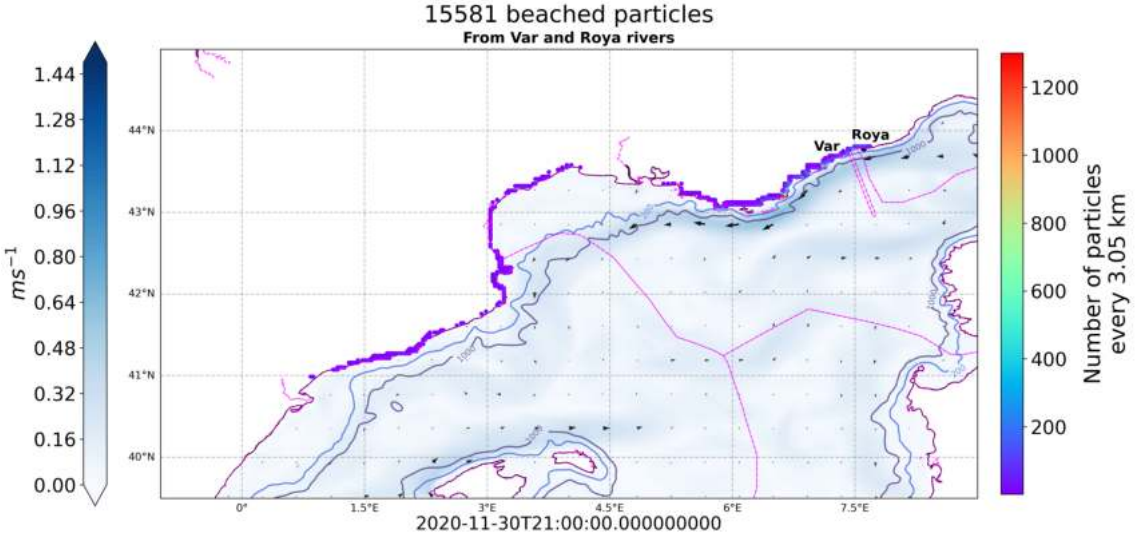

Figure 4.27: 15581 beached particles, from the CMEMS-MED MFC mean current particles simulation.

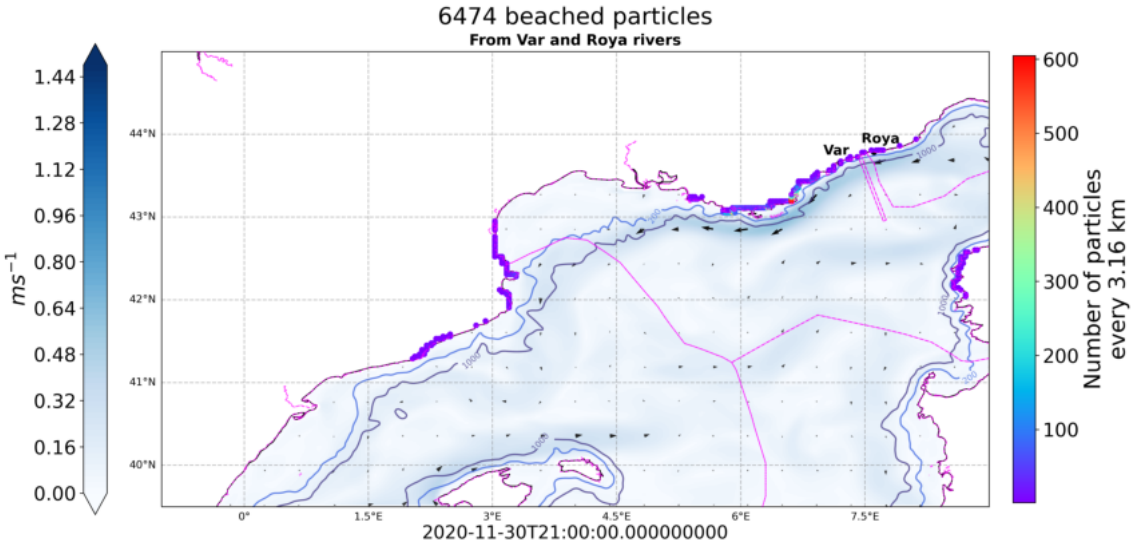

Figure 4.28: 6474 beached particles, from the CMEMS-MED MFC spatially filtered currents particles simulation.

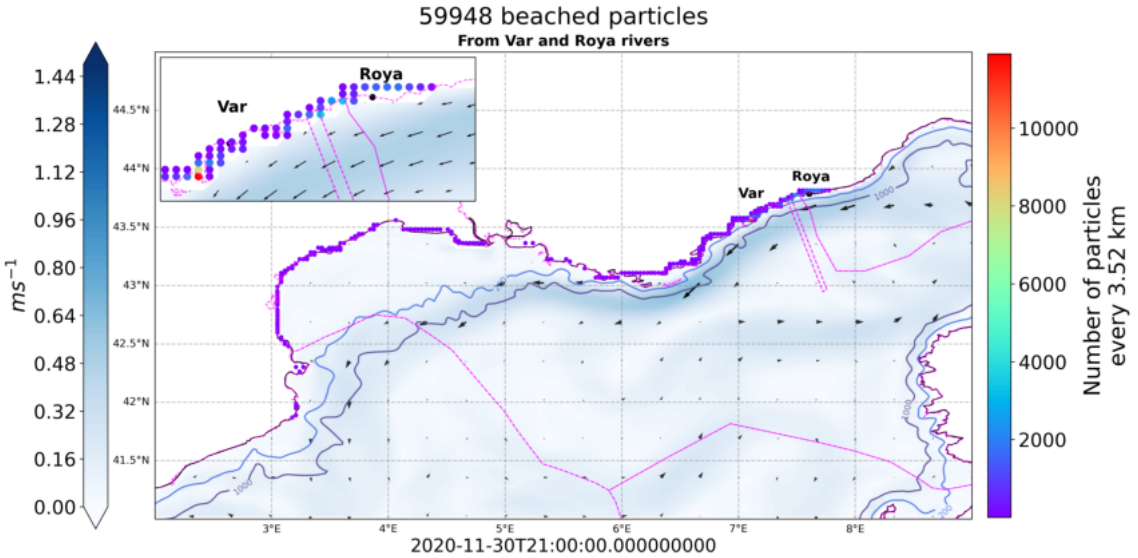

Figure 4.29: 59948 beached particles, from the CMEMS-MED MFC geostrophic currents particles simulation.

In Figures 4.26, 4.27, 4.28 and 4.29 we can see the density plots of the particles on land, from both rivers; we see that all four simulations yielded different results. The highest number of beached particles, 59948, is found in the geostrophic simulation, whereas the smallest is found in the spatially filtered simulation (6474 beached particles). In the total currents simulation and the spatially filtered one we see that some particles landed in Corsica, which we do not observe in the other simulations. The mean current simulation and the total currents one present a similar number of beached particles, 15581 and 19945 respectively, but we can see that in the mean simulation, particles spread more Southern along the Spanish coast that in the total simulation.

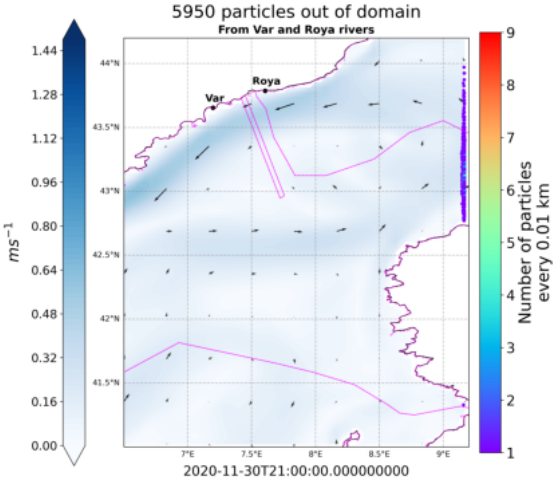

Figure 4.30: 5950 particles that left the domain of the simulations, from the CMEMS-MED MFC total currents particles simulation.

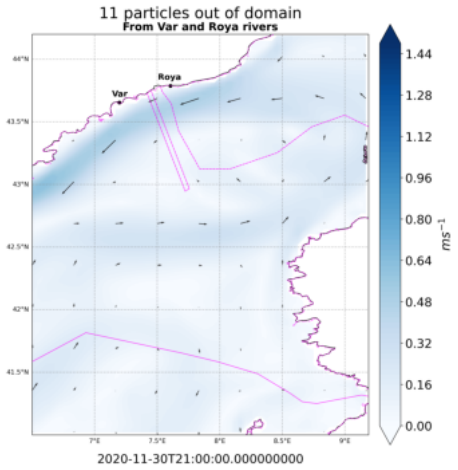

Figure 4.31: 11 particles that left the domain of the simulations, from the CMEMS-MED MFC mean current particles simulation.

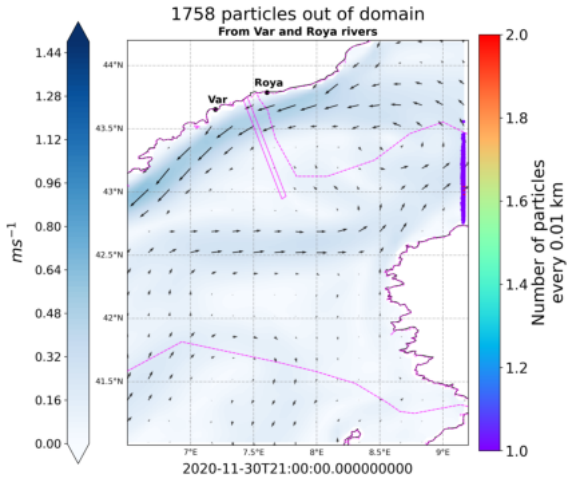

Figure 4.32: 1758 particles that left the domain of the simulations, from the CMEMS-MED MFC spatially filtered currents particles simulation.

As we can see in Figures 4.30, 4.31 and 4.32, all the particles that left the domain of our simulations did so Northern of Corsica. The largest amount of material that went out of domain was in the total simulation (5950 particles), while only 11 and 1 particles left the domains of the mean simulation and geostrophic simulation, respectively; in the spatially filtered simulation 1758 particles went out of domain.

4.3.2 Floating particles

The majority of particles from the spatially filtered simulation remained on water, that is 51768 particles (Figure 4.35) which remained very compact and did not spread out much in the water domain. Likewise, in the total simulation and in the

mean simulation more than half of all the particles stayed on water, but we can see that they were more dispersed that in the spatially filtered simulation: they reached as South as the Valencian coast in both simulations. In the geostrophic simulation we see that only 51 particles remained on water and stayed mainly in the Gulf of Lion.

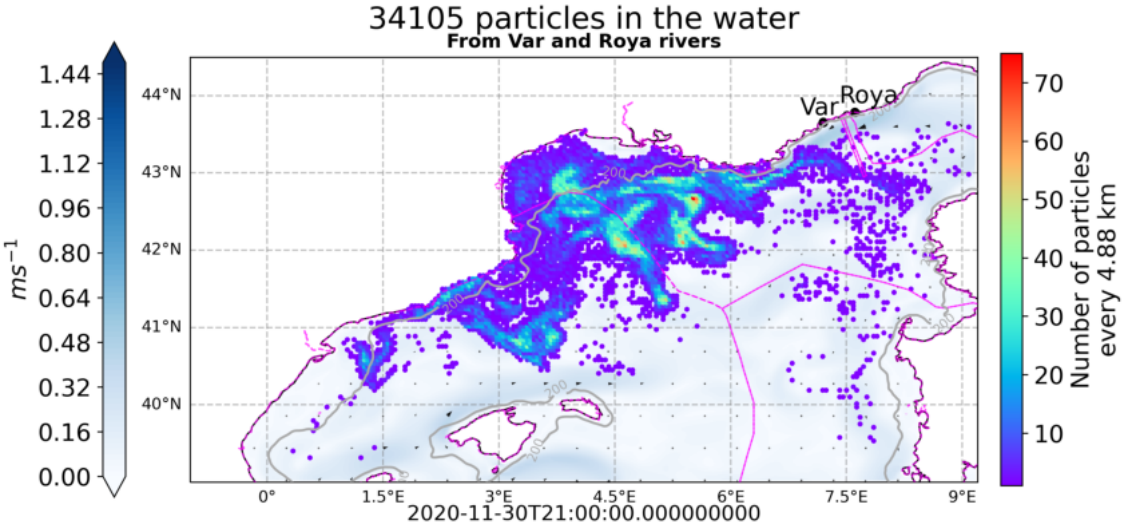

Figure 4.33: 34105 particles on water, density plot from the CMEMS-MED MFC total currents particles simulation.

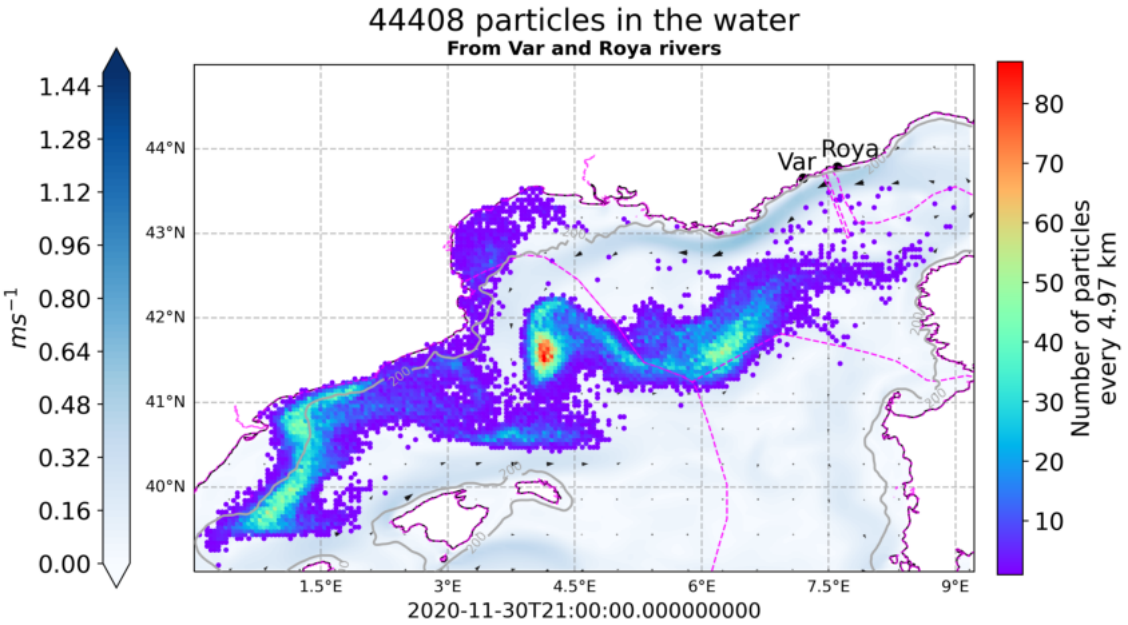

Figure 4.34: 44408 particles on water, density plot from the CMEMS-MED MFC mean current particles simulation.

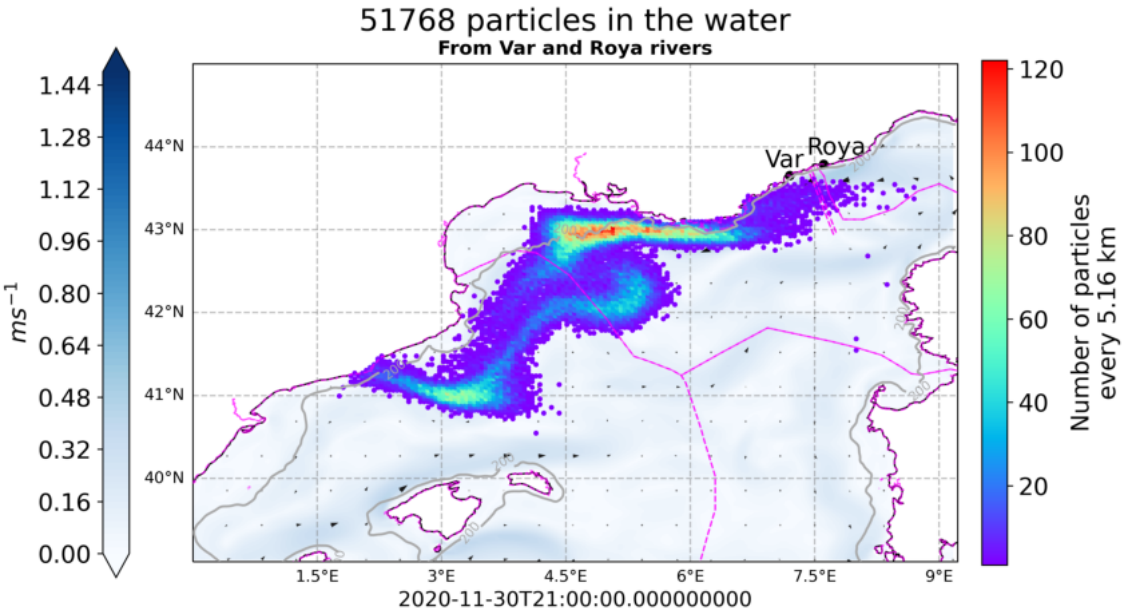

Figure 4.35: 51768 particles on water, density plot from the CMEMS-MED MFC spatially filtered currents particles simulation.

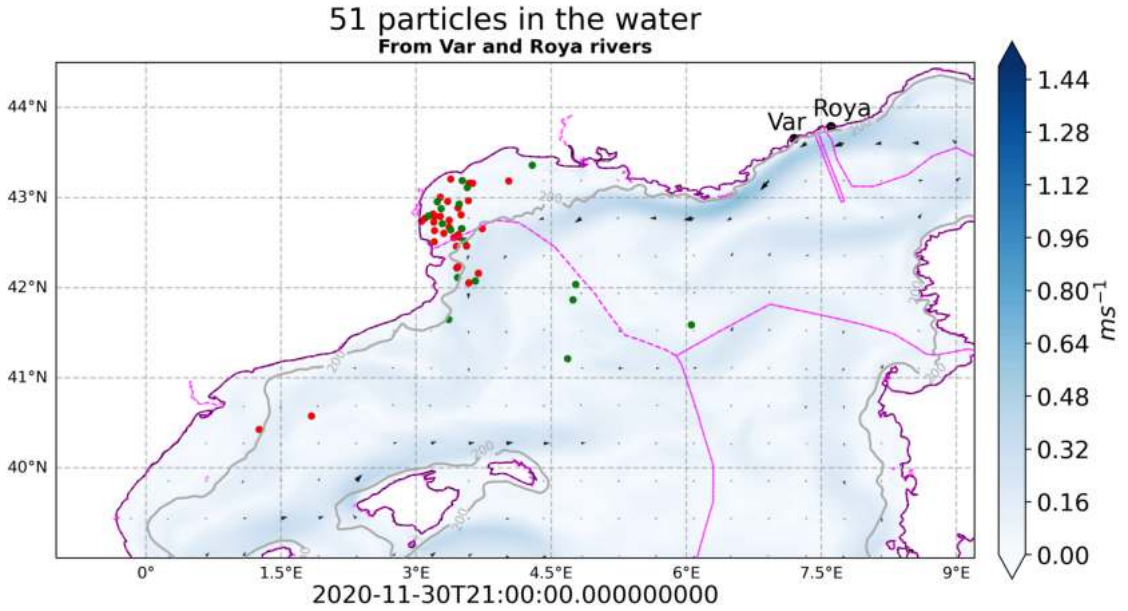

Figure 4.36: 51 particles on water, from the geostrophic currents particles simulation.

4.3.3 Shelf-slope exchanges

To study the extent of the shelf-slope exchange we look at the fraction of particles that ended up on land, out of domain, on water, and how many crossed the 200 m bathymetry line (Table 4.1). The highest percentage is found in the total and spatially filtered simulations, where, respectively, ∼46.75 % and ∼71.92 % of the particles crossed the bathymetry line. This value is followed by the mean current simulation, in which ∼19.04 % of the particles went beyond the 200 m bathymetry

line. On the other hand, only ∼0.02 % of the geostrophic particles crossed the line, which is not surprising considering that ∼99.9 % of the material in this simulation ended up on land. In fact, we need to consider that these percentages increase accordingly to the amount of particles that ended up on water, and therefore the currents characteristics that kept material close to the coast played the same role in preventing shelf-slope exchanges.
Comparing these with the WMOP results (shown in Table 3.1), we can see that in the WMOP total currents and spatially filtered simulations a much smaller number of particles crossed the 200 m bathymetry line. On the other hand, in the mean and geostrophic simulations less particles crossed the bathymetry line in the CMEMS case than in the WMOP result.
In the geostrophic simulations, we generally have similar results in both models, with most of the particles ending up on land. Contrarily, the other three simulations show noticeable differences across the two models, perhaps due to the different resolutions.

Simulation	Total	Mean	Spatially filtered	Geostrophic
On water	56.9%	74.08%	86.3%	0.1%
Beached	33.2%	25.9%	10.8%	99.898%
Out of domain	9.9%	0.02%	2.9%	0.002%
Percentage beyond the 200m bathymetry line	46.75%	19.04%	71.92%	0.02%

Table 4.1: For each CMEMS-MED MFC simulation: number of particles on water, and the percentage that crossed the 200m bathymetry line.

4.3.4 Transnational transport

As we previously investigated for the WMOP case, we want to know which countries were most affected by the pollution from the two rivers. We remind the reader that Var's delta is located between Nice and Saint-Laurent-du-Var, France, and that Roya discharges in the town of Ventimiglia, Italy. In this Section we analyse the transnational transport of material from the two rivers, for the CMEMS-MED MFC simulations, and we also draw a parallel between the two models outputs.
In Figures 4.37, 4.38, 4.39 and 4.40 are shown the Sankey diagrams of the transnational transport for the different CMEMS-MED MFC simulations.

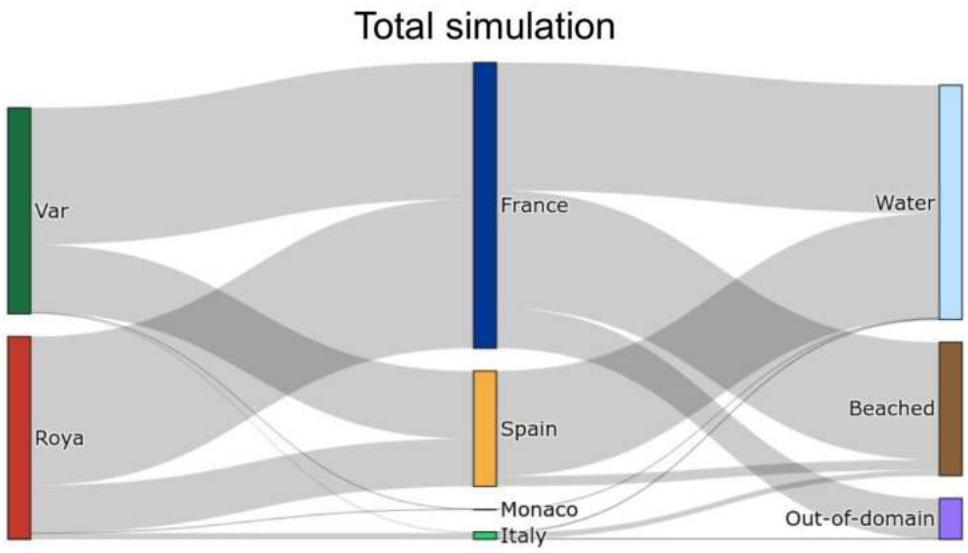

Figure 4.37: CMEMS-MED MFC total currents: Sankey plot of transnational transport of particles from rivers Var and Roya.

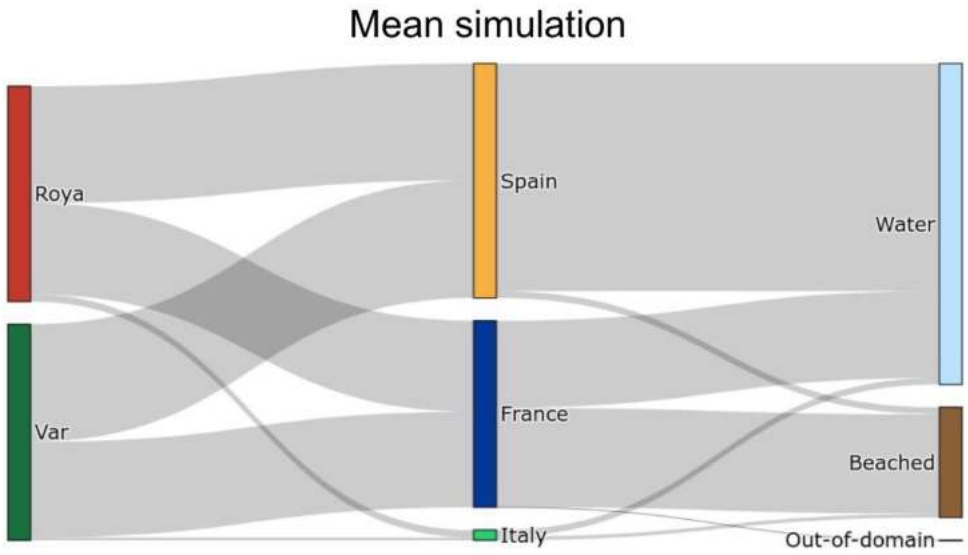

Figure 4.38: CMEMS-MED MFC mean current: Sankey plot of transnational transport of particles from rivers Var and Roya.

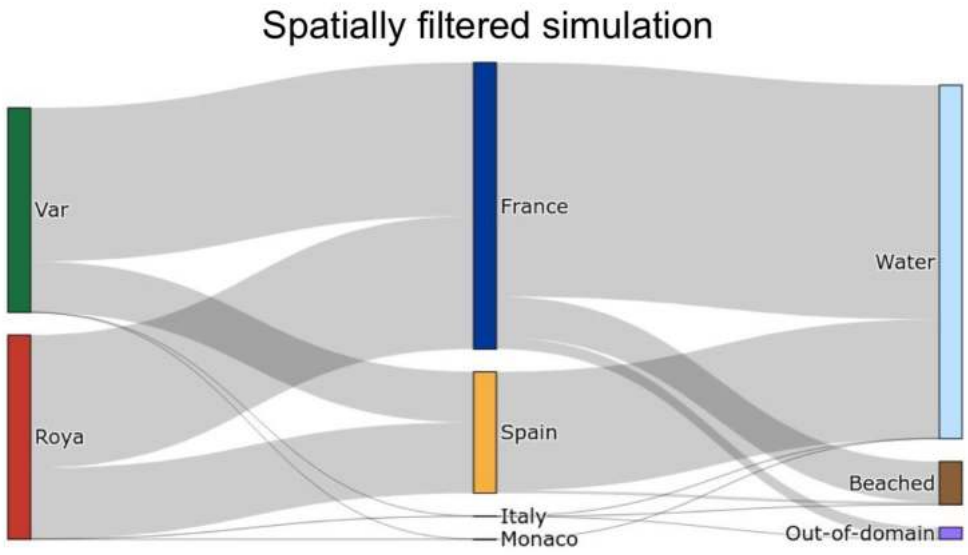

Figure 4.39: CMEMS-MED MFC spatially filtered currents: Sankey plot of transnational transport of particles from rivers Var and Roya.

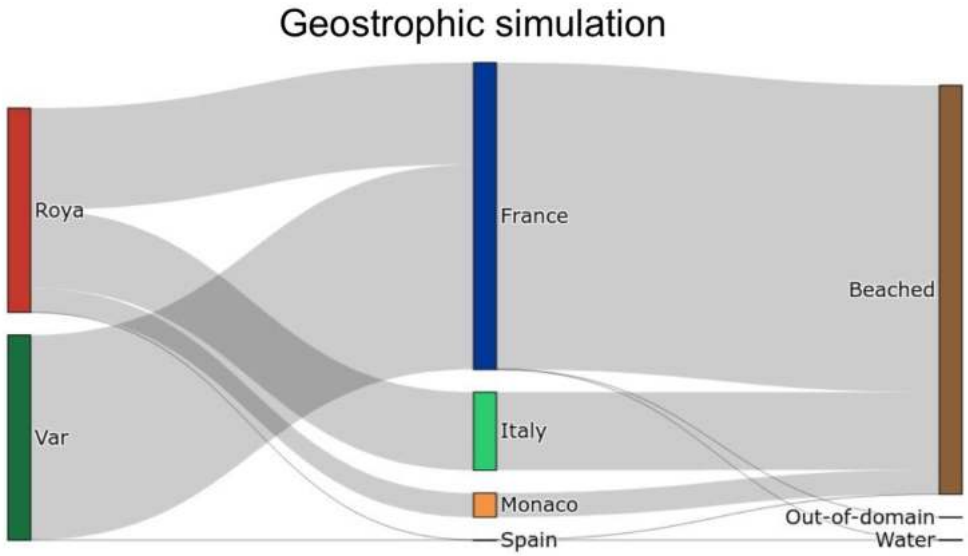

Figure 4.40: CMEMS-MED MFC geostrophic currents: Sankey plot of transnational transport of particles from rivers Var and Roya.

In the total currents simulation (Figure 4.37) we see that most of the material from both rivers ended up on the French coast or waters. Nonetheless, a substantial fraction of the particles also arrived in Spain, almost all of it on water. Italy and Monaco also took on part of the pollution, but considerably less than France and

Spain. Compared to the WMOP result (Figure 3.41), here Spain received more pollution, but France remains the prime country in which the material ends up; the main difference is that in the WMOP case most of the plastic went out of domain or was beached, whereas in the CMEMS simulation we now observe most of it on water or beached.
In the mean current simulation (Figure 4.38) Spain and France received almost all of the particles. Notably, the material from Var and Roya split between the two countries, with Italy receiving only a small fraction of the plastic and Monaco none of it. Almost all of the particles that ended up in Spain were on water (a small part was beached), whereas the pollution in French was either beached or finished on water, and a small fraction went out of domain. Particles in Italy were either out of domain or on water. This result is very different from what we saw in the WMOP mean current transport (Figure 3.42), in which less particles ended up on water and more were beached, but most importantly Italy was affected much more than in the CMEMS simulation.
In the spatially filtered simulation (Figure 4.39), the majority of the particles ended up on water and mainly in France and Spain. A small fraction of the material that arrived in France was beached or went out of domain, but it is evident that most of it stayed in the sea. Italy and Monaco also received a part of the plastic particles, but it is a very small fraction of the total. Comparing this to the WMOP spatially filtered transport (Figure 3.43), the main difference is observable in where the particles were in the different countries. In fact, in the WMOP case it is still France that receives most of the particles, with Spain and Italy having similar fractions, but the main difference is that in the WMOP case a much higher percentage of the particles went out of domain rather than staying on water.
In the geostrophic case (Figure 4.40) most of the particles were beached, in decreasing order, in France, Italy, Monaco, and Spain. This is rather similar to the result obtained with the WMOP model (Figure 3.44), with the sole difference that in the CMEMS case Monaco took on a higher percentage of material than in the WMOP case.
Except for the geostrophic simulation, in the CMEMS case it seems that the effect of removing small scale features from our currents field was that of increasing the amount of material ending up on water. For all four simulation France received the highest percentage of plastic, except for the mean current case in which Spain was first. Following France, the highest receiver in the total currents and spatially filtered simulations was Spain, and in the geostrophic case it was Italy. Monaco always received a small amount of plastic, due to it being a small country.
These results are all quite different to what we obtained with the WMOP model. Knowing that the WMOP model has a finer spatial resolution we can assume that it resolves smaller scales better than the CMEMS (as proposed by Aguiar et al. (2020)). Then, if we compare the WMOP total currents transport (Figure 3.41) to that of the CMEMS (Figure 4.37), we can see that in the CMEMS case many more particles end up on water, and in particular the fraction that went out of domain is appreciably lower than in the WMOP simulation, where this was the material's main destination.

We show in Table 4.2 the exact percentages for the beached and water configurations in the total currents simulation; we do not show here the out-of-domain percentages because ultimately we do not know where the particles end up after exiting the domain.

CMEMS	Roya	Var	Roya	Var
	On water		Beached	
Spain	20.96%	30.05%	2.12%	28.73%
France	23.13%	39.01%	40.68%	16.37%
Italy	0.22%	0.26%	2.66%	0.03%
Monaco	0.00%	0.01%	0.00%	0.00%

Table 4.2: CMEMS-MED MFC total currents simulation: transnational transport.

Chapter 5

Results and discussion

The goal of this work is to assess the impact of small scale oceanic features on the dispersion of plastic following the input from Storm Alex, and in particular the effects on beaching, cross-shelf exchanges and transboundary transport. We have used two models to study the WMED currents, with the aim of looking for differences and parallelisms in material propagation when we use currents with different magnitude of small-scale turbulence. We can compare the different results the models yielded in order to find common features and discrepancies, which can help highlight the effect of turbulence on our simulations. Aguiar et al. (2020) showed that the WMOP model was generating a larger number of small eddies, compared to the CMEMS-MED MFC model, due to its better resolution (∼2 km). On the other hand, the CMEMS-MED MFC model has proved to be a better fit at recognising mesoscale structures.

The main difference noticeable between the models is that the WMOP outputs show much more dispersion of particles than the CMEMS. In the WMOP simulations we also observed an eddy, at roughly a latitude and longitude of (41.5°N, 3°E), that is very weak or that completely disappears in the CMEMS simulations. Additionally, the Northern Current in the CMEMS model is stronger and has a bigger extent than what we see with the WMOP, which contributes in bringing the material further South. From the final positions of the particles on water, in the WMOP simulations, we can infer that the total currents simulation was slowed down by turbulence in its path along the WMED circulation. The mean current simulation didn't spread as much in terms of diffusion and as a result the particles moved faster along the main currents of the WMED, reaching the North Balearic Front. This is also the case for the CMEMS total and mean current simulations, where we have that the mean current particles arrive much more South than in the total current case, and they also move Eastern along the North Balearic Front, whereas this is not observed in the total currents case. So, when we compare the total currents with the temporal average we can deduce that the effect of removing short lived turbulence is that of allowing the material to move with the WMED main circulation pathways. This is coherent in the two models, and even though the propagation is not the same, the difference between total and mean current simulations is similar in both models.

From the analysis of the particles final positions, and by looking at Tables 5.1 and 5.2, we can see that the result of the geostrophic simulation is really similar in both models: we see that the two simulations have a high number of beached particles as well as a very low escape of material from the domain. In particular, it seems that

there is no coastal offshore significant velocity component, so that the predominant currents are pushing the particles towards the land. When we compare this with the results from the total currents simulations, where most particles are either out of domain (WMOP) or on water (CMEMS), it seems that what is causing the material to disperse is the ageostrophic terms. Ageostrophy represents any turbulence that disrupts the mean circulation of the region, due to surface forcings that can be representative of many factors, such as wind events, upwelling/downwelling or more. In Figures 5.1, 5.2, 5.3 and 5.4 we show the plots for the geostrophic and ageostrophic flows of both models, for the 4th of October 2020 at T18:00. We choose to show this date because it has remarkable features that are representative of the immediate effect of the storm.

	WMOP	CMEMS	WMOP	CMEMS
	Total currents		Mean current	
On water	14754	34105	28770	44408
Beached	17486	19945	30632	15581
Out of domain	27400	5950	598	11

Table 5.1: From both models: number of particles for each final configuration, total and mean simulations.

	WMOP	CMEMS	WMOP	CMEMS
	Spatially filtered		Geostrophic currents	
On water	27392	51768	96	51
Beached	11068	6474	59857	59948
Out of domain	21540	1758	47	1

Table 5.2: From both models: number of particles for each final configuration, spatially filtered and geostrophic simulations.

By looking at the values in Tables 5.1 and 5.2, we can infer that the main effect of small-scale features, especially in the WMOP study, was to disperse particles and to push material out of domain, towards the Ligurian and Tyrrhenian Seas.

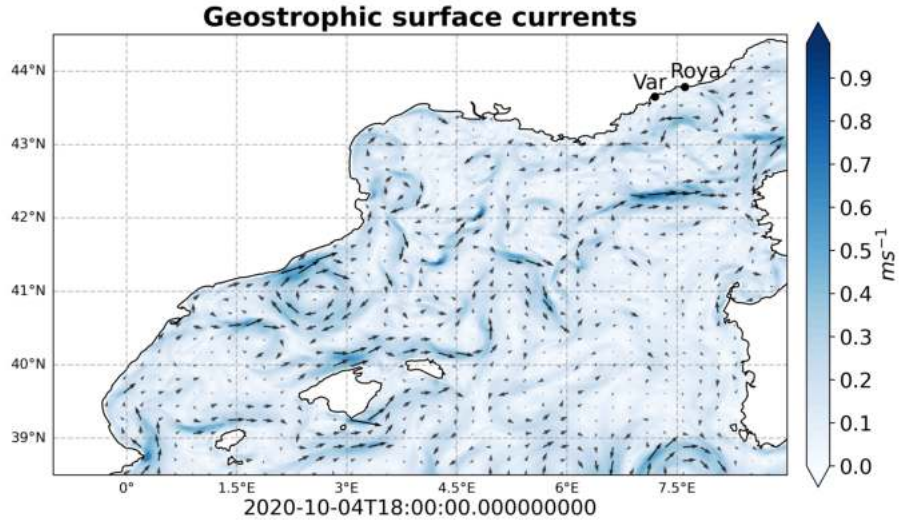

Figure 5.1: WMOP geostrophic currents on the **4th of October 2020 at T18:00**.

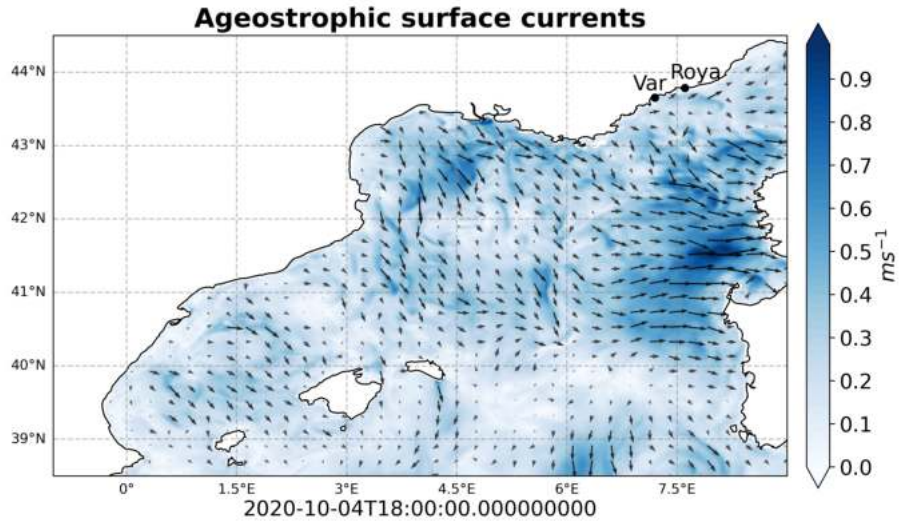

Figure 5.2: WMOP ageostrophic currents on the **4th of October 2020 at T18:00**.

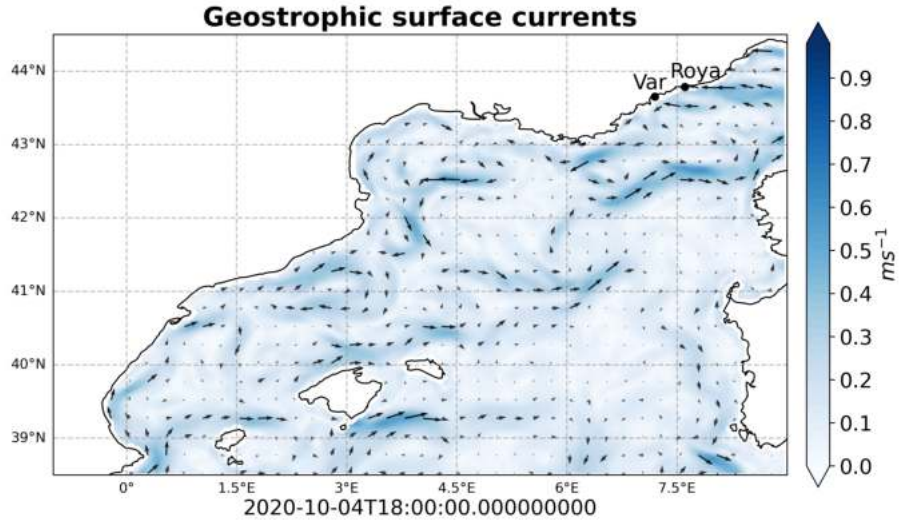

Figure 5.3: CMEMS-MED MFC geostrophic currents on the **4th of October 2020 at T18:00**.

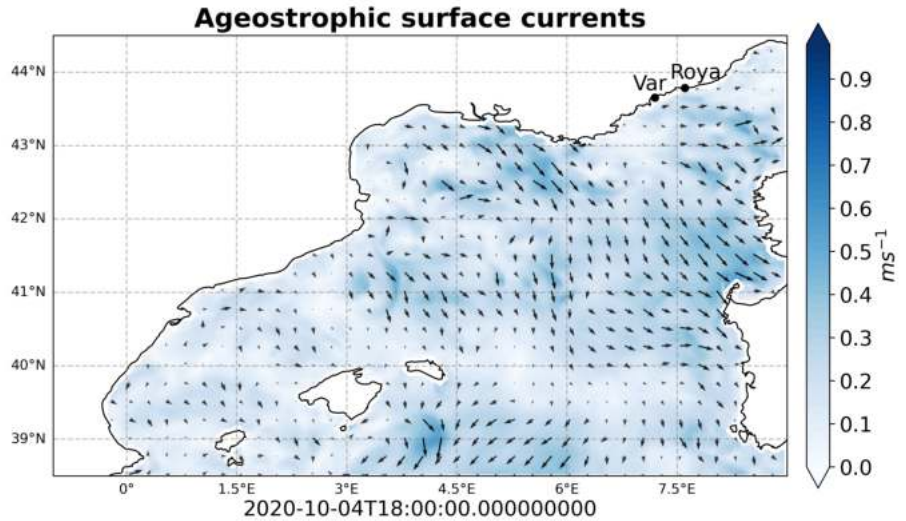

Figure 5.4: CMEMS-MED MFC ageostrophic currents on the **4th of October 2020 at T18:00**.

By looking at the geostrophic and ageostrophic currents we see that in both models the ageostrophic component flows away from the coast while the geostrophic component flows towards the coast. This would indicate that the wind effects and turbulence played an important role in bringing particles away from the coast, and specifically pushing them out of domain. In fact, in the geostrophic particles simulations we saw that almost all of the material was beached.
On the other hand, by comparing the shape and positions of on-water particles in the WMOP mean current simulation (Figure 3.38) and in the total currents simulation (Figure 3.37), it seems that the effect of short-lived eddies is that of keeping material away from the centre of the domain. In fact, in the absence of these we see that the particles reach the North Balearic Front.

The common characteristic that we find in both models, and in all four simulations, is that when we filter small scale features the amount of particles that leave the domain decreases substantially, as we showed in Tables 3.1 and 4.1.
Since we do not know what happens to the particles after they leave the domain, we want to consider the values of Tables 3.1 and 4.1 calculated as percentages of the particles that stayed in the domain, therefore excluding the out-of-domain material from the total particles. By doing so, we can better evaluate similarities and differences of the two models.
So, as we can see in Table 5.3, without accounting for the particles that left the domain, the proportionalities show a slightly different situation. From the total currents simulations we can drive to the same conclusions inferable from Tables 3.1 and 4.1, and the same can be said for the mean current simulation. It is in the spatially filtered simulation that this Table allows for a different perspective: the fact that in the WMOP case only 27392 particles are on water, compared to the 51768 particles of the CMEMS, is mainly due to the fact that a lot more particles were pushed out of domain. In fact, as highlighted in Table 5.3, the difference between the two models is only $\sim 17.7\%$ of the total. Whereas, if we keep the total as 60000 particles (as in Tables 3.1 and 4.1) then the difference would be ~ 40.6 %.
The geostrophic simulations are extremely similar, which could be due to the fact that since geostrophy is important at scales bigger than 15 km (in the Mediterranean), the difference in resolution of the two models may not have played a role in diversifying the outputs of the geostrophic simulation.

	WMOP	CMEMS	WMOP	CMEMS	WMOP	CMEMS	WMOP	CMEMS
	Total currents		Mean current		Spatially filtered		Geostrophic currents	
On water	45.26%	63.10%	48.43%	74.03%	71.22%	88.88%	0.16%	0.09%
Beached	53.64%	36.90%	51.57%	25.97%	28.78%	11.12%	99.84%	99.91%
Total particles in the domain	32600	54050	59402	59989	38460	58242	59953	59999

Table 5.3: From both models: percentage of particles for each final configuration, for every simulation. Here the total particles for every simulation has been computed by removing from the initial 60000 particles the out-of-domain particles.

Chapter 6

Conclusions

We have been able to evaluate the impact of ocean currents on the dispersion of virtual particles, representing plastic or marine litter, simulating the discharges of Var and Roya. Although the work can be extended in the future, we have already been able to quantify the role played by small scale and transient ocean features in the propagation of the plastic.
The comparison between different models simulations, performed to filter and evaluate the effect of turbulence on material dispersion, allows us to investigate the phenomena causing the discrepancies and similarities. While it is already clear that using one temporal average current to perform the particles simulation is unrealistic, we were able to use this to assess the impact of the mean currents in the absence of short-lived features. We saw, with both models, that the mean currents drive the particles along the main currents of the WMED (Figures 3.17 and 4.15), allowing them to reach the North Balearic Front in a return stream. In the total currents simulations the particles are slowed down by short-lived turbulence and eddies, and the material does not reach the NBF. Furthermore, using two different models (WMOP and CMEMS-MED MFC) to perform our investigation allowed us to back up possible assumptions, by means of finding common results in the different outputs.
We see that in the mean and geostrophic simulations the number of beached particles is much higher than in the total currents simulation (Tables 5.1 and 5.2), indicating that small scale features of turbulence played a crucial role into the transport of material away from the shelf and into open water, but while keeping it away from the centre of the domain as well. These small scale structures have been found to have a significant role on the transboundary transport of pollution, and the cross-shelf exchanges between the coast and the open ocean. With both models, most of the materials ended up in Spain or France (Tables 3.2 and 4.2), either beached or on their national waters.

Bibliography

Population and Development. In *UN environment and Mediterranean Action Plan (MAP) Barcelona convention*, 2017.

State of the Climate: Global Climate Report for Annual 2020. In *NOAA National Centers for Environmental Information.*, January 2021.

Y. account. https://www.youtube.com/c/Freepassenger-com: 1 minute Ventimiglia — Drone Bebop 2. https://www.youtube.com/watch?v=4u21VW7MW2g, a.

Y. account. https://www.youtube.com/channel/UCvD3jAzmiFoZf46ruCVDA3w: Ventimiglia After Storm ALEX - From the air (Drone footage). https://www.youtube.com/watch?v=fWWR3Pqj8GM, b.

E. Aguiar, B. Mourre, M. Juza, E. Reyes, J. Hernández-Lasheras, E. Cutolo, E. Mason, and J. Tintoré. Multi-platform model assessment in the Western Mediterranean Sea: impact of downscaling on the surface circulation and mesoscaleactivity. *Ocean Dyn.*, 70(2), 2020.

M. Berta, L. Bellomo, A. Griffa, M. G. Magaldi, A. Molcard, C. Mantovani, G. P. Gasparini, J. Marmain, A. Vetrano, L. Béguery, M. Borghini, Y. Barbin, J. Gaggelli, and C. Quentin. Wind-induced variability in the Northern Current (northwestern Mediterranean Sea) as depicted by a multi-platform observing system, 2018.

J. Bethoux, B. Gentili, P. Morin, E. Nicolas, C. Pierre, and D. Ruiz-Pino. The mediterranean sea: a miniature ocean for climatic and environmental studies and a key for the climatic functioning of the north atlantic, 1999. ISSN 0079-6611. URL https://www.sciencedirect.com/science/article/pii/S0079661199000233.

S. Brouwer et al. The Use of Diffusion for Modelling the Distribution of Plastic in the Northern Pacific, 2018.

K. Bryan and M. D. Cox. A numerical investigation of the oceanic general circulation, 1967. URL https://onlinelibrary.wiley.com/doi/abs/10.1111/j.2153-3490.1967.tb01459.x.

E. Clementi, J. Pistoia, C. Fratianni, D. Delrosso, A. Grandi, M. Drudi, G. Coppini, R. Lecci, and N. Pinardi. Mediterranean Sea Analysis and Forecast (CMEMS MED-Currents 2013-2017), 2017.

M. Evan, R. Simón, B.-B. Romain, R. Guillaume, G.-S. Marcos, , and P. Ananda. Copernicus (CMEMS) operational model intercomparison in the western Mediterranean Sea: Insights from an eddy tracker, 2019.

FloodList and News. France and Italy – Deadly Flash Floods After 630mm of Rain in 24 Hours. https://floodlist.com/europe/france-italy-floods-storm-alex-october-2020, October 2020.

J. Font, J. Salat, and J. Tintore. Permanent features of the circulation in the catalan sea. *Oceanologica Acta, Special issue*, 1988. URL https://archimer.ifremer.fr/doc/00267/37808/.

J. Font, C. Millot, J. Salas, A. Juliá, and O. Chic. The drift of modified atlantic water from the alboran sea to the eastern mediterranean. *Scientia Marina*, 62(3):211–216, Sep. 1998. doi: 10.3989/scimar.1998.62n3211. URL https://scientiamarina.revistas.csic.es/index.php/scientiamarina/article/view/965.

M. Gade, S. Karimova, and A. Buck. Mediterranean eddy statistics based on multiple sar imagery, 10 2018.

A. E. Gill. *Atmosphere-ocean dynamics / Adrian E. Gill.* Academic Press New York, 1982. ISBN 0122835204 0122835220. URL http://www.loc.gov/catdir/toc/els031/82008704.html.

J. R. Jambeck, R. Geyer, C. Wilcox, T. R. Siegler, M. Perryman, A. Andrady, R. Narayan, and K. L. Law. Plastic waste inputs from land into the ocean. *Science*, 347(6223):768–771, 2015. doi: 10.1126/science.1260352. URL https://www.science.org/doi/abs/10.1126/science.1260352.

JERICO-RI. Joint European Research Infrastructure for Coastal Observatories. https://www.jerico-ri.eu/projects/jerico-s3/pilot-supersites/.

M. Juza, B. Mourre, L. Renault, S. Gómara, K. Sebastian, S. Lora, J. Beltran, B. Frontera, B. Garau, C. Troupin, M. Torner, E. Heslop, B. Casas, R. Escudier, G. Vizoso, and J. Tintoré. Socib operational ocean forecasting system and multiplatform validation in the western mediterranean sea, 02 2016.

J. H. Lasheras. Impact of the assimilation of coastal observations on high resolution ocean model forecasts, 2022.

P. Marchesiello, J. C. McWilliams, and A. Shchepetkin. Open boundary conditions for long-term integration of regional oceanic models, 2001. ISSN 1463-5003. URL https://www.sciencedirect.com/science/article/pii/S1463500300000135.

E. C. maritime forum. Exclusive Economic Zones. https://webgate.ec.europa.eu/maritimeforum/en/node/4426, 2019.

B. Mourre, E. Aguiar, M. Juza, J. Hernández-Lasheras, E. Reyes, E. Heslop, R. Escudier, E. Cutolo, S. Ruiz, E. Mason, A. Pascual, and J. Tintoré. Assessment of high-resolution regional ocean prediction systems using multi-platform observations: Illustrations in the western mediterranean sea, 08 2018.

A. Okubo. Oceanic diffusion diagrams, 1971. ISSN 0011-7471. URL https://www.sciencedirect.com/science/article/pii/0011747171900465.

N. Pinardi, P. Cessi, F. Borile, and C. L. P. Wolfe. The mediterranean sea overturning circulation, 2019. URL https://journals.ametsoc.org/view/journals/phoc/49/7/jpo-d-18-0254.1.xml.

A. Robinson, W. Leslie, A. Theocharis, and A. Lascaratos. Mediterranean sea circulation, 12 2001.

A. Schiller, B. Mourre, Y. Drillet, and G. Brassington. *An Overview of Operational Oceanography*. 08 2018. ISBN 9781720549970. doi: 10.17125/gov2018.ch01.

S. L. Sentinel Hub. Modified Copernicus Sentinel data [2020]/Sentinel Hub. https://www.sentinel-hub.com, 2020a.

S. L. Sentinel Hub. Modified Copernicus Sentinel data [2020]/Sentinel Hub. https://www.sentinel-hub.com, 2020b.

S. L. Sentinel Hub. Modified Copernicus Sentinel data [2020]/Sentinel Hub. https://www.sentinel-hub.com, 2020c.

S. Simoncelli, C. Fratianni, N. Pinardi, A. Grandi, M. Drudi, P. Oddo, and S. Dobricic. Mediterranean Sea physical reanalysis (MEDREA 1987-2015), 2014.

J. Sommer, E. Chassignet, and A. Wallcraft. *Ocean Circulation Modeling for Operational Oceanography: Current Status and Future Challenges*. 08 2018. ISBN 9781720549970. doi: 10.17125/gov2018.ch12.

T. Tanhua, D. Hainbucher, K. Schroeder, V. Cardin, M. Alvarez, and G. Civitarese. The Mediterranean Sea system: a review and an introduction to the special issue. *Ocean Science*, 2013.

J. Tintoré, B. Casas, E. Heslop, G. Vizoso, A. Pascual, A. Orfila, S. Ruiz, L. Renault, M. Juzà, P. Balaguer, L. Gómez-Pujol, A. Álvarez-Ellacuria, S. Gómara, K. Sebastian, S. Lora, J. P. Beltrán, D. March, R. Escudier, M. Martínez-Ledesma, M. Torner, S. Cusí, D. Roque, I. Lizarán, C. Castilla, T. Cañellas, A. Lana, D. Conti, J. M. Sayol, E. Mason, B. Barceló-Llull, F. Alemany, D. Álvarez-Berastegui, P. Reglero, E. Massuti, P. Vélez-Belchí, J. Ruiz, T. Oguz, M. Gómez, E. Álvarez, L. Ansorena, and M. Manriquez. The impact of new multi-platform observing systems in science, technology development and response to society needs; from small to large scales..., 2013.

E. van Sebille, P. Delandmeter, M. Lange, W. Rath, J. S. Phillips, Simnator101, pdnooteboom, J. Kronborg, Thomas-95, D. Wichmann, nathanieltarshish, J. Busecke, R. Edwards, M. Sterl, S. Walbridge, M. Kaandorp, hart davis,

P. Miron, IsoldeGlissenaar, G. Vettoretti, and D. A. Ham. OceanParcels/parcels: Parcels v2.0.0: a Lagrangian Ocean Analysis tool for the petascale age, June 2019. URL https://doi.org/10.5281/zenodo.3257432.

H. Varkkey. Transboundary Pollution. Oxford Bibliographies, 2019.